

CHARACTERIZATION OF REMEDIATION METHODS FOR HEAVY
HYDROCARBON CONTAMINATED SOIL

A Thesis

by

THOMAS THOMPSON

Submitted to the Office of Graduate and Professional Studies of
Texas A&M University
in partial fulfillment of the requirements for the degree of

MASTER OF SCIENCE

Chair of Committee, Andrea Strzelec
Committee Members, David Staack
 Josias Zietsman

Head of Department, Andreas A. Polycarpou

August 2016

Major Subject: Mechanical Engineering

Copyright 2016 Thomas Thompson

ABSTRACT

Hydrocarbons are a prominent fuel source for many different types of applications. Due to transportation and handling, spills and leaks may contaminate the surrounding soil. Soil contamination has adverse effects on the environment that could lead to harming wildlife and humans. It is essential to find an effective remediation method in order to clean the soil. Currently, remediation methods can be categorized into two categories: non-energetic methods (includes solvents, dispersion, and bioremediation) and methods that involve energy addition.

Energy addition remediation includes incineration, thermal desorption, pyrolysis, and a newly proposed technique using an electron beam. This study focused on the characterization and quantification of hydrocarbons removed by several of the energy addition methods, including: incineration, thermal desorption, pyrolysis and electron beam treatment at several energy levels. Temperature Programmed Reaction experiments were used to characterize background, untreated, and treated soils to determine the type of hydrocarbon content, either mobile or fixed, that is in the soil sample and the efficacy of the various remediation processes.

Results from the study found that incineration is the method that removes the most hydrocarbon content, followed by thermal desorption. Pyrolysis converted a fraction of the mobile hydrocarbons content to fixed carbon content. Several (energy) levels of E-beam treatment were also able to convert a portion of the mobile hydrocarbon content to fixed carbon content, elucidating new details of how the E-beam

mechanism works; namely by a combination of thermal desorption and thermochemical conversion.

ACKNOWLEDGEMENTS

I would like to thank Dr. Strzelec for her guidance and support throughout the course of this research and for the opportunity to work in a research laboratory. I would also like to thank my committee members, Dr. Staack and Dr. Zietsman, for taking time out of their schedules to be part of my committee.

Thanks also go to my friends and colleagues and the department faculty and staff for making my time at Texas A&M University a great experience. I also would like to thank my corporate sponsor for funding my thesis research.

Finally, thanks to my mother and father for their support and encouragement throughout my entire life.

TABLE OF CONTENTS

	Page
ABSTRACT.....	ii
ACKNOWLEDGEMENTS.....	iv
TABLE OF CONTENTS.....	v
LIST OF FIGURES.....	vii
CHAPTER I INTRODUCTION AND LITERATURE REVIEW	1
CHAPTER II EXPERIMENTAL METHODS	5
2.1 Remediation Methods	5
2.1.1 Incineration.....	5
2.1.2 Thermal Desorption.....	6
2.1.3 Pyrolysis	7
2.1.4 Electron Beam	8
2.2 Characterization Methods	9
2.2.1 Microreactor	9
2.2.2 CO ₂ Calibration Procedure.....	10
2.2.3 Sample Packing	11
2.2.4 Temperature Programmed Reactions	11
2.2.4.1 Temperature Programmed Oxidation.....	11
2.2.4.2 Temperature Programmed Desorption	12
2.2.4.3 Temperature Programmed Oxidation on a Devolatilized Sample	13
CHAPTER III RESULTS AND DISCUSSION	15
3.1 Background Soils	15
3.1.1 BM2.....	15
3.1.2 BM3.....	17
3.2 GSC1AOS (Preliminary Results).....	19
3.2.1 Untreated (GSC1AOS).....	20
3.2.2 1000 kGy	22
3.2.3 Comparison of Treated and Untreated Samples (GSC1AOS)	25
3.3 SJV/BM1	30
3.3.1 Untreated (SJV/BM1).....	30
3.3.2 Incineration.....	34
3.3.3 Thermal Desorption.....	35
3.3.4 Pyrolysis	37

3.3.5 Electron Beam	40
3.3.5.1 456 kGy E-beam Treatment	40
3.3.5.2 700 kGy E-beam Treatment	43
3.3.5.3 1200 kGy E-beam Treatment	45
3.3.5.4 2200 kGy E-beam Treatment	47
3.3.6 Comparisons of Treatments.....	49
3.3.6.1 Electron Beam Dose Dependency Comparison	49
3.3.6.2 Total Treatment Comparison	52
 CHAPTER IV CONCLUSIONS	 61
4.1 Summary	61
4.2 Future Work	62
 REFERENCES	 64
 APPENDIX A CO ₂ CALIBRATION EXAMPLE	 70
 APPENDIX B UNTREATED (SJV/BM1) REPLICATE TPX.....	 71
 APPENDIX C THERMAL DESORPTION (SJV/BM1) REPLICATE TPX	 73
 APPENDIX D PYROLYSIS (SJV/BM1) REPLICATE TPX.....	 75
 APPENDIX E 456 KGY (SJV/BM1) REPLICATE TPX	 77
 APPENDIX F 700 KGY (SJV/BM1) REPLICATE TPX	 79
 APPENDIX G 1200 KGY (SJV/BM1) REPLICATE TPX.....	 81
 APPENDIX H 2200 KGY (SJV/BM1) REPLICATE TPX.....	 83

LIST OF FIGURES

	Page
Figure 1: Graphical representation of contaminated soil. The yellow layer is the MC content fraction. The black layer represents the FX content, which likely includes heavy hydrocarbons and carbon solid. The brown central region represents the soil matrix, often sand. This layer remains after incineration. ...	4
Figure 2: Graphical representation of the incineration process. Heat is applied via a programmable furnace to the contaminated soil in the presence of an oxidizer. Products of combustion are CO, CO ₂ , H ₂ O, etc. Contaminated soil is converted to a barren soil.	6
Figure 3: Graphical representation of the thermal desorption process. Heat is applied to the contaminated soil via a programmable furnace in an inert environment (in this case, Ar). A portion of the hydrocarbons will boil off of the sample leaving behind heavy hydrocarbons, carbon black, and soil.....	7
Figure 4: Graphical representation of the pyrolysis process. Heat is applied to the contaminated soil via a programmable tube furnace in an inert environment (in this case N ₂). Light hydrocarbons will desorb and H ₂ will evolve leaving behind soil and char.	8
Figure 5: Microreactor Solidworks model. Gas input is on the left. Reactor 1 (sample location) and reactor 2 (oxidation catalyst location) are shown by the glass tubes just above the white, cylindrical, temperature controlled furnaces. Gas output is shown on the right.	10
Figure 6: Diagram of the gas flow path for a TPO experiment. A gas mixture of 10% (by volume) O ₂ and Ar flow over the sample in reactor 1, where combustion occurs. Gas products are sent to the oxidation catalyst in reactor 2 in order to convert any CO to CO ₂ . The final gas product is then sent to the MS for analysis.	12
Figure 7: Diagram of gas flow path for a TPD experiment. Ar flows over the sample in reactor 1 and is heated by a temperature controlled furnace. Hydrocarbons with boiling points below the sample temperature will volatilize off of the sample and be sent to a junction right before reactor 2. This junction will add O ₂ to the mixture and then be sent to the oxidation catalyst in reactor 2. Hydrocarbons and O ₂ will react to make CO ₂ and H ₂ O. Products are then sent to the MS for analysis.....	13

Figure 8: Diagram of TPO Devol gas flow path. A gas mixture of 10% (by volume) O ₂ and Ar flow over a devolatilized sample located in reactor 1, where heat is added via a temperature controlled furnace. Products are then sent to the oxidation catalyst located at reactor 2 to convert any CO to CO ₂ . The final gas products are then sent to the MS for analysis.....	14
Figure 9: TPO CO ₂ concentration curve for BM2 background soil.....	16
Figure 10: TPD CO ₂ concentration curve for BM2 background soil.....	17
Figure 11: TPO CO ₂ concentration curve for BM3 background soil.....	18
Figure 12: TPD CO ₂ concentration curve for BM3 background soil.....	19
Figure 13: TPO CO ₂ concentration curve for untreated (hydrocarbon-contaminated) GSC1AOS soil. 6 samples of varying masses are shown.....	20
Figure 14: TPD CO ₂ concentration curve for untreated (hydrocarbon-contaminated) GSC1AOS soil. 3 samples of varying masses are shown.....	21
Figure 15: TPO Devol CO ₂ concentration curve for untreated (hydrocarbon-contaminated) GSC1AOS soil. 3 samples of varying masses are shown.....	22
Figure 16: TPO CO ₂ concentration curve for electron beam treated (1000 kGy) GSC1AOS soil. 4 samples of varying masses are shown.....	23
Figure 17: TPD CO ₂ concentration curve for electron beam treated (1000 kGy) GSC1AOS soil. 3 samples of varying masses are shown.....	24
Figure 18: TPO Devol. CO ₂ concentration curve for electron beam treated (1000 kGy) GSC1AOS soil. 3 samples of varying masses are shown.	25
Figure 19: TPO CO ₂ concentration curve comparison of the untreated (hydrocarbon-contaminated) and treated (1000 kGy) GSC1AOS soil.....	26
Figure 20: TPD CO ₂ concentration curve comparison of the untreated (hydrocarbon-contaminated) and treated (1000 kGy) GSC1AOS soil.....	27
Figure 21: TPO Devol CO ₂ concentration curve comparison of the untreated (hydrocarbon-contaminated) and treated (1000 kGy) GSC1AOS soil.....	28
Figure 22: TPX carbon mass recovery results. Units are gram of carbon per gram of sample on a percentage basis. Values are averages and error bars are the standard deviation.	29

Figure 23: TPX CO ₂ concentration curves for the untreated (hydrocarbon-contaminated) SJV/BM1 soil. TC is shown in blue, MC is shown in yellow, FX is shown in green, and temperature is shown in red.	31
Figure 24: Untreated (hydrocarbon-contaminated) SJV/BM1 carbon mass recovery on a percentage basis. Values are averages and the errors are the standard deviation. TC is shown in blue, MC is shown in yellow, FX is shown in green, and the mass balance (sum of MC and FX) is shown in gray.	33
Figure 25: TPO CO ₂ concentration curve for incineration treatment of SJV/BM1 soil. .	35
Figure 26: TPX CO ₂ concentration curves for the thermal desorption treated SJV/BM1 soil. TC is shown in blue, MC is shown in yellow, FX is shown in green, and temperature is shown in red.	36
Figure 27: Thermal desorption treated SJV/BM1 carbon mass recovery on a percentage basis. Values are averages and the errors are the standard deviation. TC is shown in blue, MC is shown in yellow, FX is shown in green, and the mass balance (sum of MC and FX) is shown in gray.	37
Figure 28: TPX CO ₂ concentration curves for the pyrolysis treated SJV/BM1 soil. TC is shown in blue, MC is shown in yellow, FX is shown in green, and temperature is shown in red.	38
Figure 29: Pyrolysis treated SJV/BM1 carbon mass recovery on a percentage basis. Values are averages and the errors are the standard deviation. TC is shown in blue, MC is shown in yellow, FX is shown in green, and the mass balance (sum of MC and FX) is shown in gray.	39
Figure 30: Untreated (hydrocarbon-contaminated) SJV/BM1 MC and pyrolysis treated SJV/BM1 MC CO ₂ concentration curve comparison. Untreated is shown in black, pyrolysis is shown in green, temperature is shown in red, and 420°C is shown in yellow.	40
Figure 31: TPX CO ₂ concentration curves for the 456 kGy electron beam treated SJV/BM1 soil. TC is shown in blue, MC is shown in yellow, FX is shown in green, and temperature is shown in red.	41
Figure 32: 456 kGy electron beam treated SJV/BM1 carbon mass recovery on a percentage basis. Values are averages and the errors are the standard deviation. TC is shown in blue, MC is shown in yellow, FX is shown in green, and the mass balance (sum of MC and FX) is shown in gray.	42

Figure 33: TPX CO ₂ concentration curves for the 700 kGy electron beam treated SJV/BM1 soil. TC is shown in blue, MC is shown in yellow, FX is shown in green, and temperature is shown in red.	43
Figure 34: 700 kGy electron beam treated SJV/BM1 carbon mass recovery on a percentage basis. Values are averages and the errors are the standard deviation. TC is shown in blue, MC is shown in yellow, FX is shown in green, and the mass balance (sum of MC and FX) is shown in gray.	44
Figure 35: TPX CO ₂ concentration curves for the 1200 kGy electron beam treated SJV/BM1 soil. TC is shown in blue, MC is shown in yellow, FX is shown in green, and temperature is shown in red.	45
Figure 36: 1200 kGy electron beam treated SJV/BM1 carbon mass recovery on a percentage basis. Values are averages and the errors are the standard deviation. TC is shown in blue, MC is shown in yellow, FX is shown in green, and the mass balance (sum of MC and FX) is shown in gray.	46
Figure 37: TPX CO ₂ concentration curves for the 2200 kGy electron beam treated SJV/BM1 soil. TC is shown in blue, MC is shown in yellow, FX is shown in green, and temperature is shown in red.	47
Figure 38: 2200 kGy electron beam treated SJV/BM1 carbon mass recovery on a percentage basis. Values are averages and the errors are the standard deviation. TC is shown in blue, MC is shown in yellow, FX is shown in green, and the mass balance (sum of MC and FX) is shown in gray.	48
Figure 39: Electron beam dose dependence on the different types of carbon in each soil sample. TC is shown in blue, MC is shown in yellow, FX is shown in green, and the mass balance (sum of MC and FX) is shown in gray.	49
Figure 40: Corrected electron beam dose dependence on the different types of carbon in each soil sample. TC is shown in blue, MC is shown in yellow, FX is shown in green, and the mass balance (sum of MC and FX) is shown in gray.	51
Figure 41: TPO CO ₂ concentration curve for each treatment and untreated (hydrocarbon-contaminated) SJV/BM1 soil. Untreated is shown in black, incineration is shown in yellow, thermal desorption is shown in pink, pyrolysis is shown in green, electron beam treatments are shown in shades of blue decreasing in brightness with increasing dosage, and temperature is shown in red.	52
Figure 42: TPD CO ₂ concentration curve for each treatment and untreated (hydrocarbon-contaminated) SJV/BM1 soil. Untreated is shown in black,	

incineration is shown in yellow, thermal desorption is shown in pink, pyrolysis is shown in green, electron beam treatments are shown in shades of blue decreasing in brightness with increasing dosage, and temperature is shown in red.....	53
Figure 43: TPO Devol. CO ₂ concentration curve for each treatment and untreated (hydrocarbon-contaminated) SJV/BM1 soil. Untreated is shown in black, incineration is shown in yellow, thermal desorption is shown in pink, pyrolysis is shown in green, electron beam treatments are shown in shades of blue decreasing in brightness with increasing dosage, and temperature is shown in red.....	55
Figure 44: TC mass recovery percentage results for each treatment and untreated (hydrocarbon-contaminated) SJV/BM1 soil. Untreated is shown in black, incineration is shown in yellow, thermal desorption is shown in pink, pyrolysis is shown in green, and electron beam treatments are shown in shades of blue decreasing in brightness with increasing dosage.	57
Figure 45: MC mass recovery percentage results for each treatment and untreated (hydrocarbon-contaminated) SJV/BM1 soil. Untreated is shown in black, incineration is shown in yellow, thermal desorption is shown in pink, pyrolysis is shown in green, and electron beam treatments are shown in shades of blue decreasing in brightness with increasing dosage.	58
Figure 46: FX mass recovery percentage results for each treatment and untreated (hydrocarbon-contaminated) SJV/BM1 soil. Untreated is shown in black, incineration is shown in yellow, thermal desorption is shown in pink, pyrolysis is shown in green, and electron beam treatments are shown in shades of blue decreasing in brightness with increasing dosage.	59
Figure 47: TPX carbon mass recovery percentage results for each treatment and untreated (hydrocarbon-contaminated) SJV/BM1 soil. Untreated is shown in black, incineration is shown in yellow, thermal desorption is shown in pink, pyrolysis is shown in green, and electron beam treatments are shown in shades of blue decreasing in brightness with increasing dosage.	60
Figure 48: CO ₂ Calibration Graph	70
Figure 49: TPO CO ₂ concentration curve for untreated (hydrocarbon-contaminated) SJV/BM1 soil. 5 samples of varying masses are shown.	71
Figure 50: TPD CO ₂ concentration curve for untreated (hydrocarbon-contaminated) SJV/BM1 soil. 5 samples of varying masses are shown.	72

Figure 51: TPO Devol. CO ₂ concentration curve for untreated (hydrocarbon-contaminated) SJV/BM1 soil. 4 samples of varying masses are shown.....	72
Figure 52: TPO CO ₂ concentration curve for thermal desorption treated SJV/BM1 soil. 4 samples of varying masses are shown.	73
Figure 53: TPD CO ₂ concentration curve for thermal desorption treated SJV/BM1 soil. 2 samples of varying masses are shown.	73
Figure 54: TPO Devol. CO ₂ concentration curve for thermal desorption treated SJV/BM1 soil. 1 sample is shown.	74
Figure 55: TPO CO ₂ concentration curve for pyrolysis treated SJV/BM1 soil. 5 samples of varying masses are shown.	75
Figure 56: TPD CO ₂ concentration curve for pyrolysis treated SJV/BM1 soil. 5 samples of varying masses are shown.	76
Figure 57: TPO Devol. CO ₂ concentration curve for pyrolysis treated SJV/BM1 soil. 4 samples of varying masses are shown.	76
Figure 58: TPO CO ₂ concentration curve for 456 kGy electron beam treated SJV/BM1 soil. 5 samples of varying masses are shown.	77
Figure 59: TPD CO ₂ concentration curve for 456 kGy electron beam treated SJV/BM1 soil. 3 samples of varying masses are shown.	78
Figure 60: TPO Devol. CO ₂ concentration curve for 456 kGy electron beam treated SJV/BM1 soil. 3 samples of varying masses are shown.	78
Figure 61: TPO CO ₂ concentration curve for 700 kGy electron beam treated SJV/BM1 soil. 5 samples of varying masses are shown.	79
Figure 62: TPD CO ₂ concentration curve for 700 kGy electron beam treated SJV/BM1 soil. 5 samples of varying masses are shown.	80
Figure 63: TPO Devol. CO ₂ concentration curve for 700 kGy electron beam treated SJV/BM1 soil. 5 samples of varying masses are shown.	80
Figure 64: TPO CO ₂ concentration curve for 1200 kGy electron beam treated SJV/BM1 soil. 5 samples of varying masses are shown.	81
Figure 65: TPD CO ₂ concentration curve for 1200 kGy electron beam treated SJV/BM1 soil. 5 samples of varying masses are shown.	82

Figure 66: TPO Devol. CO₂ concentration curve for 1200 kGy electron beam treated SJV/BM1 soil. 5 samples of varying masses are shown.82

Figure 67: TPO CO₂ concentration curve for 2200 kGy electron beam treated SJV/BM1 soil. 5 samples of varying masses are shown.83

Figure 68: TPD CO₂ concentration curve for 2200 kGy electron beam treated SJV/BM1 soil. 5 samples of varying masses are shown.84

Figure 69: TPO Devol. CO₂ concentration curve for 2200 kGy electron beam treated SJV/BM1 soil. 6 samples of varying masses are shown.84

CHAPTER I

INTRODUCTION AND LITERATURE REVIEW

Hydrocarbons are used globally every day and their use spans many applications. One major application is internal combustion engines, which use liquid hydrocarbons (gasoline and diesel) in order to create energy for transportation or electricity. Gaseous hydrocarbons are used as fuel for heating, cooking, lighters, and electrical generation [1]. Other applications include solvents for cleaning, tar for roofing or road construction, oil paint, and lipstick, to name a few [1, 2]. Hydrocarbons are a necessity, but during their production and transportation, spills and leaks may contaminate the surrounding soil.

Soil contaminated with oil could originate from sludge ponds or spills [3-8]. Oil spills may occur during transport like the Exxon Valdez spill where a tanker struck a reef, tearing the hull open and releasing millions of gallons of oil into the environment [9]. Spills can also occur through natural seepages where oil below the ocean floor can leak into the ocean through cracks [10]. Oil tankers on highways or railroad cars may crash and contaminate the soil that way. Leaks and spills may also occur around drilling platforms.

Contamination of soil often results in contaminated ground water, foul aesthetics, and prevents vegetation from growing [5, 7, 11-14]. One study conducted at RICE University shows the effect of hydrocarbon contaminated soil on lettuce growth [15]. Lettuce plants were grown in clean and hydrocarbon contaminated soil. Clean soil allowed for lettuce to grow larger in magnitude than the lettuce grown in the

contaminated soil, which shows a direct effect that hydrocarbon contaminated soil has on plant growth.

Two types of remediation methods are currently in use: non-energetic and methods that involve energy addition. Non-energetic methods include bio-remediation, redistribution, landfarming, etc [6, 16-22]. These methods have difficulty in the removal of the heavier hydrocarbons [15]. This work focused on characterizing the efficacy and mechanisms of the methods that involve energy addition.

Four energy addition remediation methods will be characterized and quantified: incineration, thermal desorption, thermochemical decomposition by pyrolysis, and electron beam.

Incineration is the oxidation of the sample at elevated temperatures. This method should destroy all of the hydrocarbon content in the sample, but it will also likely destroy some of the carbon-containing organic nutrients required for growing vegetation [15]. Incineration is mainly used for waste disposal because it reduces mass and volume of waste [23-26]. Proper exhaust after treatments must be applied when using the incineration method to avoid emission of pollutants such as carbon monoxide and nitric oxides.

Thermal desorption occurs when the sample is heated in an inert environment in order to desorb the hydrocarbons off of the sample [8, 16, 27]. All of the carbon content will not be removed due to thermal desorption. Thermal desorption will only remove the mobile carbon (MC) content. MC is a portion of the total carbon (TC) content that is volatile, meaning it will desorb in an inert environment when the sample temperature

reaches or exceeds its boiling point temperature. The remainder of TC content is comprised of fixed carbon (FX) content. FX is carbon that is not volatile and includes extra heavy hydrocarbons and solid carbon or carbon black.

Incineration will remove the TC content on the sample, whereas thermal desorption will only remove the MC content leaving the FX content.

Pyrolysis is thermochemical decomposition of organic matter at elevated temperatures in the absence of an oxidizer, typically in an inert environment. The goal of this method is to change the chemical composition, dehydrogenating the hydrocarbons *in situ*. A portion of the MC content, mainly the lighter hydrocarbons, will be removed in the process as well, but the main goal is to create char [26, 28]. Char is created by the breaking of carbon-carbon bonds and carbon-hydrogen bonds so that new carbon-carbon bonds may be formed [28, 29].

Pyrolysis of hydrocarbons have been used in the past to create smaller paraffin's and olefins from saturated hydrocarbons and isomers and polymers from unsaturated hydrocarbons [30, 31]. Converting a heavy hydrocarbon to smaller hydrocarbons will be easier to remediate. Hydrocarbon pyrolysis kinetics will help determine the best pyrolysis method for remediation [32].

Electron beam remediation uses electrons as a radiation source to generate physical and chemical changes in various substances [33]. Different doses of radiation or energy levels, in terms of Grays (Gy), will be characterized. One gray is defined as the adsorption of one joule of radiation energy per one kilogram of matter.



Figure 1: Graphical representation of contaminated soil. The yellow layer is the MC content fraction. The black layer represents the FX content, which likely includes heavy hydrocarbons and carbon solid. The brown central region represents the soil matrix, often sand. This layer remains after incineration.

In order to characterize the effect of the remediation methods performed, both untreated and treated soil samples were analyzed for TC, MC, and FX content.

A graphical representation of the contaminated soil is shown in **Figure 1**. It can be seen that the soil sample has soil, which consists of minerals and sand, FX content, and MC content.

Temperature Programmed Reaction (TPX) experiments were used to determine the TC, MC, and FX content [34-39]. Three TPX's were used: Temperature Programmed Oxidation (TPO), Temperature Programmed Desorption with Supplementary Oxidation (TPD), and Temperature Programmed Oxidation on a Devolatilized sample (TPO Devol) [40].

CHAPTER II

EXPERIMENTAL METHODS

2.1 Remediation Methods

2.1.1 Incineration

Incineration is the process of combusting organic material. It can be accomplished in the laboratory by TPO, where the sample is exposed to an oxidizing flow at increasingly higher temperatures. **Figure 2** shows a simple representation of the incineration process, where heat is applied via a programmable furnace to the contaminated soil in the presence of an oxidizer, specifically 10% oxygen (O₂) in argon (Ar). The temperature profile is as follows: the sample is held at 50⁰C held for 5 minutes, followed by a 5⁰C per minute ramp to 650⁰C, where it is held for 30 minutes. Evolved gases are the products of combustion such as carbon monoxide (CO), water (H₂O), carbon dioxide (CO₂), and are monitored by a mass spectrometer (MS). To simplify the carbon balance, the product gases are converted to complete combustion products over an oxidation catalyst, so that only CO₂ is measured by the MS as a function of time (and therefore temperature) during the experiment. At the end of the process, barren soil is the product.

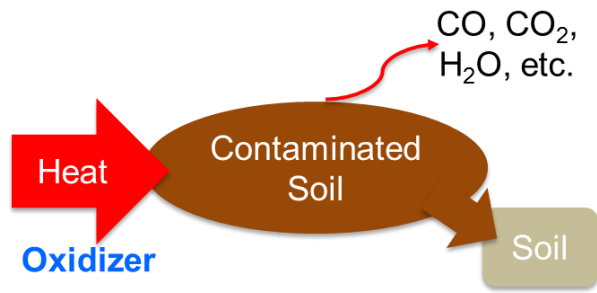


Figure 2: Graphical representation of the incineration process. Heat is applied via a programmable furnace to the contaminated soil in the presence of an oxidizer. Products of combustion are CO, CO₂, H₂O, etc. Contaminated soil is converted to a barren soil.

2.1.2 Thermal Desorption

Thermal desorption is heating the sample in an inert environment, so as to separate the hydrocarbons from the soil by volatility differences. The goal is the removal of the mobile hydrocarbon content, without combustion. In this process, it is possible that the hydrocarbons could be recovered in a secondary step. The fraction and identity of the hydrocarbons that can be removed in this manner depends on the maximum temperature the sample is exposed to. Generally, this method removes the light and medium hydrocarbons, defined as those that have boiling points below 650⁰C. The non-volatile fraction, also known as fixed carbon content, will remain. This fraction includes the elemental carbon (also known as black carbon) as well as the waxy organic carbons that have boiling points above the experimental temperature range.

Figure 3 is a graphical representation of the thermal desorption process, where heat is applied via a programmable furnace to the sample under an inert environment, specifically Ar. The goal for thermal desorption is to separate the volatile hydrocarbons from the non-volatile soil matrix. Experimentally, thermal desorption is accomplished

by flowing an inert gas, in this case Argon, over the sample during a specific temperature profile. The temperature profile is as follows: the sample is held at 50°C for 5 minutes, followed by a 5°C per minute ramp to 650°C where it is held for 30 minutes. The effluent will contain the devolatilized hydrocarbons, specifically those with a boiling point that is under the maximum temperature (650°C for this experiment). To quantify the hydrocarbons removed in this manner, the effluent hydrocarbons are converted in a secondary reactor, with added O₂. An oxidation catalyst is used to completely combust to CO₂ and water. A MS is used to measure the CO₂ concentration with time (temperature).

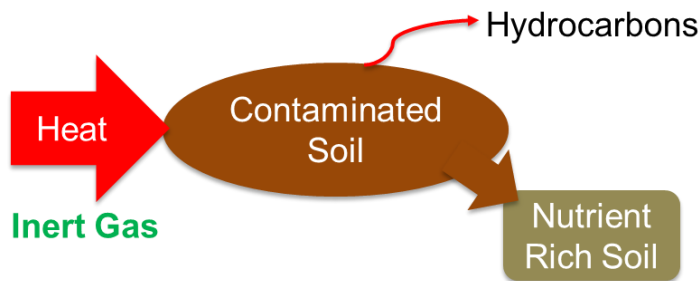


Figure 3: Graphical representation of the thermal desorption process. Heat is applied to the contaminated soil via a programmable furnace in an inert environment (in this case, Ar). A portion of the hydrocarbons will boil off of the sample leaving behind heavy hydrocarbons, carbon black, and soil.

2.1.3 Pyrolysis

Pyrolysis is thermochemical decomposition, usually carried out in an inert environment. Untreated soil is placed in a large tube furnace, heated to 420°C and held for 3 hours with nitrogen (N₂) flowing at a flow rate of 1 liter per minute through the sample. The goal of this treatment is to convert the hydrocarbons to char by breaking

the hydrogen and carbon bonds. Char has been shown to increase soil fertility, increase agricultural productivity, and can provide protection against some soil-borne diseases.

Figure 4 shows a simple diagram of the pyrolysis treatment, where heat is applied to achieve and maintain a constant temperature, 420 °C, in an inert environment. Light hydrocarbons, with a boiling point below the treatment temperature, will likely desorb. During the pyrolysis reaction, as the hydrocarbon bonds are broken and rearranged to form carbonaceous char, hydrogen (H₂) gas evolves.

Experimentally, the sample is packed between quartz wool plugs in a 2” diameter quartz tube, inserted in a tube furnace, heated to 420°C and held for 3 hours with N₂ flowing at a flow rate of 1 liter per minute through the sample.

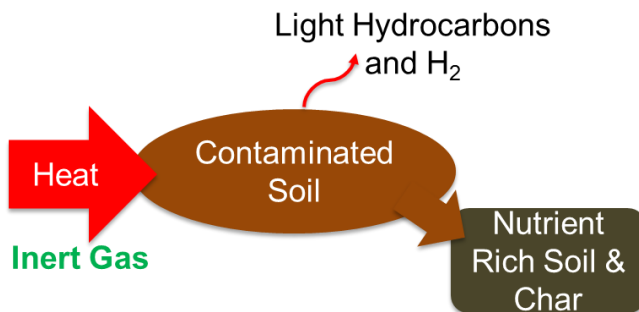


Figure 4: Graphical representation of the pyrolysis process. Heat is applied to the contaminated soil via a programmable tube furnace in an inert environment (in this case N₂). Light hydrocarbons will desorb and H₂ will evolve leaving behind soil and char.

2.1.4 Electron Beam

The electron beam treatment was conducted by Dr. Staack’s research group, the Plasma Engineering and Diagnostics Laboratory (PEDL) and performed at the National Center for Electron Beam Research at Texas A&M University (TAMU). Detailed

procedures for treatment can be found in [33]. Briefly, the sample is placed in an aluminum container for treatment. The samples are dosed with varying kGy levels of energy.

2.2 Characterization Methods

2.2.1 Microreactor

Characterization experiments were conducted in a fixed-bed flow-through microreactor, designed in the Combustion and Reaction Characterization Laboratory (CRCL) and shown in **Figure 5**. This two-stage system consists of two 0.5-inch diameter quartz u-tube reactors cells. Thermocouples are placed inside the u-tube so that measurements of the sample temperature can be recorded. Both reactor cells (the left which holds the sample and the right, which holds the oxidation catalyst) are heated by cylindrical, ceramic, radiant furnaces, which are placed around the reactors. A second thermocouple is used on the outside of the u-tube for feedback control of the furnace heater. Temperatures for the sample are recorded for data analysis. Reactor 1 (left) holds the sample under study and reactor 2 (right) holds a Pt/Al₂O₃ oxidation catalyst for complete conversion of the reactor 1 products. Products from reactor 1 will be sent to reactor 2 in order to convert any CO or remaining hydrocarbons to CO₂ for detection by the MS. Gas flow is metered by digital mass flow controllers (MKS instruments, Inc. Andover, MA) from compressed gas bottles. CO₂ content was measured with a quadrupole mass spectrometer (HIDEN QGA), which was regularly calibrated with 3.5vol%, 3.0vol%, 2.5vol%, 2.0vol%, 1.5vol%, 1.0vol%, 0.5vol%, and 0.25vol% CO₂.



Figure 5: Microreactor Solidworks model. Gas input is on the left. Reactor 1 (sample location) and reactor 2 (oxidation catalyst location) are shown by the glass tubes just above the white, cylindrical, temperature controlled furnaces. Gas output is shown on the right.

2.2.2 CO₂ Calibration Procedure

A Hiden Analytical Quantitative Gas Analysis (QGA) MS was used to analyze the partial pressure of CO₂. In order to increase the accuracy of the TPX results, CO₂ calibrations were performed monthly. A flow of 175 standard cubic centimeters per minute (sccm) with Ar as a carrier gas and with varying concentrations of CO₂ was used during the calibration. 3.5vol% of CO₂ is the first step and this concentration is held till a flat baseline is obtained. The concentration is then decreased by 0.5vol% until a new baseline is attained. This process is repeated until the concentration is 0.5vol% CO₂. At this point, the concentration is decreased to 0.25vol% and held until a baseline is obtained. The baseline of 0vol% of CO₂ is obtained at the beginning of each TPX experiment. Appendix A is an example of the CO₂ calibration graph.

2.2.3 Sample Packing

Quartz wool was used to create a gas permeable plug at the bottom of the tube to prevent the solid sample from flowing out of the tube. Zirconium Oxide beads of 1 millimeter (mm) diameter are mixed with the sample for thermal stability throughout the bed. Sample sizes were kept close to 200 milligrams (mg). Another quartz wool plug was inserted atop the sample to prevent gas line contamination in the rare event of backflow.

2.2.4 Temperature Programmed Reactions

TPX was used to analyze the different remediation methods. The three TPX experiments that were used to determine the effectiveness of the remediation methods are TPO, TPD, and TPO Devol.

These experiments allowed for the determination of the TC, MC, and FX content of the sample. Each experiment used the same temperature profile: a 5-minute hold at 50°C, followed by a 5°C per minute ramp to 650°C where the sample was held for 30 minutes. Partial pressure of CO₂ measured by the MS was recorded during all of the TPX experiments and was converted to concentration using the CO₂ calibration. In each experiment, the measured CO₂ trace can be integrated to find the total amount of CO₂ evolved. This value was used to find the total amount of carbon that came off of the sample in the experiment.

2.2.4.1 Temperature Programmed Oxidation

TPO flows 10% O₂ in Ar directly over the sample in reactor 1, where combustion occurs. Products of combustion are then sent to reactor 2, the oxidation catalyst, to

convert any CO to CO₂. TC content in the original sample can be found by measuring the amount of CO₂ that came off of the sample. **Figure 6** shows the gas flow path for the TPO experiment.

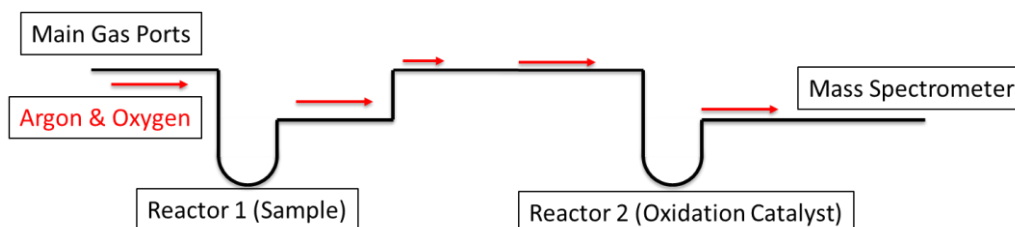


Figure 6: Diagram of the gas flow path for a TPO experiment. A gas mixture of 10% (by volume) O₂ and Ar flow over the sample in reactor 1, where combustion occurs. Gas products are sent to the oxidation catalyst in reactor 2 in order to convert any CO to CO₂. The final gas product is then sent to the MS for analysis.

2.2.4.2 Temperature Programmed Desorption

TPD solely flows inert Ar over the sample. The increasing temperature causes mobile hydrocarbons, those with boiling points at or below the sample temperature, to volatilize off of the sample during the temperature profile. The effluent mixture from reactor 1 was mixed with O₂ right before the oxidation catalyst to completely combust the hydrocarbons, and CO₂ concentration was measured by the MS, allowing for the calculation of the MC content of the sample. **Figure 7** shows the gas flow path for the TPD experiment.

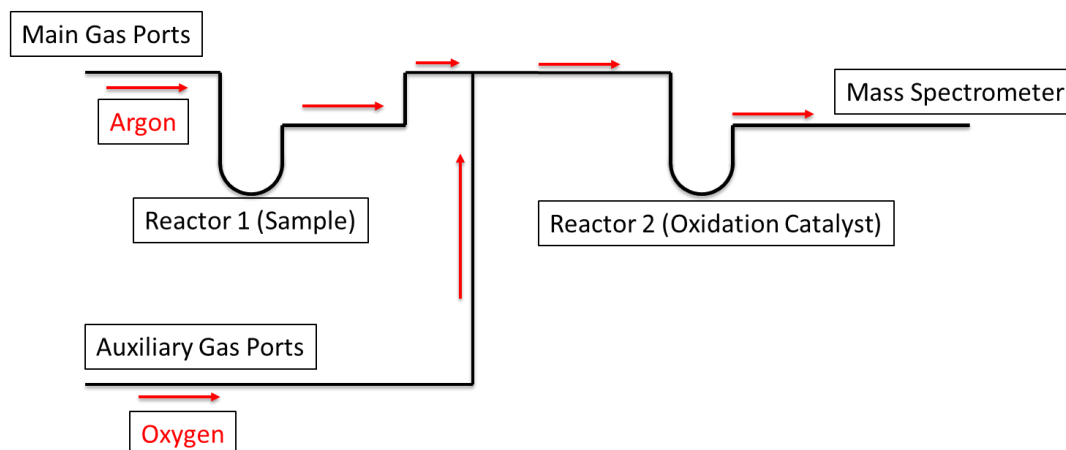


Figure 7: Diagram of gas flow path for a TPD experiment. Ar flows over the sample in reactor 1 and is heated by a temperature controlled furnace. Hydrocarbons with boiling points below the sample temperature will volatilize off of the sample and be sent to a junction right before reactor 2. This junction will add O₂ to the mixture and then be sent to the oxidation catalyst in reactor 2. Hydrocarbons and O₂ will react to make CO₂ and H₂O. Products are then sent to the MS for analysis.

2.2.4.3 Temperature Programmed Oxidation on a Devolatilized Sample

TPO Devol is a TPO experiment on a sample that has been through a TPD, which should only have the fixed (non-mobile) carbon fraction (containing waxy, heavy hydrocarbons and any solid carbon) remaining. It follows the same procedures as the TPO experiment described in 2.2.4.1. Results from this experiment allow for the calculation of the FX content of the sample. **Figure 8** show the gas flow path for a TPO Devol experiment.

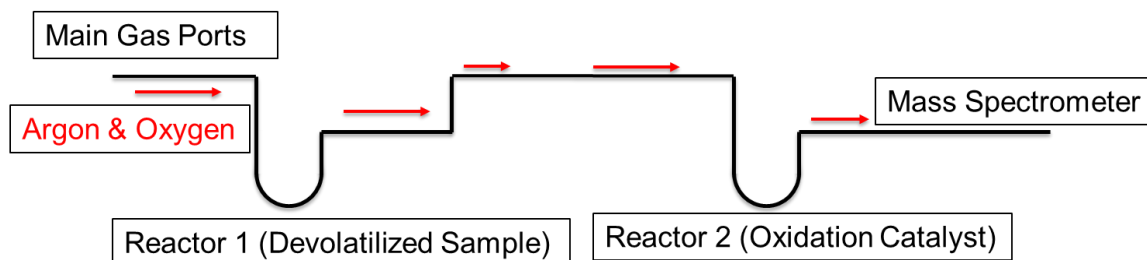


Figure 8: Diagram of TPO Devol gas flow path. A gas mixture of 10% (by volume) O₂ and Ar flow over a devolatilized sample located in reactor 1, where heat is added via a temperature controlled furnace. Products are then sent to the oxidation catalyst located at reactor 2 to convert any CO to CO₂. The final gas products are then sent to the MS for analysis.

CHAPTER III

RESULTS AND DISCUSSION

3.1 Background Soils

Background soils are samples of clean soil that are taken from locations near the contamination site but are not themselves hydrocarbon contaminated. Characterization of these soil samples will help determine how much carbon content in the sample came from the original soil. TPX characterization of two background soils will be discussed.

3.1.1 BM2

Both TPO and TPD experiments were conducted for the BM2 soil sample. Results from both experiments show insignificant levels of carbon recovery. A TPO Devol test was not performed because the results would have been insignificant. **Figure 9**, shown below, is the TPO plot for the BM2 background soil. The total carbon mass recovered is 0.71% in the uncontaminated soil. This value is significantly lower than the contaminated soil results, which are shown in later sections.

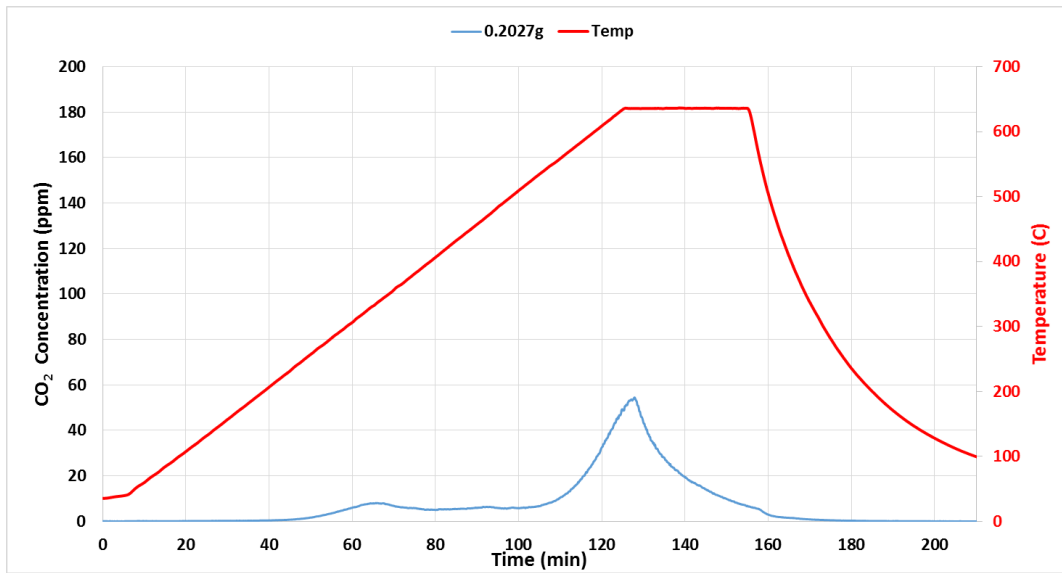


Figure 9: TPO CO₂ concentration curve for BM2 background soil.

Figure 10 is the TPD plot for the BM2 background soil sample. Mobile carbon mass recovered is 0.83%. It is interesting to note that the mobile fraction was measured to be higher than the total carbon mass, because the mobile carbon as measured by TPD should be a fraction of the total carbon measured by TPO. This discrepancy may be explained by the error tolerance of the experiments since the low percentage values are more sensitive to change in sample size.

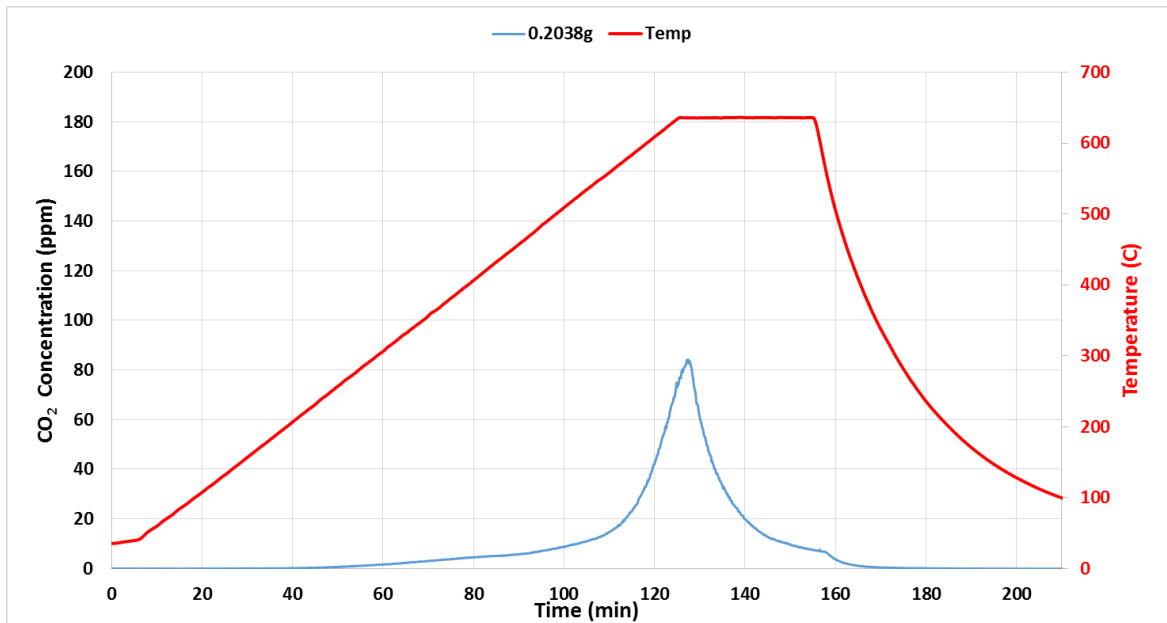


Figure 10: TPD CO₂ concentration curve for BM2 background soil.

3.1.2 BM3

Characterization by TPO and TPD was conducted on the BM3 background soil.

Figure 11, shown below, is the TPO result for the BM3 background soil. The total carbon mass recovered is 0.29%. This value is very low and in fact, negligible compared to the contaminated soil values, which are shown in later sections.

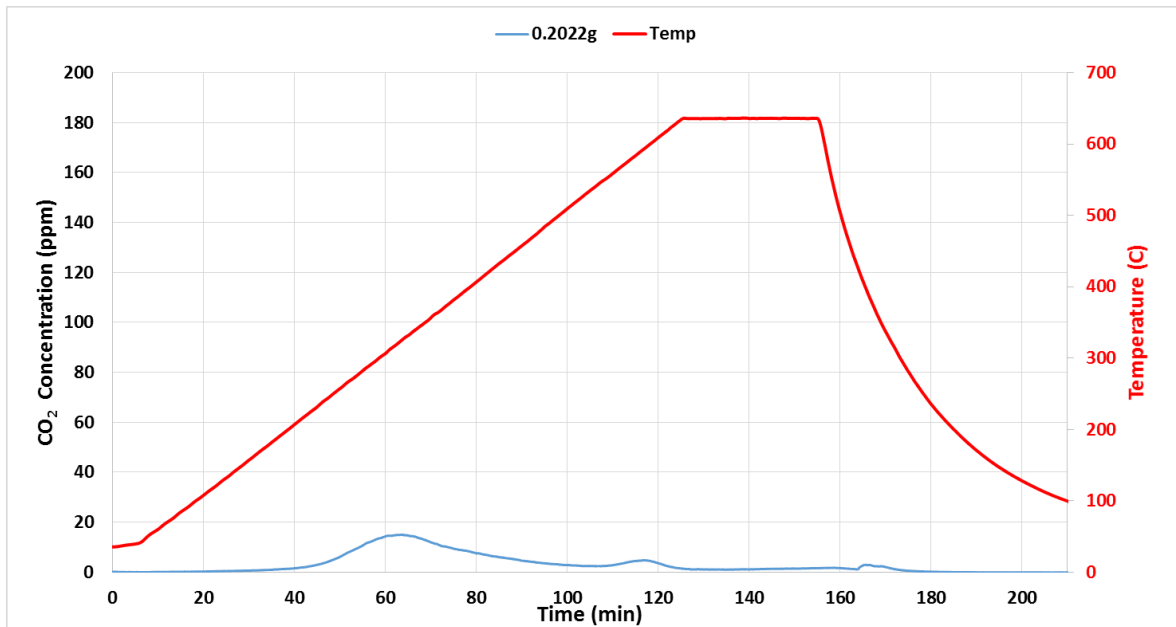


Figure 11: TPO CO₂ concentration curve for BM3 background soil.

Lastly, **Figure 12** shows the TPD plot for the BM3 background soil. The mobile carbon mass recovered is 0.28%. This value is lower than the TPO value, which is expected.

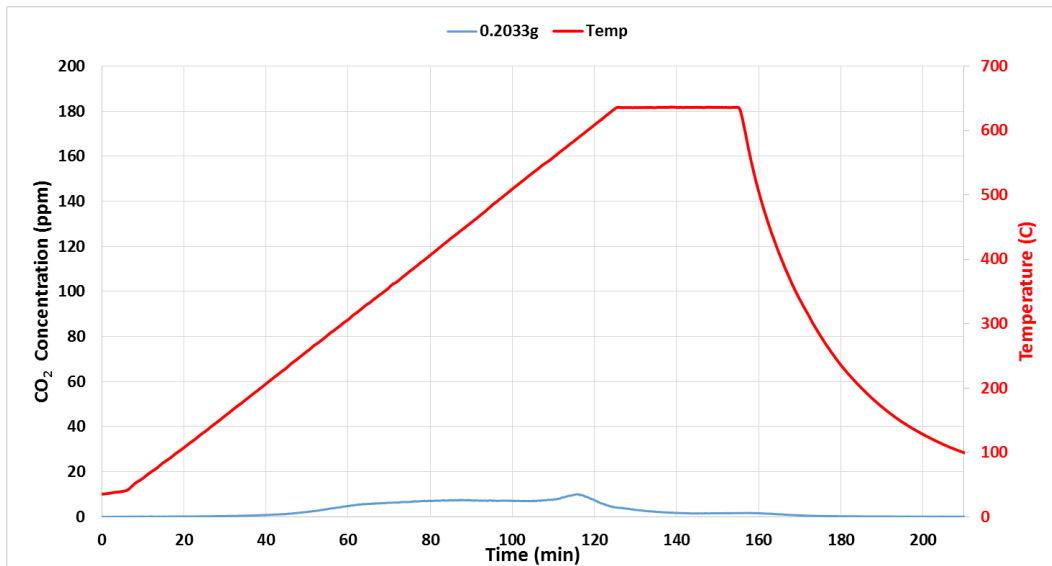


Figure 12: TPD CO₂ concentration curve for BM3 background soil.

Results from the background soils show that naturally occurring carbon content in the soils is very low and realistically negligible compared to the content coming from the hydrocarbon contamination. Therefore, while incineration is destroying some organic content in the soil, the carbon fractions measured in the experiments reported in this work can be attributed to the contaminating hydrocarbons.

3.2 GSC1AOS (Preliminary Results)

The following results are based on the first soil sample characterized for proof-of-concept for the electron beam method, GSC1AOS. A sweep of TPX experiments were conducted on the untreated sample and an electron beam treated (1000 kGy) sample in order to show changes in the hydrocarbon content.

3.2.1 Untreated (GSC1AOS)

Figure 13, shows CO₂ concentration versus time curves from replicated TPO experiments for the untreated (hydrocarbon-contaminated) soil.

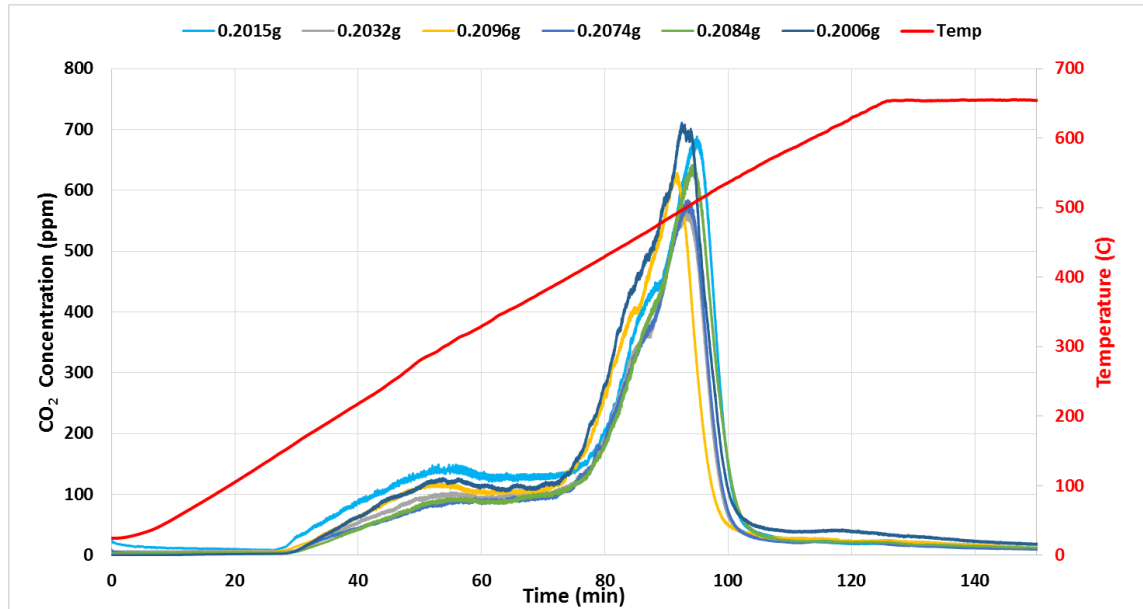


Figure 13: TPO CO₂ concentration curve for untreated (hydrocarbon-contaminated) GSC1AOS soil. 6 samples of varying masses are shown.

The graph shown above has two axes: CO₂ concentration in ppm vs. time (left axis) and temperature vs. time (right axis). At the top of the graph, the legend is shown for the different curves and is separated by sample mass size. Six sample sizes were tested and the final curve, shown in red, is the temperature curve.

The figure clearly shows that all of the samples have the same general CO₂ profile. At the beginning of the temperature ramp, the CO₂ baseline remains constant. This implies that any hydrocarbons that are on the sample are not reacting with the O₂. Once the temperature reaches around 150°C, the CO₂ concentration begins to increase, indicating that reaction is occurring. The CO₂ concentration begins to increase rapidly

around 375°C and peaks around 475°C. The concentration then decreases after this peak eventually returning to the baseline as the sample is consumed.

Figure 14 is the concentration versus time graph of the untreated sample for a TPD experiment. This concentration is the portion of the sample that is mobile carbon content. It shows that the concentration does not go to the baseline at 150 minutes even though baseline is reached at a later time.

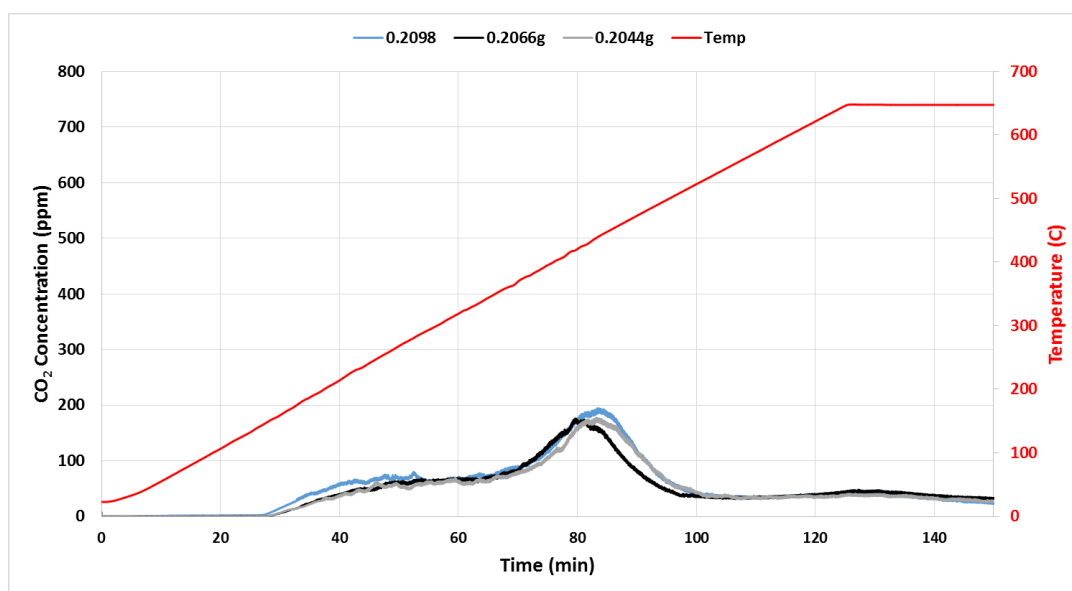


Figure 14: TPD CO₂ concentration curve for untreated (hydrocarbon-contaminated) GSC1AOS soil. 3 samples of varying masses are shown.

Figure 15 shows the CO₂ concentration versus time curves for the untreated TPO Devol, which is a TPO experiment on a sample that has previously undergone a TPD. The carbon mass that is oxidized in this sample is considered to be the fixed portion of the nascent (untreated) sample, representing heavy, waxy hydrocarbons with boiling points above 650°C and elemental carbon. The peak at around 425°C is notable for later comparison.

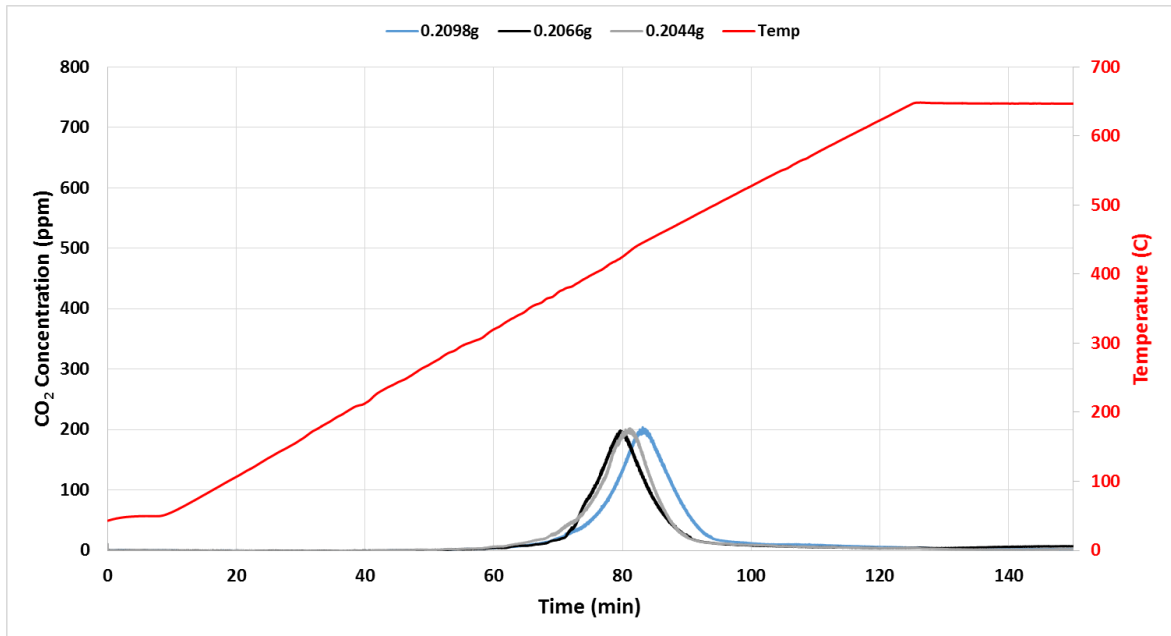


Figure 15: TPO Devol CO₂ concentration curve for untreated (hydrocarbon-contaminated) GSC1AOS soil. 3 samples of varying masses are shown.

3.2.2 1000 kGy

Figure 16, below, shows the CO₂ concentration versus time plots for TPO experiments on the electron beam treated soil. Comparing this graph to **Figure 13**, it can be seen that the initial “peak” in CO₂ concentration in the 300°C-400°C temperature range is no longer present. The E-beam treatment removed at least a portion of the mobile carbon content. There remains a peak in the CO₂ concentration that occurs at around 480°C, showing that not all of the hydrocarbon content was removed by the electron beam treatment.

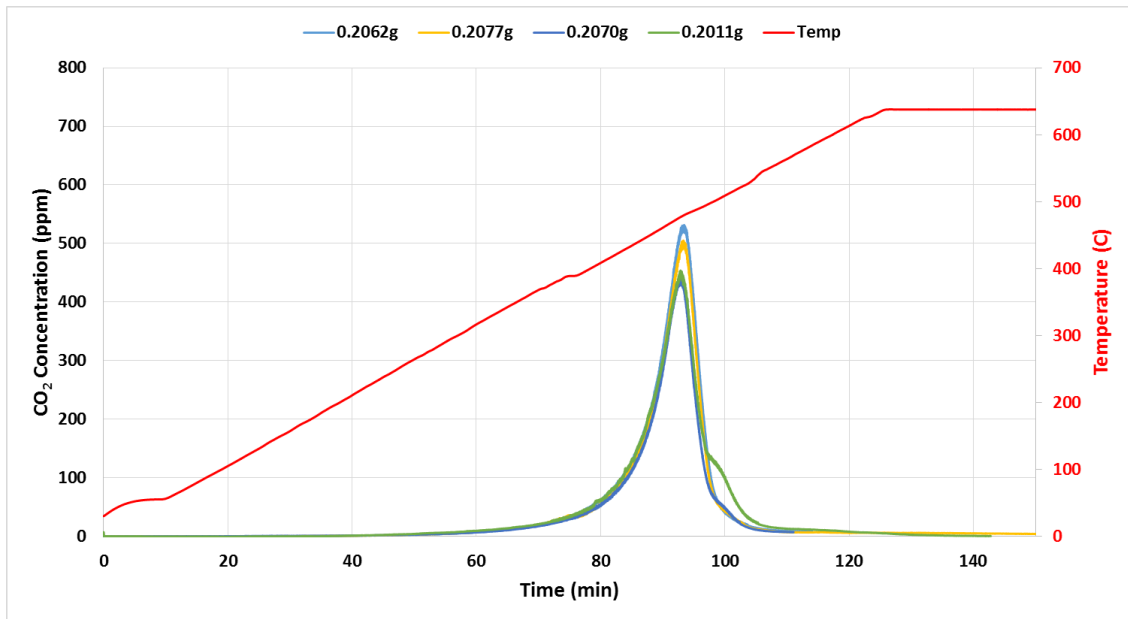


Figure 16: TPO CO₂ concentration curve for electron beam treated (1000 kGy) GSC1AOS soil. 4 samples of varying masses are shown.

Figure 17, shown below, is the TPD experiment CO₂ concentration versus time plots for the E-Beam treated soil. It can be seen that there is a slight bump at around 80 minutes. The slight bump would result in minor amounts of mobile carbon content, which will be quantified in a later section.

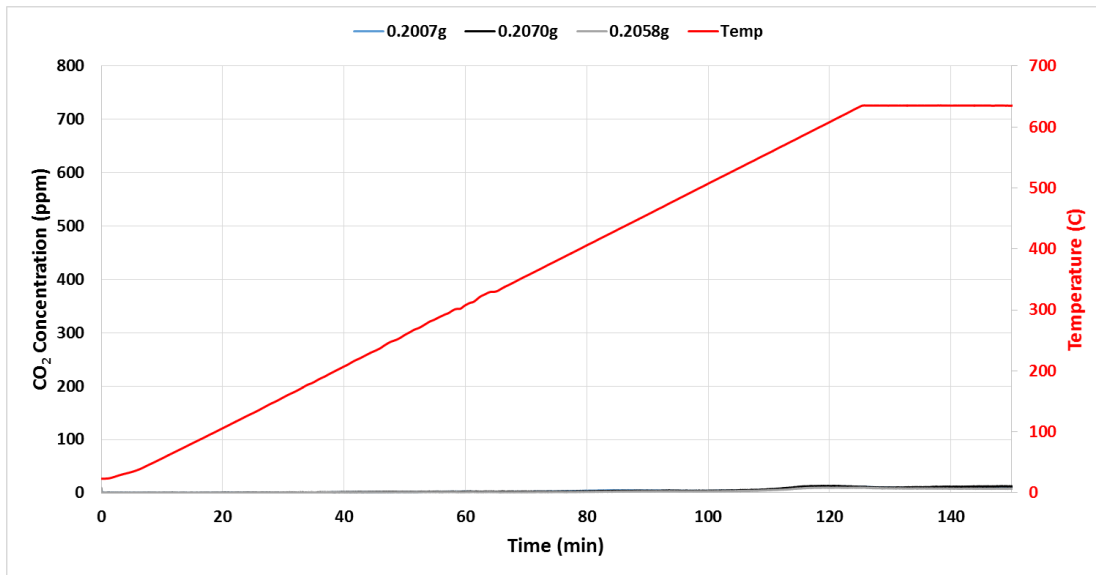


Figure 17: TPD CO₂ concentration curve for electron beam treated (1000 kGy) GSC1AOS soil. 3 samples of varying masses are shown.

Figure 18, shows the CO₂ concentration versus time plots for the TPO experiments on the previously devolatilized E-Beam treated samples, known as TPO Devol experiments. The plot shows that the early time peaks that we associated with the mobile carbon fraction is missing and that the peak concentration occurs around 475°C. This plot represents the removal of the remaining FX fraction from the sample.

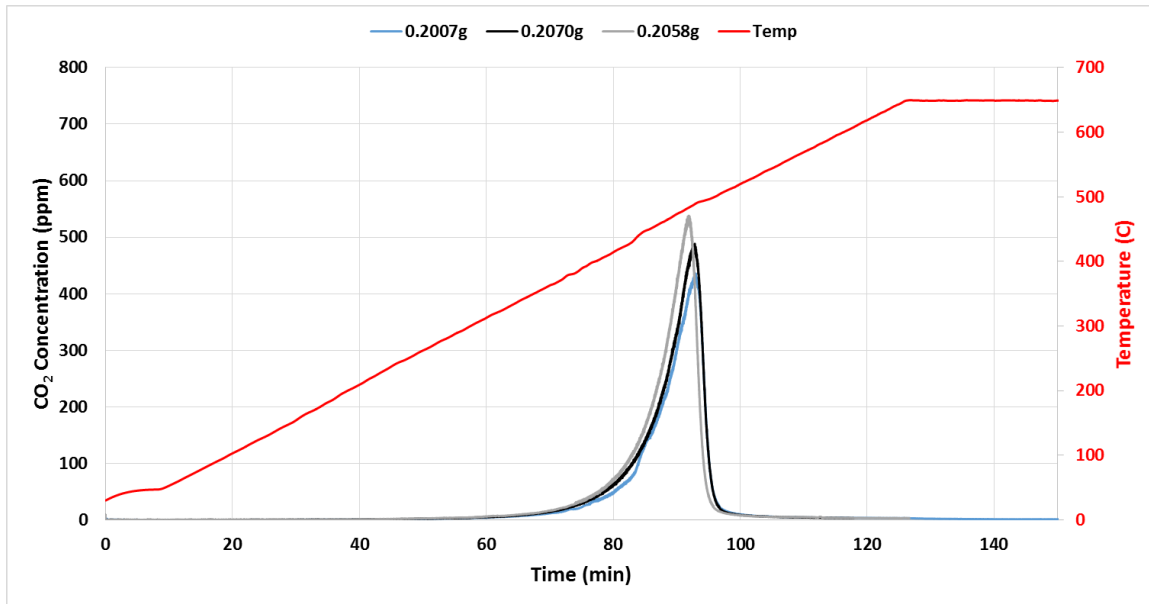


Figure 18: TPO Devol. CO₂ concentration curve for electron beam treated (1000 kGy) GSC1AOS soil. 3 samples of varying masses are shown.

3.2.3 Comparison of Treated and Untreated Samples (GSC1AOS)

CO₂ calibration is done regularly and is used to convert the partial pressure of CO₂ and Ar measured by the MS into concentrations of CO₂ for the temperature programmed experiments.

Multiple TPX replicate experiments were conducted for each sample to investigate both the reproducibility of the result and the sample variation. Since the samples were taken from real contamination sites, they were not homogeneous and some amount of variability was expected and seen.

Based on the TPO and TPD plots shown previously and from the comparison of the treated and untreated samples, we can identify the first, smaller peak in **Figure 19** at around 40 minutes for the untreated sample represents the mobile carbon content. It can

also be seen in the figure that, because the area under the curve for the untreated sample is greater than that of the treated sample, the untreated sample has more TC content than the treated sample.

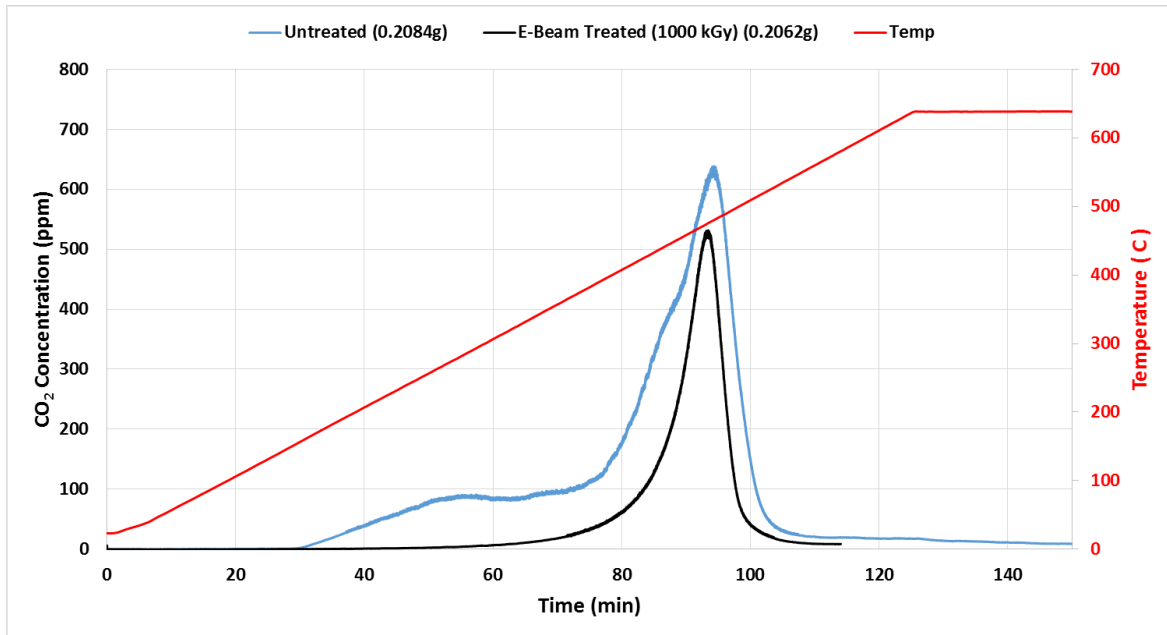


Figure 19: TPO CO₂ concentration curve comparison of the untreated (hydrocarbon-contaminated) and treated (1000 kGy) GSC1AOS soil.

Figure 20 shows the comparison of the CO₂ concentration versus time curves of the TPD experiments for the treated and untreated GSC1AOS soil samples.

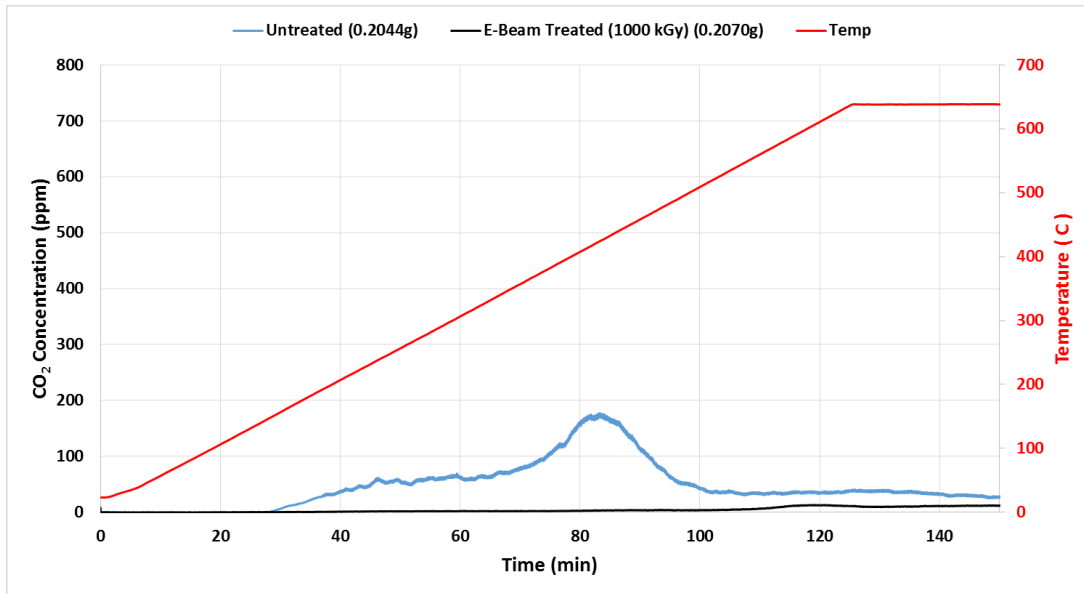


Figure 20: TPD CO₂ concentration curve comparison of the untreated (hydrocarbon-contaminated) and treated (1000 kGy) GSC1AOS soil.

The comparison of the TPD experiments, which are used to measure the mobile content, verifies that the initial smaller peak is the mobile carbon content. The untreated sample has mobile carbon content where the treated sample has virtually none. **Figure 21**, shown below, compares the FX fractions of the treated and untreated soil samples as measured by TPO Devol experiments.

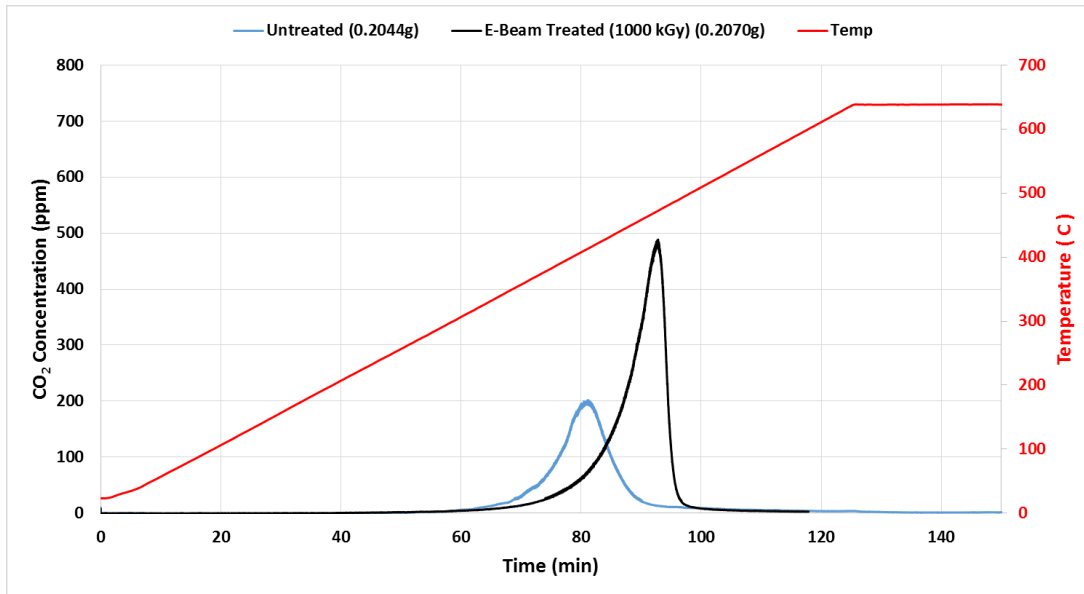


Figure 21: TPO Devol CO₂ concentration curve comparison of the untreated (hydrocarbon-contaminated) and treated (1000 kGy) GSC1AOS soil.

The TPO Devol comparison of the treated and untreated samples, shows that there is significantly more fixed carbon content on the treated sample as well as a shift in the peak. This shift is both in temperature and in magnitude, indicating that additional elemental carbon has been created in the sample, likely by thermochemical conversion of the hydrocarbons into elemental carbon.

Multiple experiments were repeated to ensure high quality results and define the experimental error. **Figure 22** compares the carbon mass recovery results from integrating the concentration curves on a percentage of the sample mass basis. It shows the TC content and calculates the sum of the measured mobile and fixed fractions, which are nearly identical to the TC content as measured by TPO, demonstrating that the overall mass balance on the carbon is closed in these experiments.

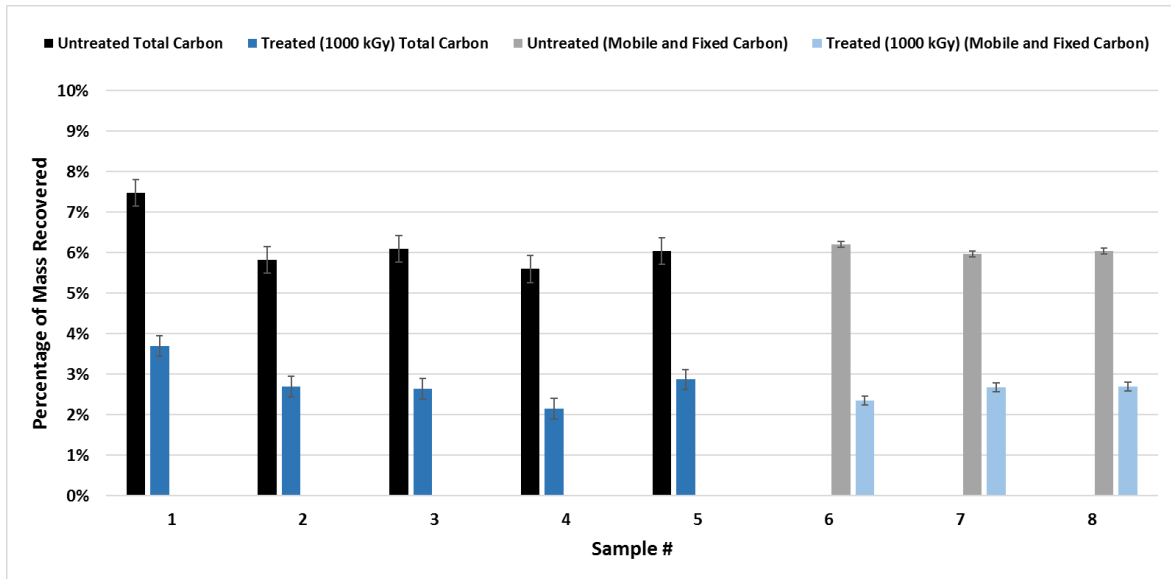


Figure 22: TPX carbon mass recovery results. Units are gram of carbon per gram of sample on a percentage basis. Values are averages and error bars are the standard deviation.

It can be seen that the replicate TPO results (samples 1-5) for both soil samples are on average close to the same value. Samples 6-8 are the recovery percentages summed from the TPD and the TPO Devol experiments to show continuity as their totals are nearly identical to the total measured directly by TPO.

Table 1 is a summary of the carbon mass recovery percentage results.

Table 1: Carbon mass recovered as a percentage of sample mass (GSC1AOS)

TPX Type	(g of C from CO ₂)/(g of sample) %	
	Untreated	E-Beam Treated (1000 kGy)
TC	6.21	2.81
MC	4.24	0.32
FX	1.83	2.26
Sum of MC and FX	6.07	2.58

Approximately 68% of the carbon content in the untreated soil is mobile carbon content. E-beam treatment removes about 55% of the total carbon content on the sample. 88% of the carbon content that is remaining on the E-Beam treated samples is fixed carbon content. Since a majority of the carbon content on the untreated soil is mobile carbon content and a majority of the carbon content on the E-Beam treated soil is fixed carbon content, it can be said that the electron beam is effective at removing some of the mobile carbon content and converting a portion of the mobile carbon content to fixed carbon content.

3.3 SJV/BM1

SJV/BM1 is the first soil sample that we received sufficient quantities of to compare multiple remediation methods. The GSC1AOS soil sample results were used as proof of the usefulness of our characterization tools for comparing remediation methods. Representative plots of each experiment will be presented in this section in order to show the shape of the curve for each TPX experiment. Replicate results can be seen in Appendix B-Appendix H.

3.3.1 Untreated (SJV/BM1)

The untreated soil sample was dried at 100⁰C for 30 minutes in order to remove any water in the soil. TPX experiments were then conducted on sample sizes of approximately 200 mg. **Figure 23** is an overlay plot of the TPX experimental CO₂ concentration curves for the untreated SJV/BM1 soil sample.

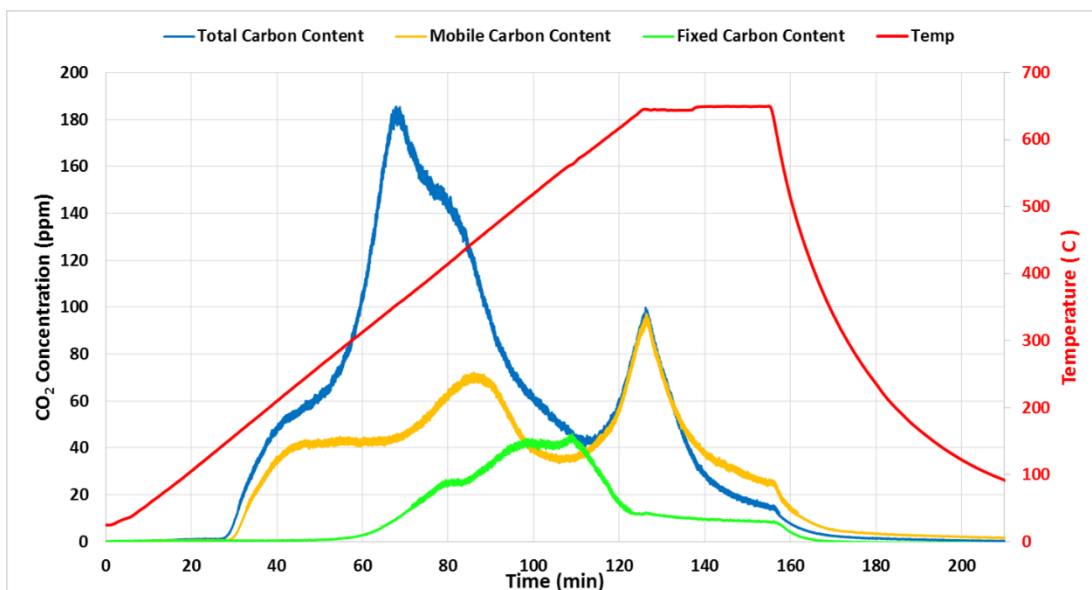


Figure 23: TPX CO₂ concentration curves for the untreated (hydrocarbon-contaminated) SJV/BM1 soil. TC is shown in blue, MC is shown in yellow, FX is shown in green, and temperature is shown in red.

Each of the overlay graphs for the TPX experiments have the same structure: the x-axis is the time in minutes, the left y-axis is the concentration of CO₂ in ppm and the right y-axis is the temperature of the sample in degrees Celsius (°C). As the legend shows, the temperature line is in red, and each type of carbon in the sample is given a different color: blue for TC (TPO), yellow for MC (TPD) and green for FX (TPO Devol). All sample sizes were kept equivalent to one another so the graphs need not be normalized and mass recovery analysis will yield the normalized results. The temperature profile for the TPX reactions is over after the 30-minute soak at 650°C but graphs are shown after this time to recover the baseline. Integration of the CO₂ concentration curve yields the total amount of CO₂ that came off of the sample for that

experiment, which is then used to find the total amount of carbon that was on the sample.

The TC content curve, shown in blue in **Figure 23**, shows that CO₂ formation (indicative of combustion) begins at around 30 minutes (150°C) and starts to increase rapidly until it peaks at 68 minutes where it reaches 180 ppm (350°C). After the initial small peak, the curve dips to a trough at 40 ppm and 110 minutes (575°C). After the trough, the curve increases rapidly again, to a peak of 100 ppm at 125 minutes (650°C). After the second peak, the curve returns to baseline. Integration of this curve yields the total carbon content of the sample. It is worth noting that the concentration axis for the SJV/BM1 samples are 0 to 200 ppm where the GSC1AOS is 0 to 800 ppm – however, these were dissimilar samples, from different locations and contaminated by different hydrocarbons – so they were not expected to be similar.

The MC content, shown in yellow in **Figure 23**, is the CO₂ concentration curve for the TPD experiment. CO₂ formation begins at around 30 minutes (150°C) with 3 peaks occurring in the trace at 50 ppm at 42 minutes (220°C), 80 ppm at 85 minutes (445°C), and 100 ppm at 125 minutes (650°C), respectively. Integration of this curve yields the MC content on the sample.

FX content, shown in green in **Figure 23**, shows the TPO Devol plot for the untreated soil sample. CO₂ begins to form at 60 minutes (305°C) and starts to increase till it reaches a small plateau at 25 ppm (400°C), which occurs for about 5 minutes (until 425°C). After the initial plateau, it begins to increase again, more rapidly this time, to another plateau at 40 ppm (505°C), which lasts for 15 minutes (until 560°C). After the

second plateau, the curve returns to baseline. Integration of this curve yields the FX content on the soil sample.

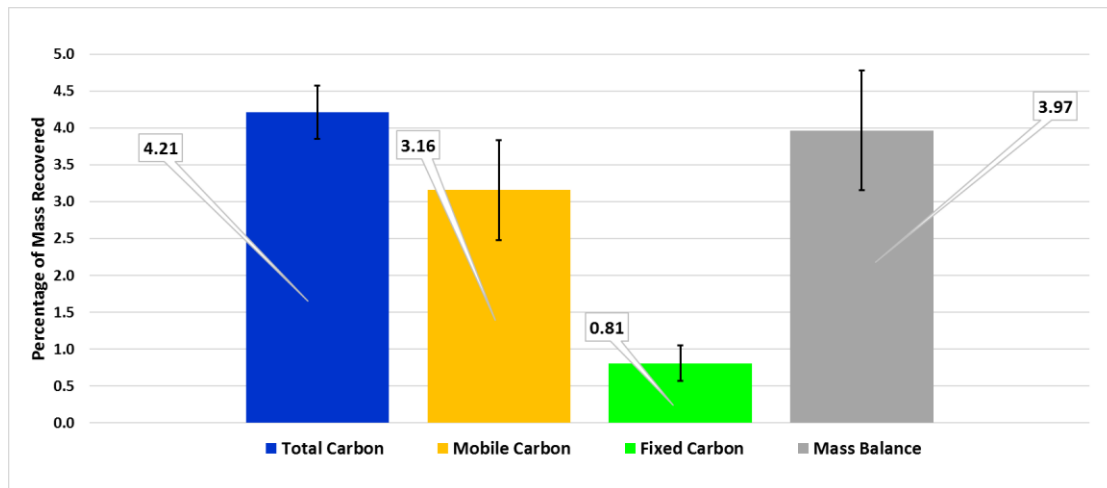


Figure 24: Untreated (hydrocarbon-contaminated) SJV/BM1 carbon mass recovery on a percentage basis. Values are averages and the errors are the standard deviation. TC is shown in blue, MC is shown in yellow, FX is shown in green, and the mass balance (sum of MC and FX) is shown in gray.

Figure 24 is a bar graph of the mass recovery results from the integrated curves for the TPX experiments. These values are a ratio of carbon mass to sample mass on a percentage basis. Results shown are averages and the error bars represent a single standard deviation. The y-axis is the percentage of the sample mass burned or recovered as CO₂ as measured by the MS. Four bars are shown: Total Carbon, Mobile Carbon, Fixed Carbon, and Calculated Mass Balance (sum of the Mobile and Fixed Carbon fractions, which is nearly equal to the Total Carbon) are displayed in blue, yellow, green, and gray, respectively. Graphs in the later sections will have this same structure.

Approximately 75% of the total carbon content on the untreated sample is mobile carbon and 25% is fixed carbon. It can be seen that the mass balance is closed by summation of the mobile and fixed fractions, as expected.

3.3.2 Incineration

It is known that incineration will remove all of the hydrocarbon content by completely combusting any carbon in the sample, therefore it is not necessary to try to understand the mechanism by which the carbon is removed – or which fraction is affected by this remediation method. It is noteworthy that the TPO experiment which has been used in the characterization studies to evaluate the total carbon is one way of accomplishing the incineration method. In order to verify that the method does remove all of the combustible hydrocarbon content, an untreated sample was run through two consecutive TPO experiments. The first one represents the incineration method of remediation and the second one is the TPO characterization results from the incinerated sample.

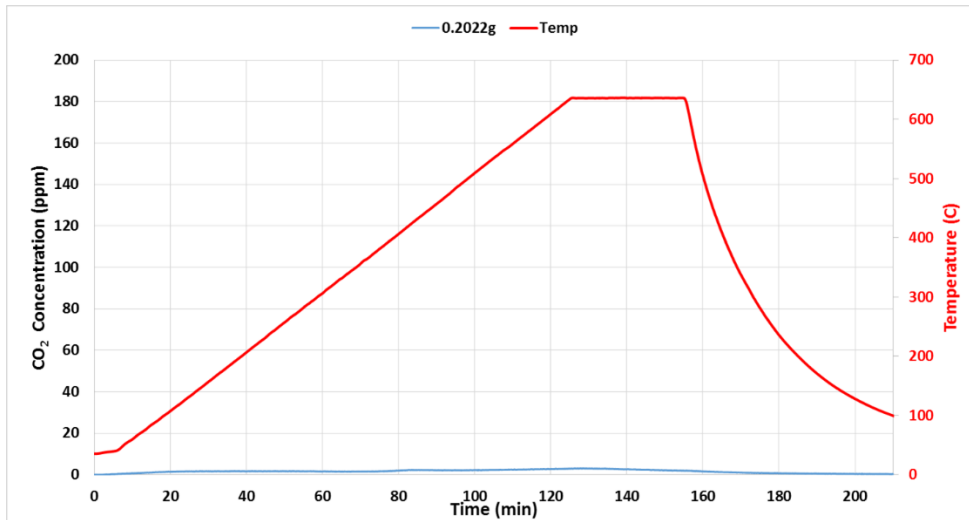


Figure 25: TPO CO₂ concentration curve for incineration treatment of SJV/BM1 soil.

Figure 25 shows the CO₂ concentration curve of a TPO experiment for an incinerated sample of the SJV/BM1. It can be seen that there is almost no carbon recovered from the sample. Due to the very little amount of carbon on this sample, no further TPX experiments were conducted, as there was no mobile or fixed carbon remaining to measure.

3.3.3 Thermal Desorption

Industrially, Thermal Desorption (TD) is done by heating the sample with the hot exhaust gas from a combustion source. This exhaust gas can have residual oxygen remaining and therefore there is the possibility for some combustion to occur. This would cause a mixed mechanism for remediation that would be difficult to understand fundamentally, so for this work, we only considered the desorption mechanism by running our TD under inert conditions.

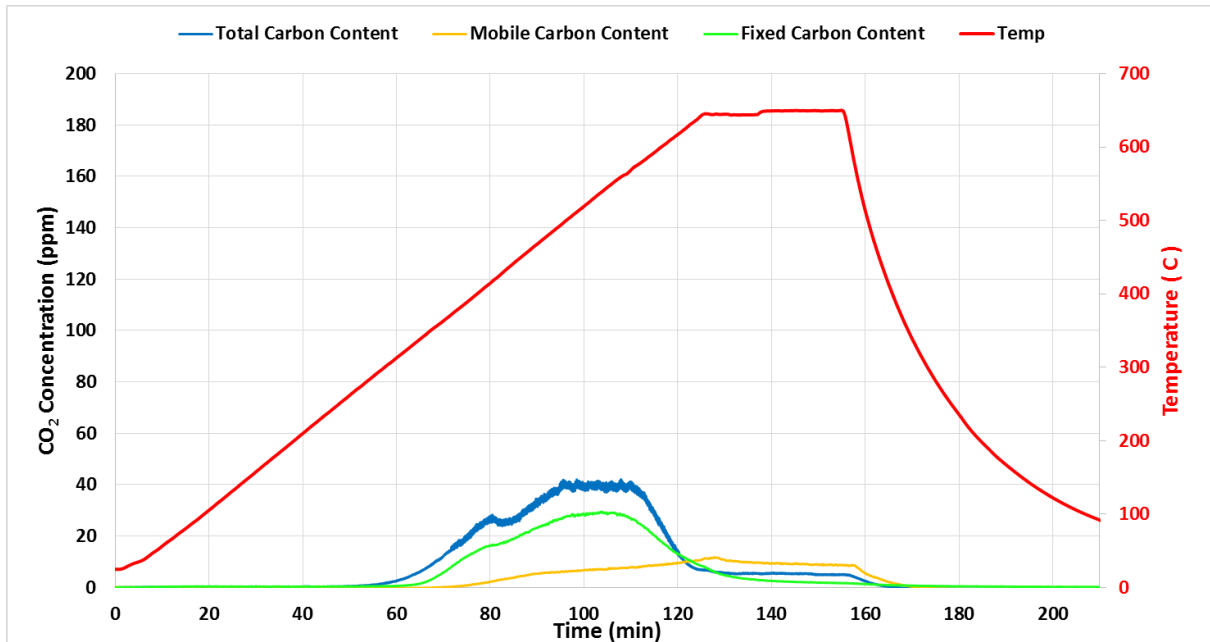


Figure 26: TPX CO₂ concentration curves for the thermal desorption treated SJV/BM1 soil. TC is shown in blue, MC is shown in yellow, FX is shown in green, and temperature is shown in red.

Figure 26 is the TPX overlay plot for the thermal desorption remediation method. Total carbon content, shown in blue, and fixed carbon content, shown in green, should be the same exact plot because the thermal desorption procedure is the same as the TPD procedure. It can be seen that this is not the case, although it is very close. Mobile carbon content, shown in yellow, shows the TPD for the thermal desorption remediation method. It can be seen that there is a minor bump that mimics the shape of the temperature profile.

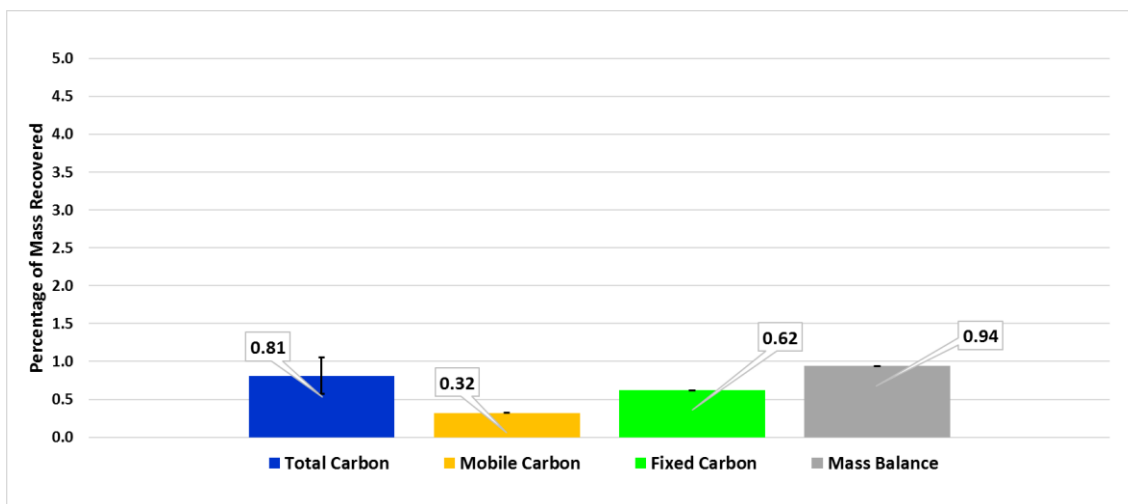


Figure 27: Thermal desorption treated SJV/BM1 carbon mass recovery on a percentage basis. Values are averages and the errors are the standard deviation. TC is shown in blue, MC is shown in yellow, FX is shown in green, and the mass balance (sum of MC and FX) is shown in gray.

Figure 27 is a bar graph of the integrated TPX CO₂ plots. Ideally, the value for the mobile carbon content should be zero. Fixed carbon content and the total carbon content should have matching values as well. Discrepancies may arrive from the low sample size for the TPD and TPO Devol experiments. The mass balance value is close to the total carbon content value.

3.3.4 Pyrolysis

Figure 28, shows the TPX overlay plot for pyrolysis. For the total carbon content curve, shown in blue, CO₂ formation begins at 40 minutes (205°C) and increases to a peak at 100 ppm at around 88 minutes (450°C). After this peak, CO₂ decreases to a trough at 55 ppm at around 115 minutes (540°C). Then, CO₂ begins to increase to a

sharp peak at 100 ppm at around 125 minutes (650°C). Once CO₂ reaches this sharp peak, it decreases to the baseline.

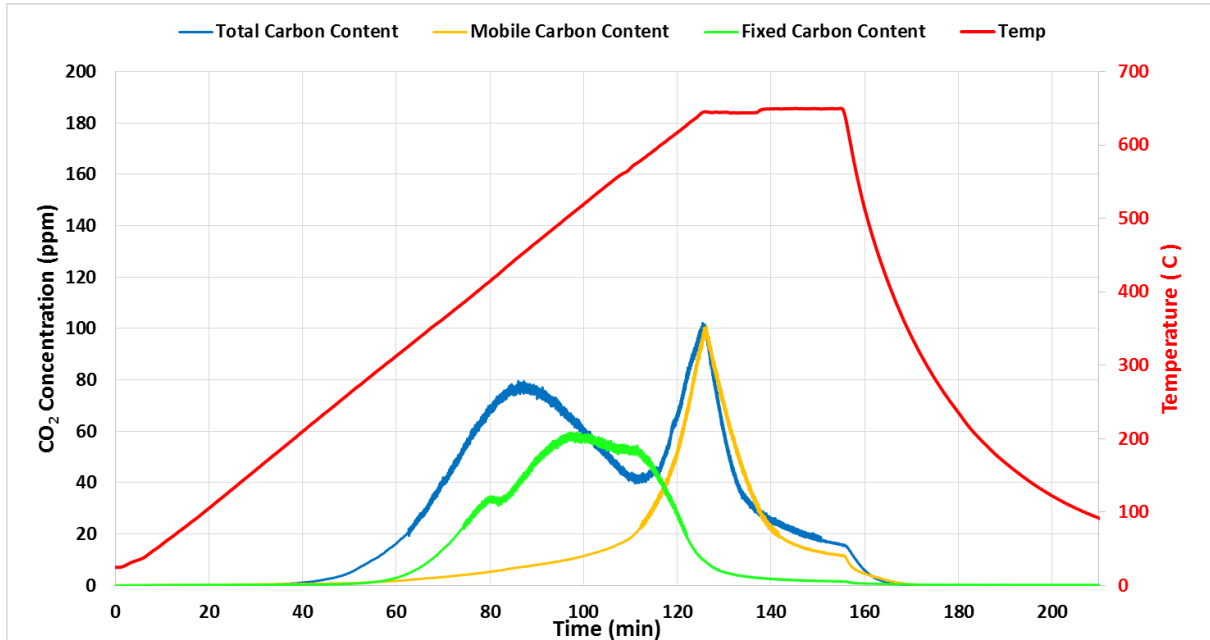


Figure 28: TPX CO₂ concentration curves for the pyrolysis treated SJV/BM1 soil. TC is shown in blue, MC is shown in yellow, FX is shown in green, and temperature is shown in red.

The curve shown in yellow is the Mobile Carbon Content. CO₂ formation begins at 60 minutes (305°C) and increases to a sharp peak at 100 ppm at 125 minutes (650°C). After this peak, CO₂ decreases to the baseline.

Lastly, the curve in green shows the fixed carbon content. CO₂ begins to increase at 55 minutes (280°C) to a small plateau at 40 ppm for about 5 minutes (until 305°C). CO₂ increases again after the minor plateau to a section that decreases linearly, at a slower rate than the rate of increase, for 15 minutes (500°C-575°C). After the slower linear decrease, CO₂ decrease sharply to the baseline.

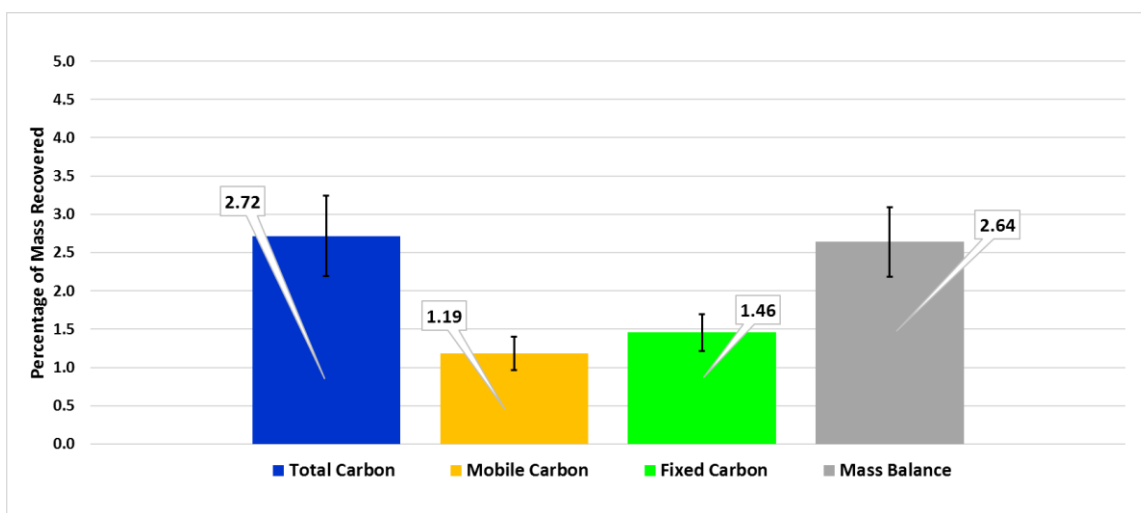


Figure 29: Pyrolysis treated SJV/BM1 carbon mass recovery on a percentage basis. Values are averages and the errors are the standard deviation. TC is shown in blue, MC is shown in yellow, FX is shown in green, and the mass balance (sum of MC and FX) is shown in gray.

Figure 29 is a bar graph of the integrated TPX results. Pyrolysis removed 35% of the total carbon content. 44% of the carbon content is mobile carbon. It can be seen that the fixed carbon content increased from the untreated fixed carbon content. This result is expected because the goal of pyrolysis is to create char and char will be in the fixed carbon content portion. The mass balance result matches with the total carbon content.

Figure 30 is an overlay plot of the mobile carbon content curves for the untreated soil (shown in black) and pyrolysis (shown in green). The temperature profile is shown in red and the yellow, vertical line is the time where 420°C is reached. 420°C is the hold temperature for the pyrolysis method and it can be seen on the pyrolysis curve that there is only one peak located at 650°C. The procedure for pyrolysis is also achieving thermal desorption because it is an open system with a volumetric flow rate.

Any carbon content to the left of the yellow line on the untreated sample will desorb off of the sample because its boiling point is under 420°C.

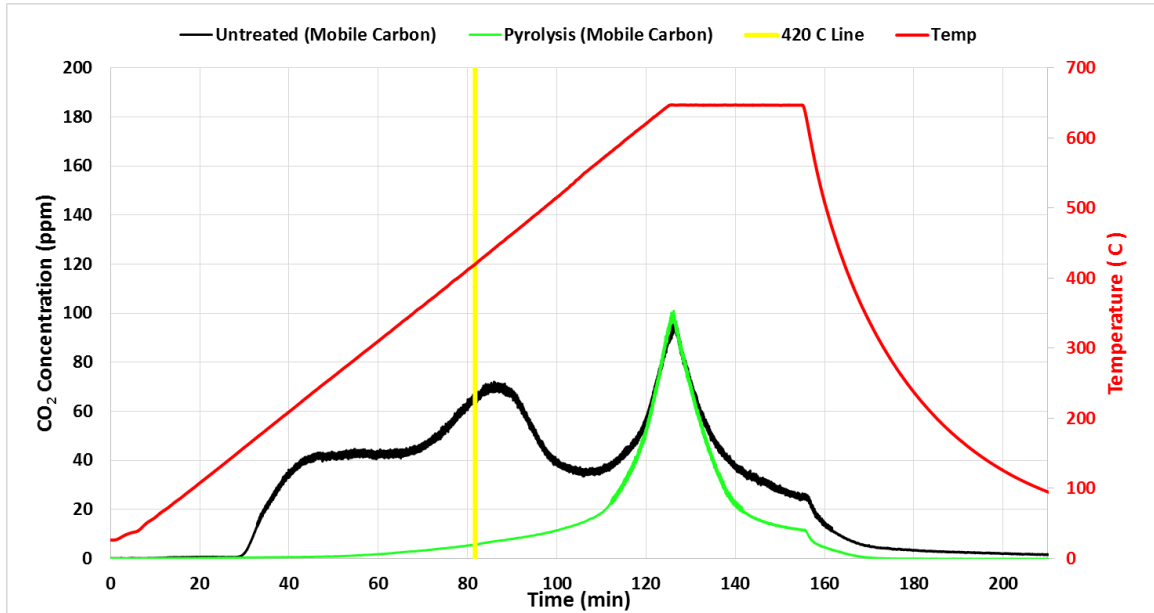


Figure 30: Untreated (hydrocarbon-contaminated) SJV/BM1 MC and pyrolysis treated SJV/BM1 MC CO₂ concentration curve comparison. Untreated is shown in black, pyrolysis is shown in green, temperature is shown in red, and 420°C is shown in yellow.

3.3.5 Electron Beam

Several energy levels, measured in kGy were used for the electron beam treatments: 456 kGy, 700 kGy, 1200 kGy, and 2200 kGy.

3.3.5.1 456 kGy E-beam Treatment

The first electron beam remediation method is the lowest dose at 456 kGy.

Figure 31 shows the TPX CO₂ concentration curves for the 456 kGy remediation method.

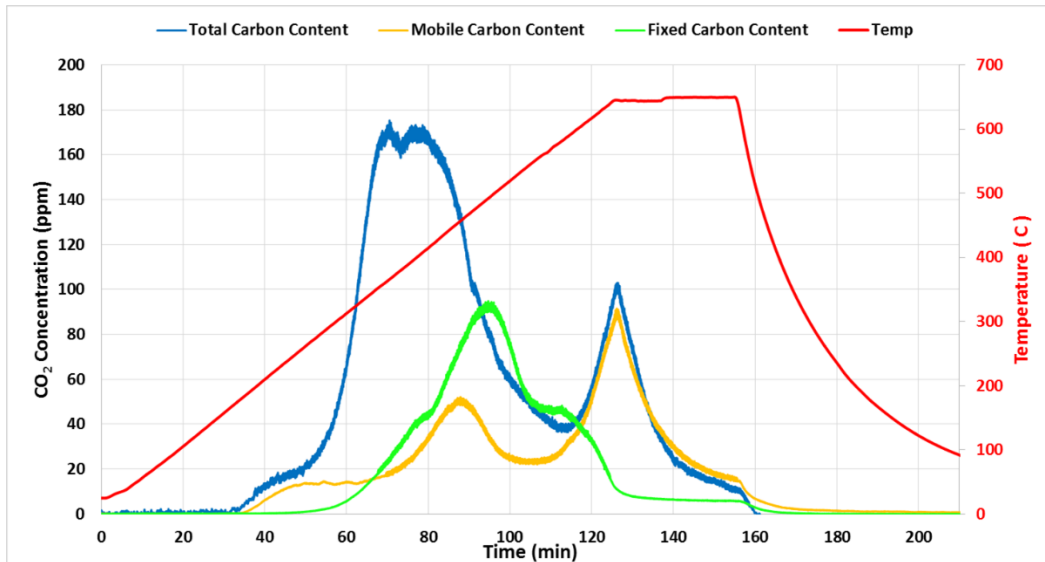


Figure 31: TPX CO₂ concentration curves for the 456 kGy electron beam treated SJV/BM1 soil. TC is shown in blue, MC is shown in yellow, FX is shown in green, and temperature is shown in red.

Total carbon content (blue line) shows the CO₂ formation beginning at 32 minutes (160°C) and increases to a plateau at 130 ppm and lasts for about 20 minutes (260°C). After the plateau, CO₂ decreases to a trough at 40 ppm at 115 minutes (260°C). CO₂ increases again to a sharp peak at 100 ppm (650°C), then decreases to the baseline.

Mobile carbon content, shown in yellow, is the TPD plot for the 456 kGy treated sample. CO₂ begins to form at 35 minutes (175°C) and increases to a minor peak at 50 ppm at 88 minutes (450°C). After this peak, CO₂ decreases to a trough located at 25 ppm and 105 minutes (550°C). CO₂ increases to a sharp peak at 90 ppm and 125 minutes (650°C). The curve decreases back down to the baseline after this sharp peak.

The fixed carbon portion of the 456 kGy treated sample, shown by the green curve in **Figure 31**, shows CO₂ formation beginning at 30 minutes (150°C) and

increases to a peak located at 85 ppm and 95 minutes (495°C). After this peak, the curve decreases to the baseline. At first glance, this peak implies creation of fixed carbon due to the electron beam likely thermochemically decomposing some of the hydrocarbons. This is verified in a later section.

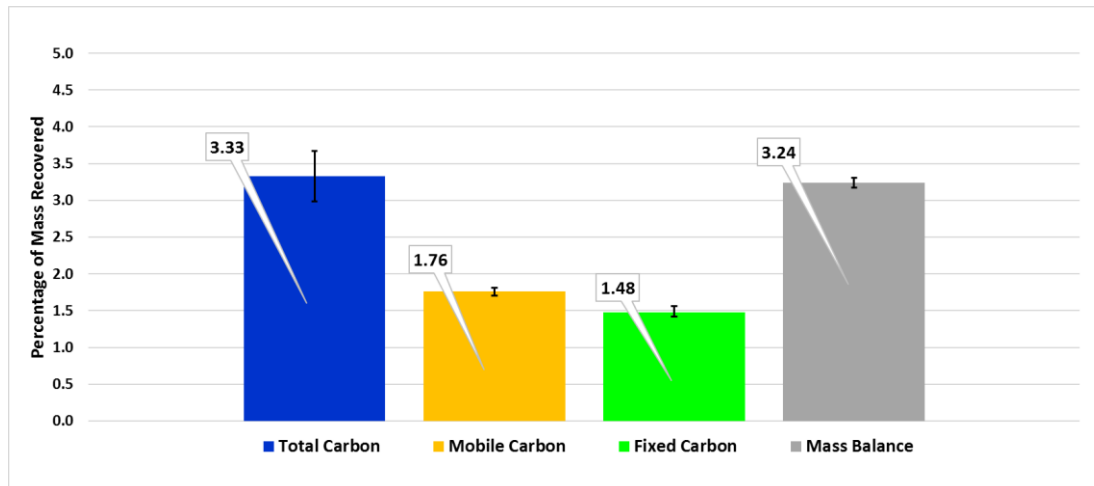


Figure 32: 456 kGy electron beam treated SJV/BM1 carbon mass recovery on a percentage basis. Values are averages and the errors are the standard deviation. TC is shown in blue, MC is shown in yellow, FX is shown in green, and the mass balance (sum of MC and FX) is shown in gray.

Figure 32 is a bar graph of the TPX carbon mass recovery on a percentage basis. The 456 kGy E-beam treatment removed 20% of the total carbon content, 53% of which is mobile fraction carbon. The fixed carbon content is higher for the 456 kGy E-beam treated sample than for the untreated, meaning that this method has converted a portion of the mobile carbon content to fixed carbon. In support of this theory, the mass balance from the summation of the mobile and fixed matches the total carbon content as measured by TPO.

3.3.5.2 700 kGy E-beam Treatment

The second electron beam treatment energy level is 700 kGy. **Figure 33** shows the TPX results for the 700 kGy E-beam treated sample. CO₂, for the total carbon content shown in blue, forms at 35 minutes (175°C) and increases to a peak at 110 ppm and 73 minutes. After this first peak, CO₂ decreases to a trough located at 40 ppm and 112 minutes (585°C). CO₂ increases again, after the trough, to a sharp peak located at 90 ppm and 125 minutes (175°C), then decreases to the baseline.

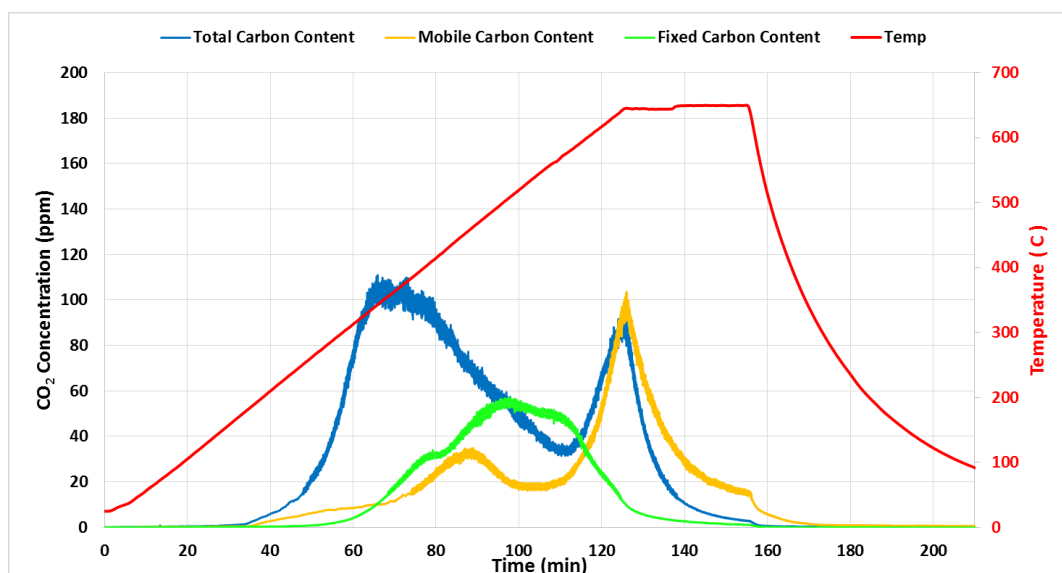


Figure 33: TPX CO₂ concentration curves for the 700 kGy electron beam treated SJV/BM1 soil. TC is shown in blue, MC is shown in yellow, FX is shown in green, and temperature is shown in red.

Mobile carbon content, shown in yellow, is the TPD overlay plot for the 700 kGy E-beam treated sample. CO₂ formation begins at 38 minutes (190°C) and increases to small peak located at 38 ppm and 88 minutes (450°C). Small peak is emphasized because this peak occurs at the same time as the first peak in the 456 kGy E-beam

treated TPD plot but it is smaller in magnitude. Initially, this indicates that the 700 kGy E-beam treatment removed more of the lighter hydrocarbons than the 456 kGy E-beam treatment. After the first peak, CO₂ decreases, slightly, to a trough located at 20 ppm and 105 minutes (550°C). Once the curve reaches the trough, CO₂ quickly increases to a sharp peak located at 90 ppm and 125 minutes (650°C) and then decreases to the baseline.

Fixed carbon content, shown in green, is the TPO Devol overlay plot for the 700 kGy treated sample. CO₂ begins to form at 58 minutes (295°C) and increases to a peak located at 50 ppm and 97 minutes (495°C). After this peak, CO₂ decreases linearly at a slow rate for about 20 minutes (495°C-595°C). Once the curve reaches the end of the 20 minutes, it decreases at a faster rate than before to the baseline.

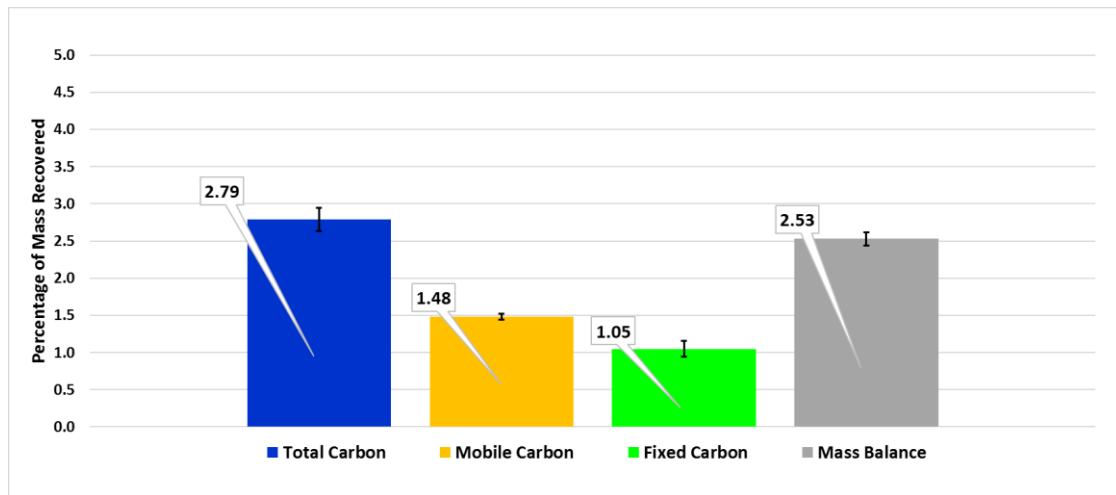


Figure 34: 700 kGy electron beam treated SJV/BM1 carbon mass recovery on a percentage basis. Values are averages and the errors are the standard deviation. TC is shown in blue, MC is shown in yellow, FX is shown in green, and the mass balance (sum of MC and FX) is shown in gray.

Figure 34 is the carbon mass recovery percentage results for the TPX experiments for the 700 kGy treated sample. 700 kGy has removed 34% of the total carbon content. 53% of the carbon content is mobile carbon and some portion of the mobile carbon was converted to fixed carbon. The mass balance value is close to the total carbon content, which is expected.

3.3.5.3 1200 kGy E-beam Treatment

Figure 35, shown below, is the TPX overlay plot for the 1200 kGy treated sample. CO₂, for the total carbon content curve shown in blue, begins to form at 32 minutes (160°C) and increases to a peak at 120 ppm and 80 minutes (425°C). After this peak, CO₂ decreases to a trough located at 40 ppm and 115 minutes (540°C). Once the CO₂ reaches the trough, the curve increases to a sharp peak at 110 ppm and 125 minutes (650°C). Lastly, CO₂ decreases to baseline after the sharp peak.

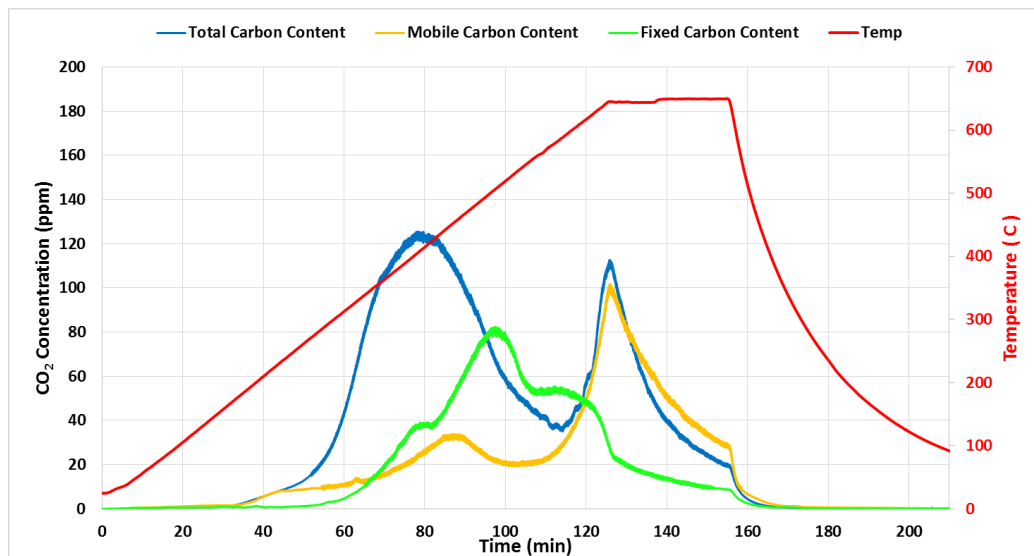


Figure 35: TPX CO₂ concentration curves for the 1200 kGy electron beam treated SJV/BM1 soil. TC is shown in blue, MC is shown in yellow, FX is shown in green, and temperature is shown in red.

The mobile carbon content curve (TPD experiment) is shown in **Figure 35** by the yellow curve. CO₂ formation begins at 32 minutes (160°C) and increases to a small peak, in reference to other treatments, at 35 ppm and 85 minutes (445°C). From the small peak, CO₂ decreases to a trough located at 20 ppm and 105 minutes (550°C). After the trough, CO₂ increases to a sharp peak at 100 ppm and 125 minutes and then decreases down to baseline.

The final TPX experiment for the 1200 kGy treated sample is the TPO Devol (Fixed Carbon Content), shown by the green curve in **Figure 35**. CO₂ forms at 50 minutes (255°C) and increases to a peak at 80 ppm and 95 minutes (500°C). CO₂ decreases after the peak to a plateau at 55 ppm for 15 minutes (550°C-625°C). After the plateau, CO₂ decreases down to baseline.

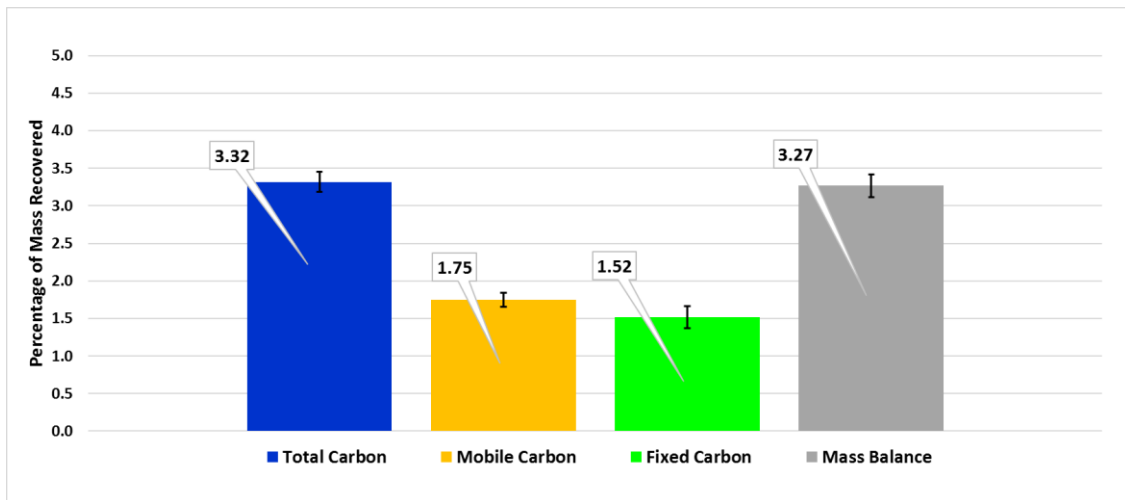


Figure 36: 1200 kGy electron beam treated SJV/BM1 carbon mass recovery on a percentage basis. Values are averages and the errors are the standard deviation. TC is shown in blue, MC is shown in yellow, FX is shown in green, and the mass balance (sum of MC and FX) is shown in gray.

Figure 36 is the carbon mass recovery results for the 1200 kGy TPX experiments on a percentage basis. From the plot, we see that 21% of the total carbon mass was removed due to this treatment; 53% of the carbon content is mobile carbon and a portion of the mobile carbon was converted to fixed carbon. The mass balance value is again very close to the total carbon content value.

3.3.5.4 2200 kGy E-beam Treatment

The final electron beam treatment is the 2200 kGy, shown in **Figure 37**. CO₂ for the total carbon content curve begins to form at 42 minutes (215°C) and increases to a small peak, in reference to previous treatments, at 60 ppm and 92 minutes (470°C). After this peak, CO₂ decreases to a trough located at 28 ppm and 115 minutes (600°C). Once the curve reaches the trough, CO₂ increases to a sharp peak at 52 ppm and 125 minutes (650°C), then decreases to baseline.

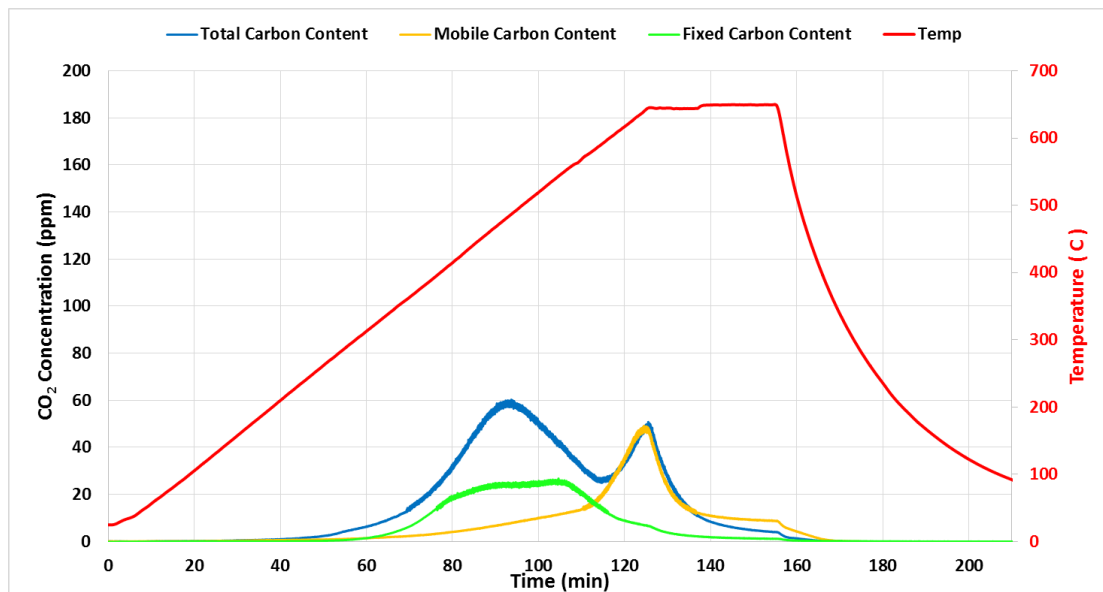


Figure 37: TPX CO₂ concentration curves for the 2200 kGy electron beam treated SJV/BM1 soil. TC is shown in blue, MC is shown in yellow, FX is shown in green, and temperature is shown in red.

Mobile carbon content, shown by the yellow curve, is the TPD plot for the 2200 kGy treated sample. CO₂ forms at 60 minutes (305°C) and increases to a sharp peak at 55 ppm and 125 minutes (650°C). After the sharp peak, the curve decreases to baseline.

The fixed carbon content (TPO Devol) plot for the 2200 kGy is shown by the green curve in **Figure 37**. CO₂ forms at 57 minutes (290°C) and increases to a plateau (note: this is not a plateau but it is a section that is increasing at very slow rate compared to other sections.) located at 25 ppm for 25 minutes (450°C-575°C). After the plateau, the curve decreases to baseline.

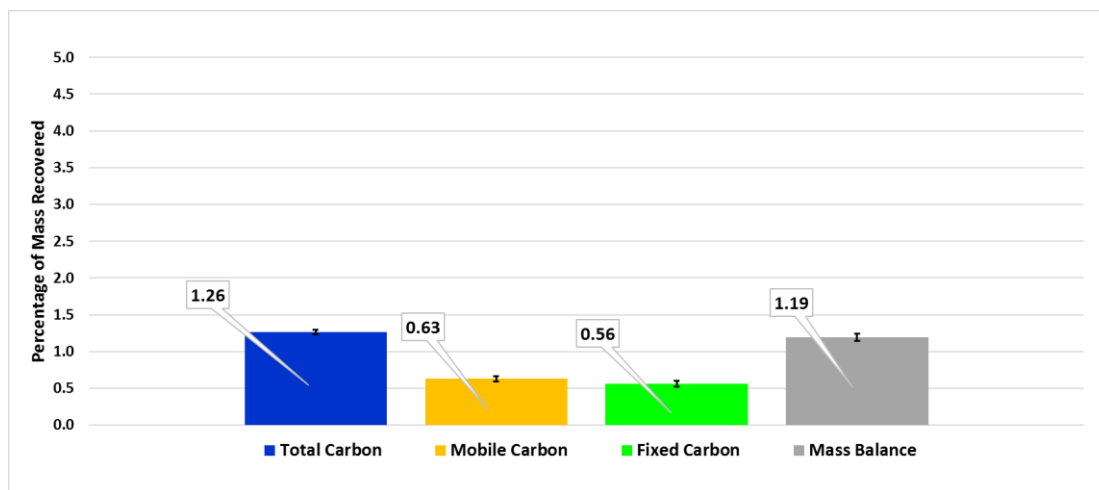


Figure 38: 2200 kGy electron beam treated SJV/BM1 carbon mass recovery on a percentage basis. Values are averages and the errors are the standard deviation. TC is shown in blue, MC is shown in yellow, FX is shown in green, and the mass balance (sum of MC and FX) is shown in gray.

Figure 38 is a bar graph of the carbon mass recovery percentage for the TPX experiments for the 2200 kGy E-beam treated sample. 70% of the total carbon content was removed due to the 2200 kGy E-beam treatment. Mobile carbon content is about

half of the total carbon content. Notably, unlike other electron beam methods, fixed carbon content is less than the value of fixed carbon from the untreated sample. The mass balance value is close to the total carbon content value.

3.3.6 Comparisons of Treatments

Comparisons of the treatments will be conducted in two types of studies. The first is a comparison of the electron beam treatment to determine a dose dependence. The second study is a comparison of all of the treatments.

3.3.6.1 Electron Beam Dose Dependency Comparison

The electron beam treatment, carried out by the PEDL used different magnitudes of dosage to treat the contaminated soil in order to determine the effects of dosage. The graphs in this section are presented with dosage as the independent variable, to investigate this dependence.

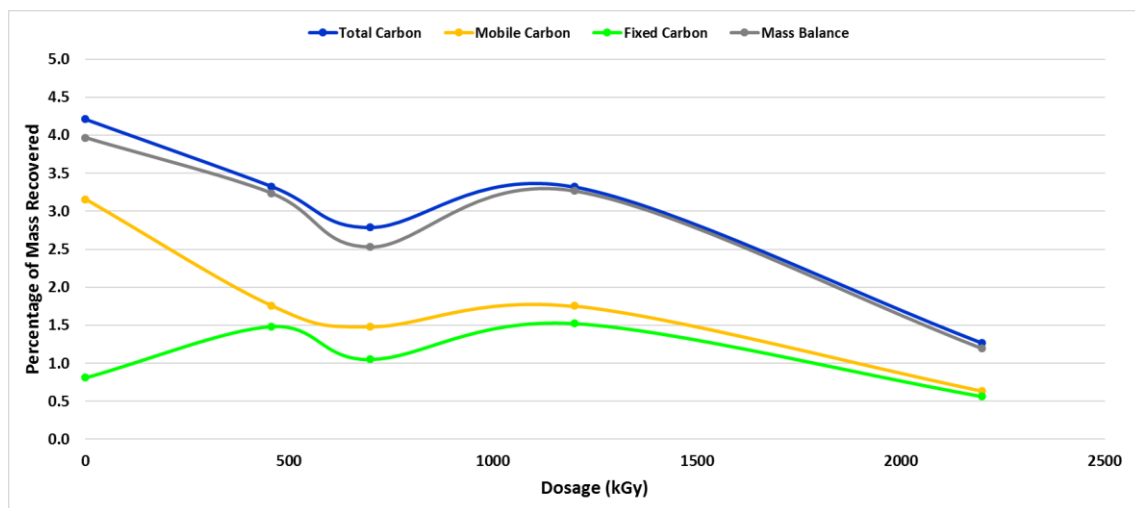


Figure 39: Electron beam dose dependence on the different types of carbon in each soil sample. TC is shown in blue, MC is shown in yellow, FX is shown in green, and the mass balance (sum of MC and FX) is shown in gray.

Figure 39 is a plot of the effect of the E-beam on the percent of carbon mass recovered. The x-axis is the dosage in kGy's. The y-axis is the mass of carbon recovered per unit of sample mass on a percentage basis. Mass recovery percentage is an average of 5 samples. Four curves occupy this plot. Total carbon content is shown in blue, mobile carbon content is shown in yellow, fixed carbon content is shown in green, and the mass balance is shown in gray.

Dosage that corresponds to 0 kGy of E-beam treatment are the values of the untreated soil sample. Total carbon content and the mass balance curves are the same, which is expected. During the lowest energy level treatment (456 kGy), mobile carbon content decreases and fixed carbon content increases. After this value, both mobile and fixed carbon content decrease at 700 kGy, increase at 1200 kGy, and decreases, yet again, at 2200 kGy level. The most interesting observation of this graphs is that mobile and fixed carbon content curves have the same shape in between the doses of 456 kGy and 2200 kGy.

However, there are some discrepancies with this graph that may be able to be explained by experimental variation. There were variables, such as flow rate and whether or not the container was closed, that were not held constant across all of the experiments, making it difficult to draw concrete conclusions. The 456 kGy E-beam treatment used a container open to the atmosphere, allowing evolved gasses to escape. However, the 1200 kGy E-beam used a closed container with a low volumetric flow rate, allowing time for volatilized material to recondense on the sample. The 700 and 2200 kGy E-beam treatments used the same (though different from the 456 and 1200 kGy

samples) high volumetric flow rate in a closed container. Given this knowledge of the experimental protocols, a new graph is shown below with 456 kGy E-beam and 1200 kGy E-beam removed to make a more level comparison, where dosage is the only variable.

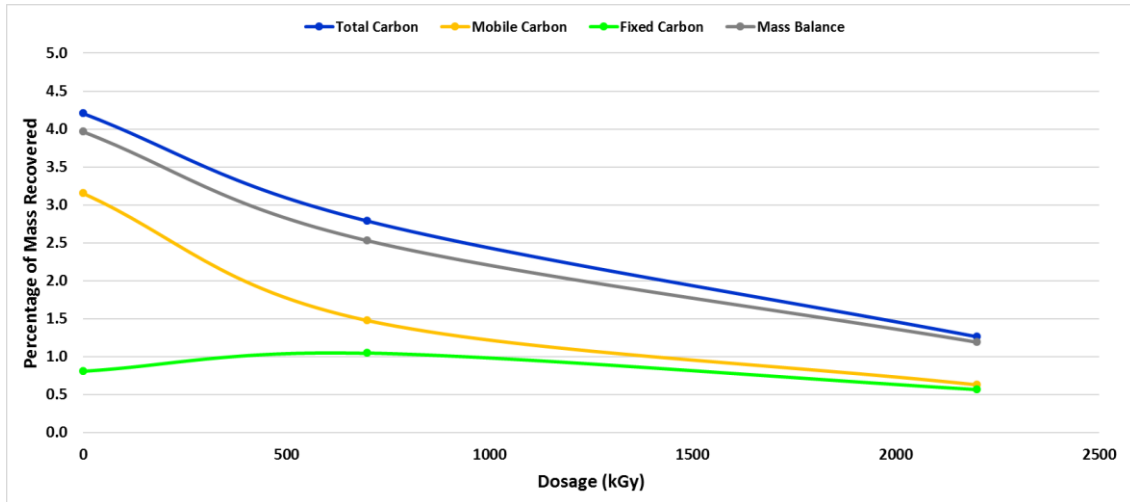


Figure 40: Corrected electron beam dose dependence on the different types of carbon in each soil sample. TC is shown in blue, MC is shown in yellow, FX is shown in green, and the mass balance (sum of MC and FX) is shown in gray.

Figure 40 is the dose dependence graph, with dose as the only variable – allowing for a true comparison. The total carbon content and the mass balance curve are the same shape and decreasing monotonically for increasing dosage. A large amount of mobile carbon content is removed by the lowest treatment level while a small amount of fixed carbon is converted from mobile carbon. Mobile carbon continues to decrease with increasing dosage, but the fixed carbon has a maximum value at the 700 kGy treatment level.

3.3.6.2 Total Treatment Comparison

This section will compare all of the treatments against one another in order to determine the most effective method for removing hydrocarbons from soil.

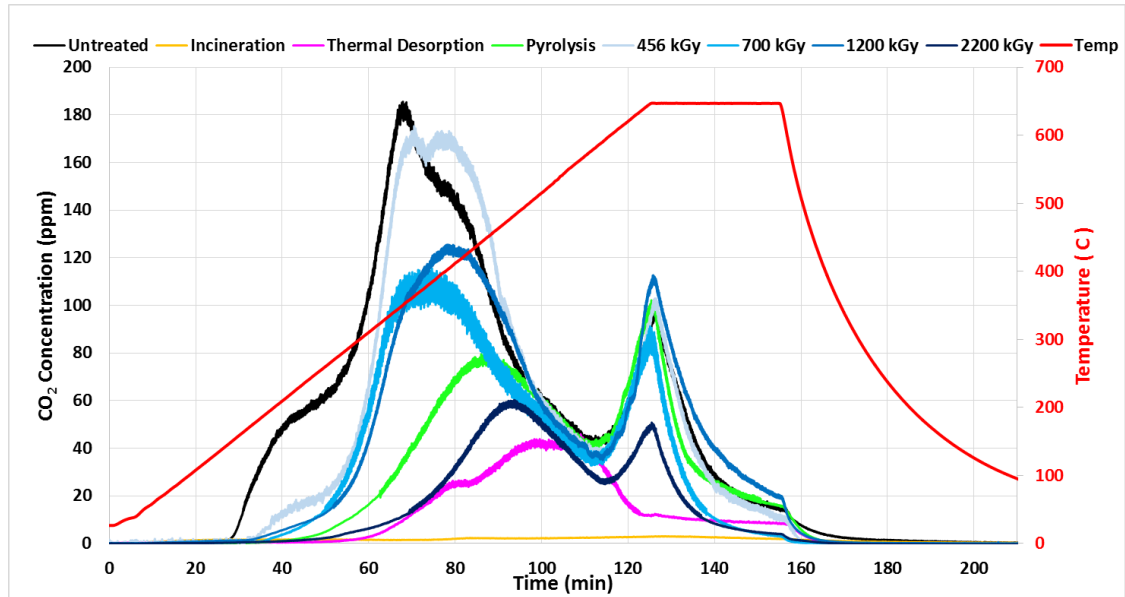


Figure 41: TPO CO₂ concentration curve for each treatment and untreated (hydrocarbon-contaminated) SJV/BM1 soil. Untreated is shown in black, incineration is shown in yellow, thermal desorption is shown in pink, pyrolysis is shown in green, electron beam treatments are shown in shades of blue decreasing in brightness with increasing dosage, and temperature is shown in red.

Figure 41, shown above, is the concentration overlay plot for all treated soil samples and the untreated sample for the TPO experiment. The area under the curve will yield the total amount of CO₂ that was removed from the sample. Therefore, larger curves represent more hydrocarbons (remaining) on the sample, meaning the treatment was less effective.

Untreated soil has the highest amount of hydrocarbon remaining on it, which is to be expected – as it is the worst case scenario and has not been treated in any way to

remove them. It can be seen that each of the remediation methods does at least lower the amount of hydrocarbon in the sample by some amount. Looking at the E-Beam treatment levels, shown in different shades of blue, it can be seen that as the dose increases, the total amount of hydrocarbon remaining on the sample decreases. Pyrolysis removed more hydrocarbon than the three lower dose levels of the electron beam. Thermal desorption removes the second most amount of carbon content while still keeping the fixed carbon content intact. Incineration clearly removed the most (in fact all of the) hydrocarbons from the sample.

There are only three methods that remove the sharp peak that occurs at 100 ppm

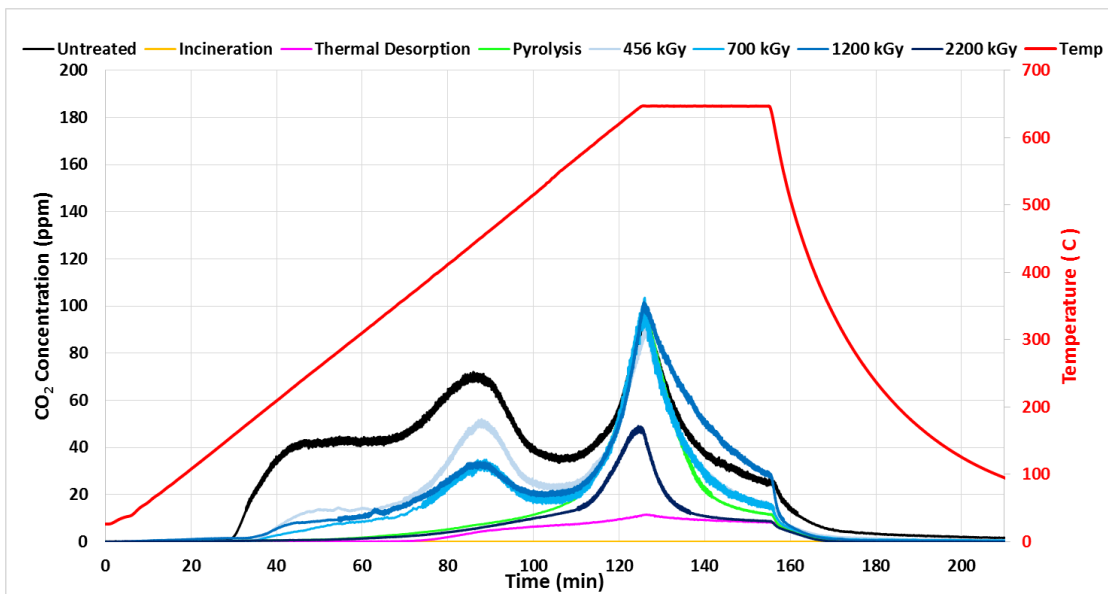


Figure 42: TPD CO₂ concentration curve for each treatment and untreated (hydrocarbon-contaminated) SJV/BM1 soil. Untreated is shown in black, incineration is shown in yellow, thermal desorption is shown in pink, pyrolysis is shown in green, electron beam treatments are shown in shades of blue decreasing in brightness with increasing dosage, and temperature is shown in red.

and 125 minutes (650°C), associated with the MC and TC content. Incineration and thermal desorption both remove the peak completely, while the 2200 kGy E-beam sample decreased the peak magnitude by a factor of 2.

TPD results shows the mobile carbon content on each treated and untreated sample. **Figure 42** shows the comparison overlay plot for the TPD experiment.

Untreated soil is shown in black and it has the most volatile hydrocarbon content. All of the remediation method curves are lower than the untreated curve, which is expected and the desired effect from remediation methods.

The first initial peak on the untreated curve, located at 40 ppm and 42 minutes (220°C), represents the lighter hydrocarbons and each method is effective at removing that initial peak. A second peak is located at 70 ppm and 85 minutes (445°C) on the untreated curve. Four of the remediation methods remove these peaks entirely: incineration, thermal desorption, pyrolysis and 2200 kGy E-beam treatment.

The other electron beam treatment levels lower the magnitude of the second peak, but do not completely remove it. One hypothesis as to why the pyrolysis completely removes the second peak is because it occurs at around 420°C. It could be that the pyrolysis procedure acted as a thermal desorption for any of the hydrocarbons with a boiling point lower than 420°C since the pyrolysis procedure has gas constantly flowing over the soil during the procedure.

Lastly, the third peak is located at 100 ppm and 125 minutes (650°C) for the untreated soil. This peak could have very heavy hydrocarbons in addition to fixed carbon because they would have very high boiling points. Incineration and thermal desorption completely remove this third peak as they reach much higher temperatures.

The 2200 kGy electron beam treatment lowers the magnitude of this peak, as discussed in the TPO comparison plot. The other remediation methods do not lower the magnitude of the third peak.

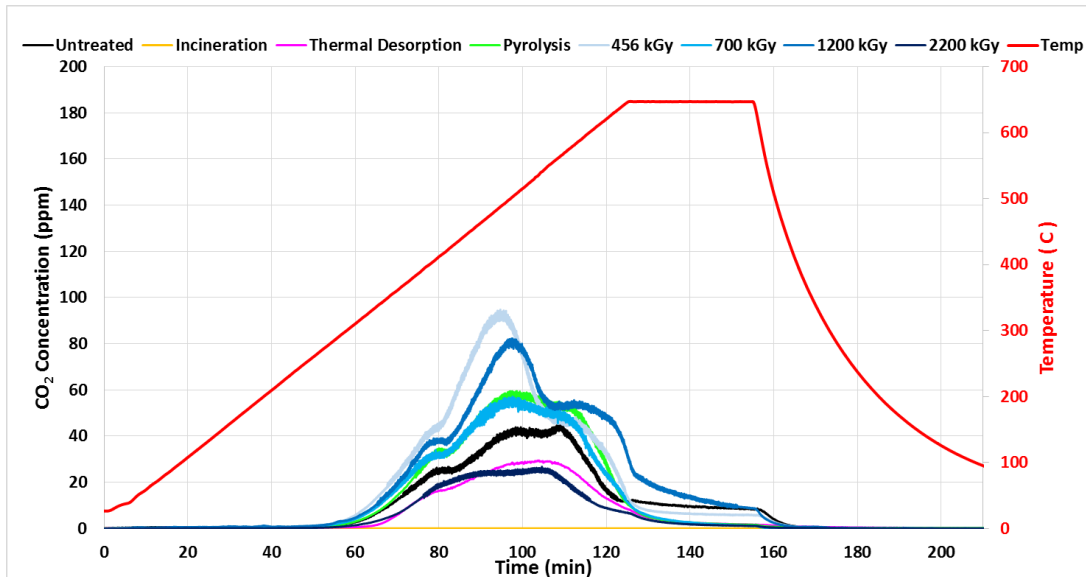


Figure 43: TPO Devol. CO₂ concentration curve for each treatment and untreated (hydrocarbon-contaminated) SJV/BM1 soil. Untreated is shown in black, incineration is shown in yellow, thermal desorption is shown in pink, pyrolysis is shown in green, electron beam treatments are shown in shades of blue decreasing in brightness with increasing dosage, and temperature is shown in red.

Figure 43 shows the comparison of the TPO Devol results for all remediation methods and the untreated soil on one plot. Untreated soil is shown in black and it can be seen that four remediation methods have larger areas under their curves as compared to the untreated soil, indicating that they created new fixed carbon, which was not in the initial sample. The two methods are E-beam treatment at 3 levels; the 456 kGy level E-beam treatment, 1200 kGy level E-beam treatment, 700 kGy level E-beam treatment, and pyrolysis. Pyrolysis was expected to show an increase in the fixed carbon content

because the goal of pyrolysis is to create char. This plot verifies that there was some char created due to the pyrolysis method. It is interesting to note that three of electron beam treatment levels create fixed carbon as well. This likely means that the electron beam method includes thermochemical decomposition.

Thermal desorption has the about the same amount of fixed carbon remaining in the sample as the untreated soil because thermal desorption only removes the mobile content. Incineration removes all of the carbon content, including the fixed fraction.

Finally, the 2200 kGy E-beam treatment level has the most interesting and complex results. Since the other three electron beam treatment levels showed the conversion of fixed carbon from the decomposition of hydrocarbons, it was expected that the 2200 kGy level would have at least as much fixed carbon as the other treatment levels. However, the overlay plot shows *less* fixed carbon. Additionally, we noticed that the color of the 2200 kGy E-beam treated samples post-TPX are different than any of the other remediation methods post-TPX. Typically, the color of the soil post-TPX is a light, reddish, brown – coming from its sandy soil base. However, soil from the 2200 kGy E-beam treatment level post-TPX has a darker color, appearing black, the black color implies that there is some carbon left over on the sample. Further tests would be needed in order to determine the reason behind these results.

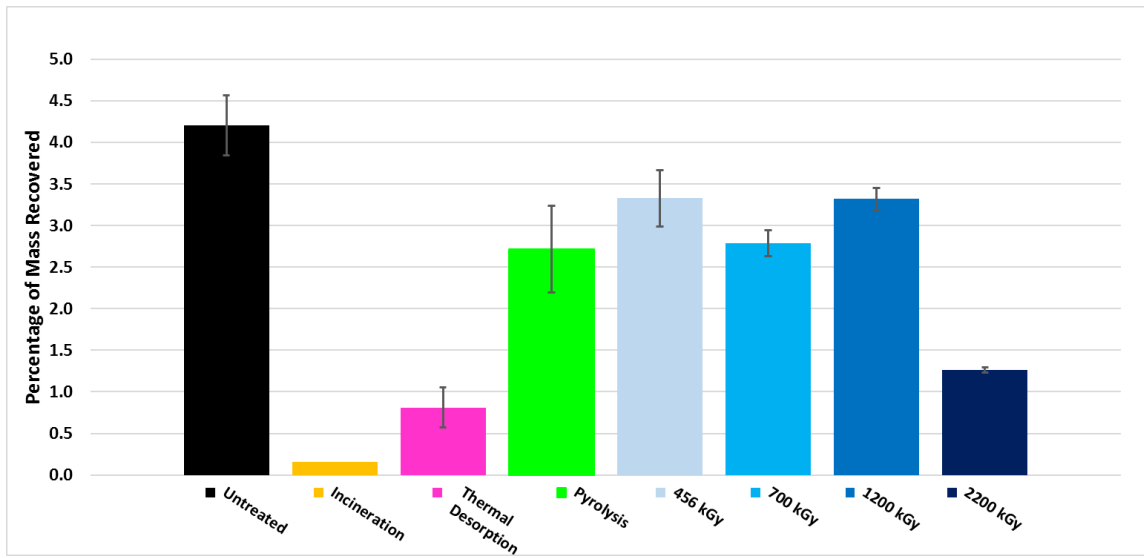


Figure 44: TC mass recovery percentage results for each treatment and untreated (hydrocarbon-contaminated) SJV/BM1 soil. Untreated is shown in black, incineration is shown in yellow, thermal desorption is shown in pink, pyrolysis is shown in green, and electron beam treatments are shown in shades of blue decreasing in brightness with increasing dosage.

Figure 44 shows the average value of carbon mass recovered by the TPO experiment per unit of total sample mass. Error bars are +/- one standard deviation. As shown from the concentration comparison plots, the untreated sample has the most carbon content. Untreated and pyrolysis samples have large error bars, likely due to the non-homogeneity of the starting material. The incineration sample does not have an error bar because the initial value was so low that it defines the zero point and any further testing would have offered insignificant insight.

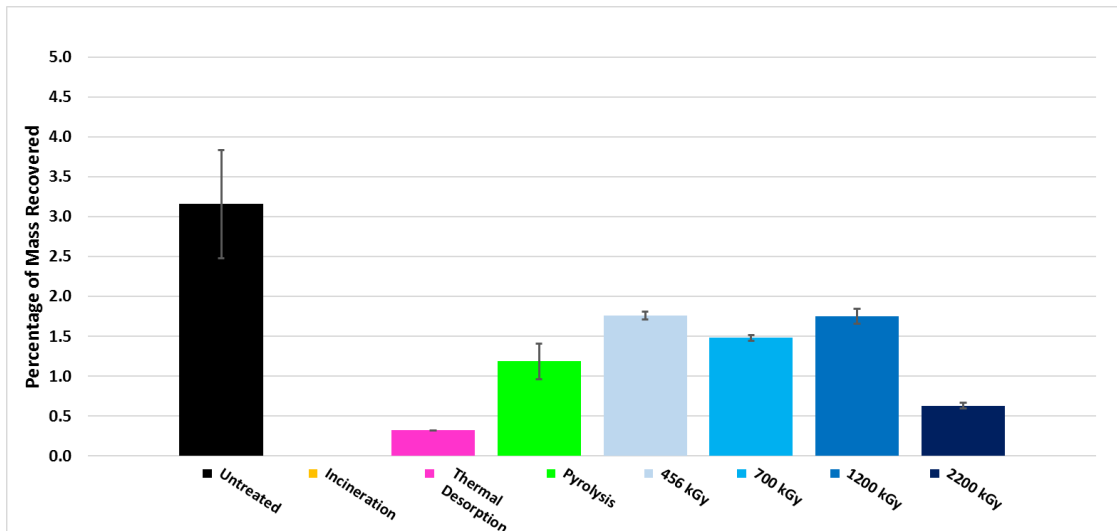


Figure 45: MC mass recovery percentage results for each treatment and untreated (hydrocarbon-contaminated) SJV/BM1 soil. Untreated is shown in black, incineration is shown in yellow, thermal desorption is shown in pink, pyrolysis is shown in green, and electron beam treatments are shown in shades of blue decreasing in brightness with increasing dosage.

The mobile carbon content on a mass percentage basis is shown in **Figure 45**.

The mobile hydrocarbons remaining are measured in this experiment, which means that effective remediation methods should have a lower value than the untreated sample. It can be seen that every remediation method removes at least some mobile content. Incineration and thermal desorption remove the most. Error bars are small for the various remediation methods but larger for the non-homogeneous untreated sample.

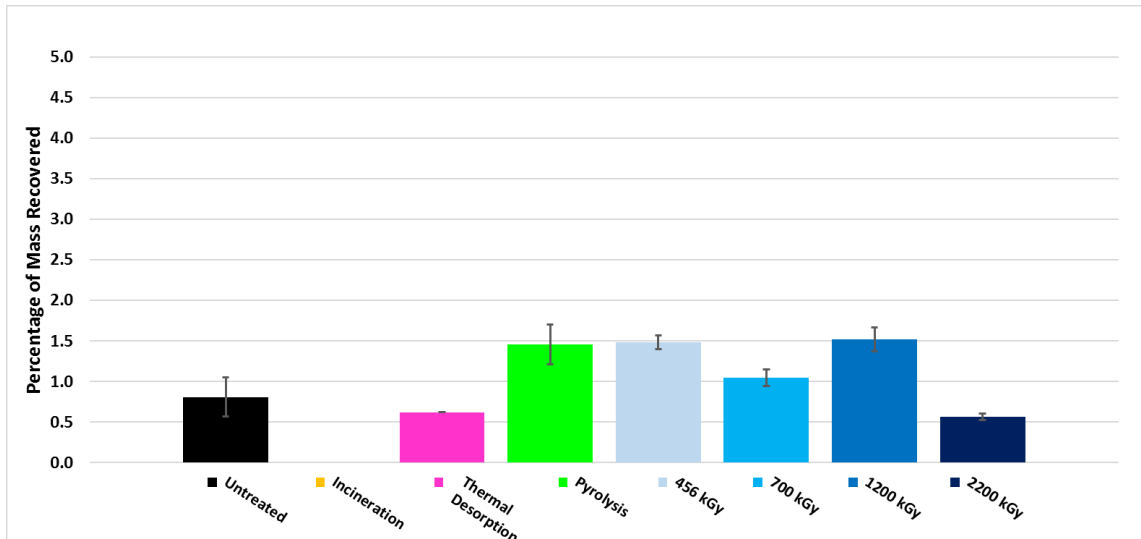


Figure 46: FX mass recovery percentage results for each treatment and untreated (hydrocarbon-contaminated) SJV/BM1 soil. Untreated is shown in black, incineration is shown in yellow, thermal desorption is shown in pink, pyrolysis is shown in green, and electron beam treatments are shown in shades of blue decreasing in brightness with increasing dosage.

Lastly, the fixed carbon mass percentage bar graph is shown in **Figure 46**. This graph shows the fixed carbon content of each sample and it can be seen that a majority of the remediation methods have more fixed carbon than the untreated sample. This was expected for the pyrolysis because that is the goal, but some electron beam treatment levels (456 kGy, 700 kGy, 1200 kGy) include some thermochemical decomposition. Thermal desorption leaves the same amount of fixed carbon as the untreated sample, which is expected because the procedure should not affect the fixed carbon content. 2200 kGy E-beam has less fixed carbon content than the untreated sample and further investigation is required.

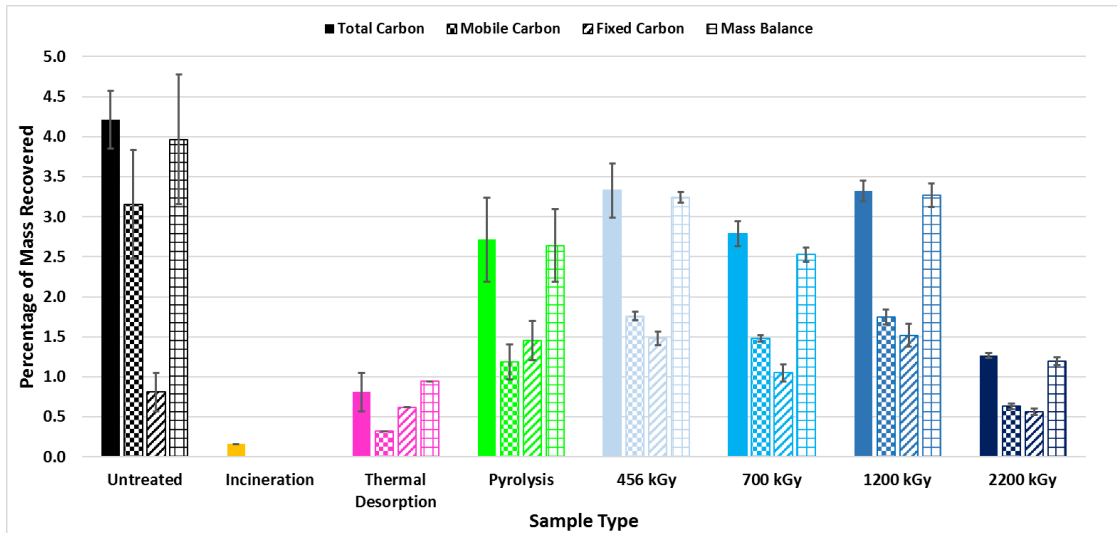


Figure 47: TPX carbon mass recovery percentage results for each treatment and untreated (hydrocarbon-contaminated) SJV/BM1 soil. Untreated is shown in black, incineration is shown in yellow, thermal desorption is shown in pink, pyrolysis is shown in green, and electron beam treatments are shown in shades of blue decreasing in brightness with increasing dosage.

Figure 47, shown above, is a comparison of the mass remaining after all remediation methods normalized to the original pre-treated sample mass. Solid bars are the total carbon content (from TPO), checkerboard bars are the mobile carbon content (from TPD), diagonal lined bars are the fixed carbon content (from TPO Devol), and the final wire pattern is the sum of the mobile and fixed carbon content added together to compare directly to the total carbon content because they should be equal. Again, we can see that incineration removes the most hydrocarbons and thermal desorption removes the second most. Pyrolysis is better than the three lower dose electron beam treatments.

CHAPTER IV

CONCLUSIONS

4.1 Summary

Initially, the preliminary results show that TPX experiments are a useful tool in analyzing different remediation methods. Results from the TPX experiments for the GSC1AOS soil sample clearly shows differences in total carbon, mobile carbon, and fixed carbon content between the untreated (hydrocarbon-contaminated) soil and E-beam treated (1000 kGy) soil. E-beam treatment removed 54% of the total carbon content. Mobile carbon content decreased from 4.3% to 0.9% showing that this method can remove a majority of the mobile hydrocarbon content. The final result for the GSC1AOS soil is fixed carbon content increased from 1.8% to 2.3% meaning that newly fixed carbon was created from a portion of the mobile carbon. These results show that the mechanism of the E-beam method is a combination of thermal desorption and thermochemical decomposition.

It has been shown that each remediation method can remove hydrocarbon content from contaminated soil. Incineration is the best method at removing hydrocarbon content because it will burn off all of the carbon content, along with the organic matter required to grow plants. Thermal desorption is the second best method at removing hydrocarbon content. This method will also leave the organic matter in the soil in case there is any need for plant life. 2200 kGy E-beam is the third best method at removing hydrocarbons. One downside of this method is that it has the largest energy cost of the electron beam treatments due to the high dosage. Pyrolysis and the 700 kGy E-beam

treatments are similar in terms of total carbon content amount but pyrolysis has a higher fixed carbon content value, which is expected because that is the goal of pyrolysis.

Lastly, 456 kGy E-beam and 1200 kGy E-beam have equivalent results. This is important because one has a lower energy cost than the other.

4.2 Future Work

A natural next step for this work is to determine the amount of energy input required for each method. This will be useful for determining the efficiency and cost-effectiveness of each method as it is considered for use at large scale remediation facilities. Additionally, soil fertility analysis should be conducted in order to evaluate the potential of the treated soils to grow plants.

One of the E-beam treatments, 2200 kGy, did not create new FX like the other E-beam energy levels. Instead, it removed a portion of the original FX but the color of the soil post-TPX was darker than the other soil samples post-TPX. One theory is that this dark color comes from carbon that is still in the soil. To help determine this theory, a TPO with a higher maximum temperature can be used. For example, a TPO that reaches 800°C may provide some insight. These experiments should be done on the untreated soil, 2200 kGy treated soil, and 2200 kGy treated (Post-TPX) soil.

The pyrolysis method, developed by Rice University and analyzed in this work seems to have a combination of thermal desorption and thermochemical decomposition mechanisms. Addition of char to soil has shown to increase soil fertility [15] so it is important that pyrolysis is creating the maximum amount of char if this method is chosen for large scale remediation. Pyrolysis optimization would include different

temperatures, hold times, and open/closed systems. Closed systems may be problematic due to the increase in pressure. Understanding the kinetics of hydrocarbon pyrolysis will be a vital in the optimization procedure.

REFERENCES

1. N/A. *Hydrocarbons*. 2015. Accessed on 5/4/2016; Available from:
<http://www.petroleum.co.uk/hydrocarbons>.
2. Renneboog, R.M.J. *Use of Hydrocarbons*. ScienceIQ.com. Accessed on
5/4/2016; Available from: <http://scienceiq.com/Facts/UsesOfHydrocarbons.cfm>.
3. Durand, C., et al., *Characterization of the Organic Matter of Sludge:
Determination of Lipids, Hydrocarbons and PAHs from Road
Retention/Infiltration Ponds in France*. Environmental Pollution, 2004. **132**(3):
p. 375-384.
4. Gogoi, B., et al., *A Case Study of Bioremediation of Petroleum-Hydrocarbon
Contaminated Soil at a Crude Oil Spill Site*. Advances in Environmental
Research, 2003. **7**(4): p. 767-782.
5. Jacki M. Aislabie, M.R.B., Julia M. Foght, and Emma J. Waterhouse,
Hydrocarbon Spills on Antarctic Soils: Effects and Management. Environmental
Science & Technology, 2004. **38**(5): p. 10.
6. Paudyn, K., et al., *Remediation of Hydrocarbon Contaminated Soils in the
Canadian Arctic by Landfarming*. Cold Regions Science and Technology, 2008.
53(1): p. 102-114.
7. Atlas, R. and J. Brown, *Introduction to the Workshop on Ecological Effects of
Hydrocarbon Spills in Alaska*. Arctic, 1978. **31**(3): p. 155-157.

8. Troxler, W.L., et al., *Treatment of Nonhazardous Petroleum-Contaminated Soils by Thermal Desorption Technologies*. *Air & Waste*, 1993. **43**(11): p. 1512-1525.
9. Taylor, A. *The Exxon Valdez Oil Spill: 25 Years Ago Today*. 2014. Accessed on 4/16/2016; Available from: <http://www.theatlantic.com/photo/2014/03/the-exxon-valdez-oil-spill-25-years-ago-today/100703/>.
10. N/A. *Oil Spills*. 2000. Accessed on 5/1/2016; Available from: http://events.awma.org/enviro_edu/resources1/additional/fact_sheets/oil_spills.html.
11. Tang, J., et al., *Eco-Toxicity of Petroleum Hydrocarbon Contaminated Soil*. *Journal of Environmental Sciences*, 2011. **23**(5): p. 845-851.
12. Aislabie, J., et al., *Effects of Oil Spills on Microbial Heterotrophs in Antarctic Soils*. *Polar Biology*, 2001. **24**(5): p. 308-313.
13. Fraser, G.S. and J. Ellis, *Offshore Hydrocarbon and Synthetic Hydrocarbon Spills in Eastern Canada: The Issue of Follow-up and Experience*. *Journal of Environmental Assessment Policy and Management*, 2008. **10**(02): p. 173-187.
14. Beckett, G. and D. Huntley, *Soil Properties and Design Factors Influencing Free-Phase Hydrocarbon Cleanup*. *Environmental Science & Technology*, 1998. **32**(2): p. 287-293.
15. Julia E. Vidonish, K.Z., Caroline A. Masiello. Xiaodong Gao, Jacques Mathieu, and Pedro J. J. Alvarez, *Pyrolytic Treatment and Fertility Enhancement of Soils Contaminated with Heavy Hydrocarbons*. *Environmental Science & Technology*, 2016. **50**(5): p. 9.

16. Lighty, J.S., et al., *Characterization of Thermal Desorption Phenomena for the Cleanup of Contaminated Soil*. Nuclear and Chemical Waste Management, 1988. **8**(3): p. 225-237.
17. Kanaly, R.A. and S. Harayama, *Biodegradation of High-Molecular-Weight Polycyclic Aromatic Hydrocarbons by Bacteria*. Journal of Bacteriology, 2000. **182**(8): p. 2059-2067.
18. Ghazali, F.M., et al., *Biodegradation of Hydrocarbons in Soil by Microbial Consortium*. International Biodeterioration & Biodegradation, 2004. **54**(1): p. 61-67.
19. Margesin, R. and F. Schinner, *Biodegradation and Bioremediation of Hydrocarbons in Extreme Environments*. Applied Microbiology and Biotechnology, 2001. **56**(5-6): p. 650-663.
20. Marchal, R., et al., *Gasoline and Diesel Oil Biodegradation*. Oil & Gas Science and Technology, 2003. **58**(4): p. 441-448.
21. Leahy, J.G. and R.R. Colwell, *Microbial Degradation of Hydrocarbons in the Environment*. Microbiological Reviews, 1990. **54**(3): p. 305-315.
22. Lu Lu, T.H., Song Jin, Yi Zuo, and Zhiyong Jason Ren, *Microbial Metabolism and Community Structure in Response to Bioelectrochemically Enhanced Remediation of Petroleum Hydrocarbon-Contaminated Soil*. Environmental Science & Technology, 2014. **48**: p. 9.

23. Zhang, F.-S., S.-i. Yamasaki, and M. Nanzyo, *Application of Waste Ashes to Agricultural land—Effect of Incineration Temperature on Chemical Characteristics*. *Science of the Total Environment*, 2001. **264**(3): p. 205-214.
24. Gautam, V., R. Thapar, and M. Sharma, *Biomedical Waste Management: Incineration vs. Environmental Safety*. *Indian Journal of Medical Microbiology*, 2010. **28**(3): p. 191.
25. Oppelt, E.T., *Hazardous Waste Destruction*. *Environmental Science & Technology*, 1986. **20**(4): p. 312-318.
26. Fife, J.A., *Solid Waste Disposal. Incineration or Pyrolysis*. *Environmental Science & Technology*, 1973. **7**(4): p. 5.
27. Marline T. Smith, F.B., and Anil K. Mehrotra, *Thermal Desorption Treatment of Contaminated Soils in a Novel Batch Thermal Reactor*. *Industrial & Engineering Chemistry Research*, 2001. **40**(23): p. 10.
28. Sterba, V.H.a.M.J., *Pyrolysis of Hydrocarbons*. *Industrial & Engineering Chemistry*, 1948. **40**(9): p. 11.
29. Srinivasan, V., et al., *Catalytic Pyrolysis of Torrefied Biomass for Hydrocarbons Production*. *Energy & Fuels*, 2012. **26**(12): p. 7347-7353.
30. Hurd, C.D., *Pyrolysis of Unsaturated Hydrocarbons*. *Industrial & Engineering Chemistry*, 1934. **26**(1): p. 50-55.
31. Frey, F., *Pyrolysis of Saturated Hydrocarbons*. *Industrial & Engineering Chemistry*, 1934. **26**(2): p. 198-203.

32. BENSON, S.W., *Some Recent Developments in the Gas-Phase Pyrolysis of Hydrocarbons*. 1970: Refining Petroleum for Chemicals Advances in Chemistry. p. 19.
33. III, K.W.B., *Experimental Setup and Preliminary Results for Electron Beam Remediation of Heavy Hydrocarbon Contaminated Soils*, in *Mechanical Engineering*. 2015, Texas A&M University. p. 136.
34. Strzelec, A., *Kinetic Model Development for the Combustion of Particulate Matter from Conventional and Soy Methyl Ester Diesel Fuels*, in *Combustion Engineering*. 2009, University of Wisconsin. p. 168.
35. Noelia Alonso-Morales, M.A.G., Francisco Heras, Juan J. Rodriguez, and Semih Eser, *Oxidation Reactivity and Structure of LDPE-Derived Solid Carbons: A Temperature-Programmed Oxidation Study*. *Energy & Fuels*, 2013. **27**(2): p. 11.
36. Yezerets, A., et al., *Quantitative Flow-Reactor Study of Diesel Soot Oxidation Process*. 2002, SAE Technical Paper.
37. Bin Geng, J.C., Shao-Xiong Liu, Pu Zhang, Zhi-Qiang Tang, Dong Chen, Qian Tao, Yan-Xia Chen, and Shou-Zhong Zou, *Temperature Programmed Desorption - An Application to Kinetic Studies of CO Desorption at Electrochemical Interfaces*. *The Journal of Physical Chemistry C*, 2009. **113**(47): p. 4.
38. Semih Eser, R.V., and Orhan Altin, *Utility of Temperature-Programmed Oxidation for Characterization of Carbonaceous Deposits from Heated Jet Fuel*. *Industrial & Engineering Chemistry Research*, 2006. **45**(26): p. 7.

39. A. N. Il'ichev, D.P.S., V. A. Matyshak, and V. N. Korchak, *A Temperature-Programmed Desorption and IR Spectroscopic Study of the Mechanism of Carbon Monoxide Oxidation on Copper-Containing Catalysts*. *Kinetics and Catalysis*, 2015. **56**(2): p. 9.
40. Yezerets, A., et al., *Investigation of the Oxidation Behavior of Diesel Particulate Matter*. *Catalysis Today*, 2003. **88**(1): p. 17-25.

APPENDIX A

CO₂ CALIBRATION EXAMPLE

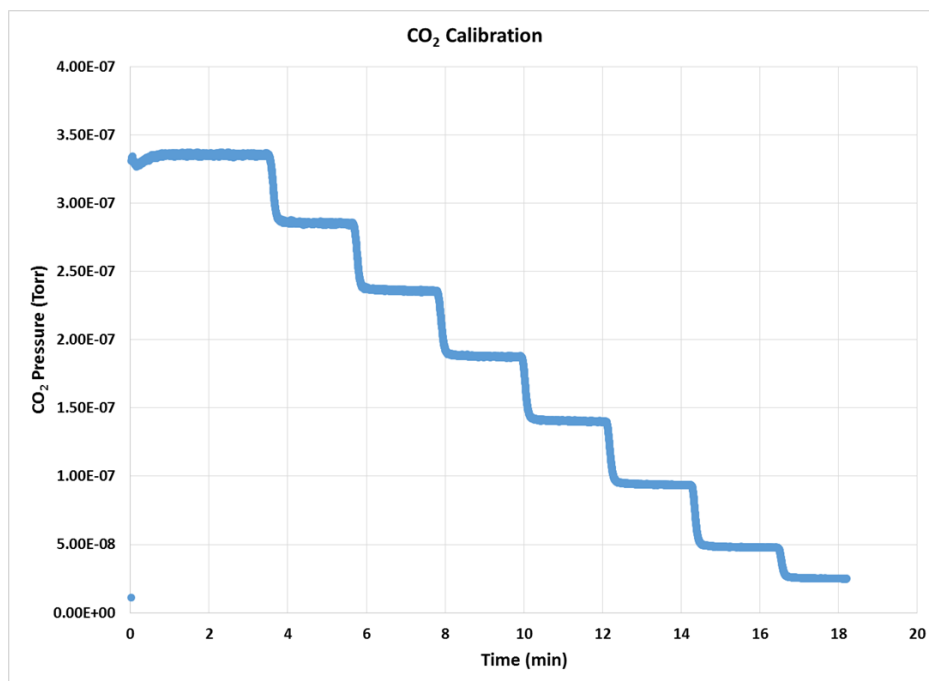


Figure 48: CO₂ Calibration Graph

Figure 48 is a plot of the CO₂ calibration. CO₂ pressure in torr is on the y-axis. Time in minutes is on the x-axis. Each flat line corresponds to a known concentration of CO₂. The first step located at 3.4×10^{-7} torr and in between 1-3 minutes is 3.5% CO₂, by volume, with Ar as the carrier gas. Each step decreases in concentration by 0.5% until the second to last step at 0.5%. The last step is 0.25%. Slope and intercept values are created for analysis. Concentration values are the dependent variable and ratio of the CO₂ and Ar pressures are the independent variables. R² values were consistently greater than 0.999.

APPENDIX B

UNTREATED (SJV/BM1) REPLICATE TPX

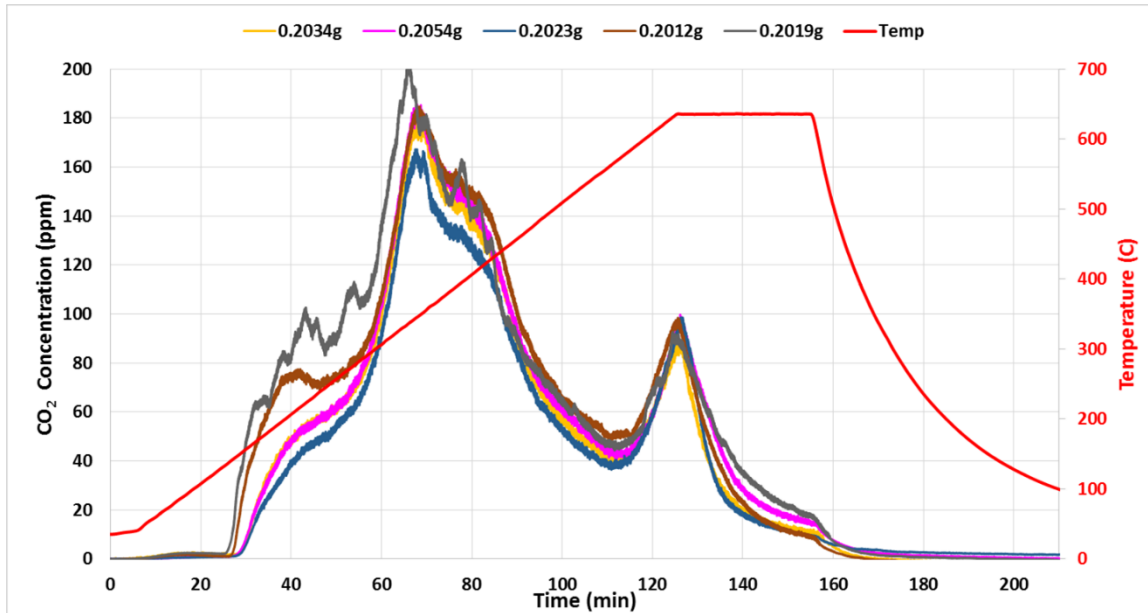


Figure 49: TPO CO₂ concentration curve for untreated (hydrocarbon-contaminated) SJV/BM1 soil. 5 samples of varying masses are shown.

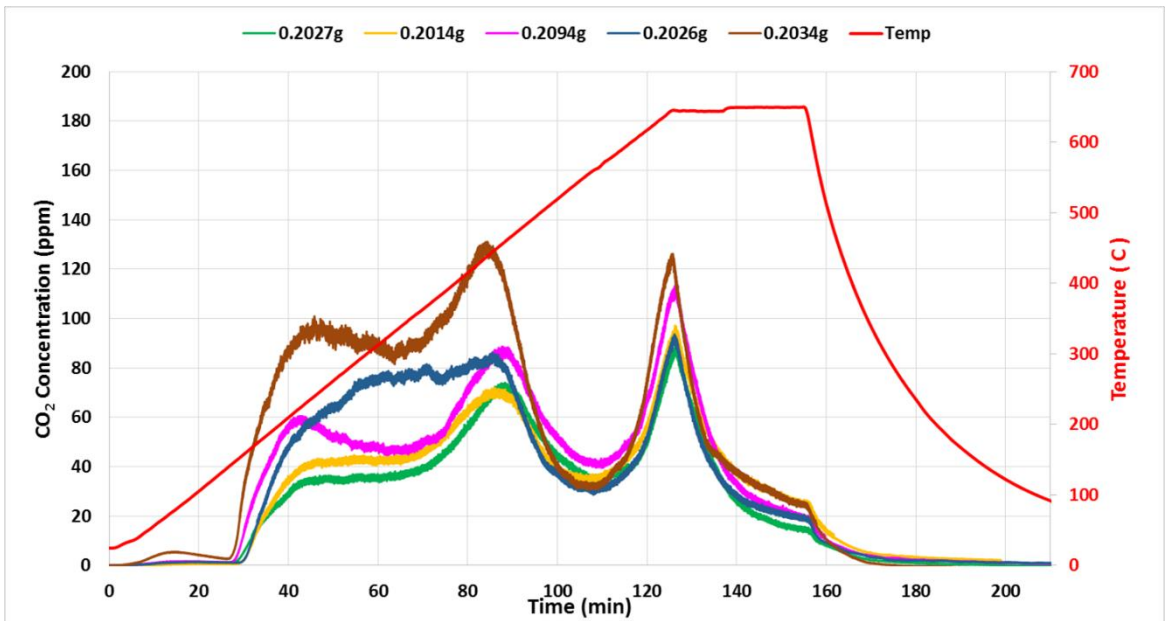


Figure 50: TPD CO₂ concentration curve for untreated (hydrocarbon-contaminated) SJV/BM1 soil. 5 samples of varying masses are shown.

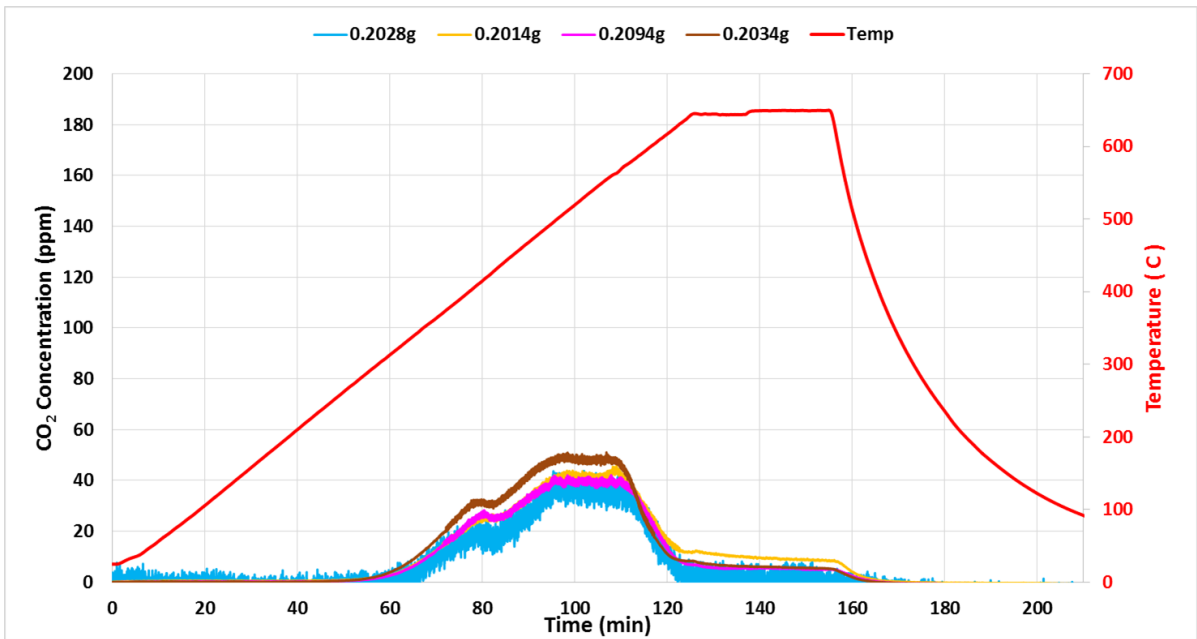


Figure 51: TPO Devol. CO₂ concentration curve for untreated (hydrocarbon-contaminated) SJV/BM1 soil. 4 samples of varying masses are shown.

APPENDIX C

THERMAL DESORPTION (SJV/BM1) REPLICATE TPX

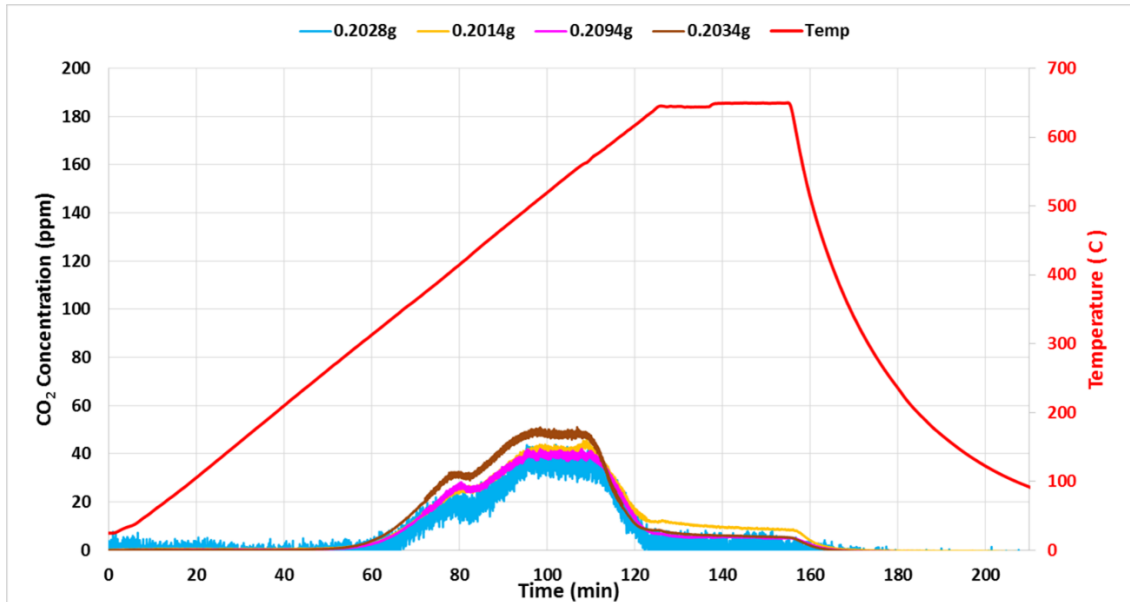


Figure 52: TPO CO₂ concentration curve for thermal desorption treated SJV/BM1 soil. 4 samples of varying masses are shown.

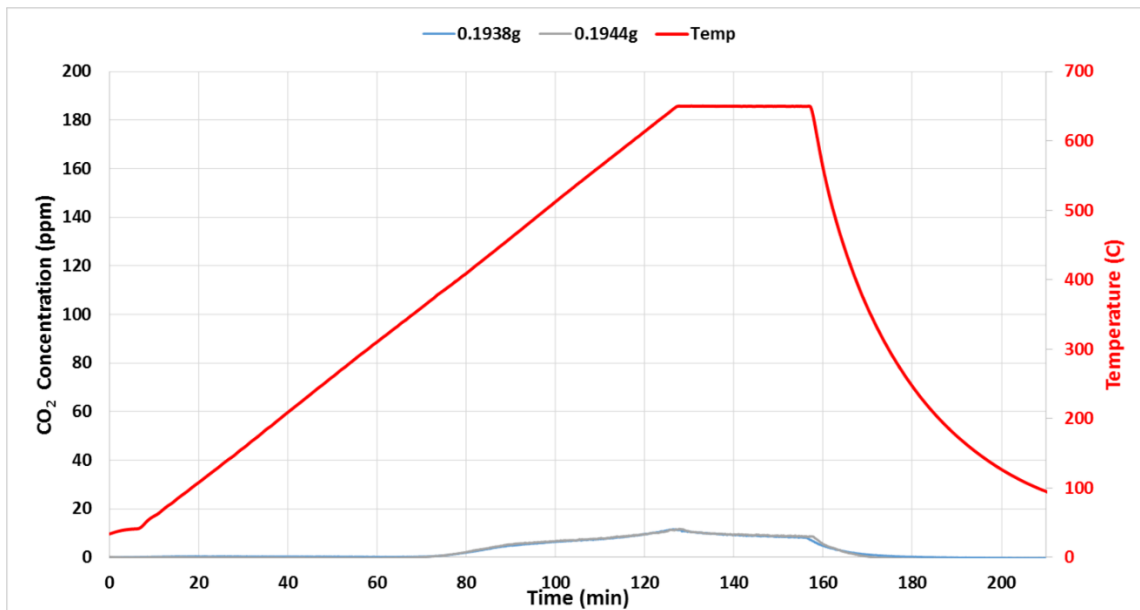


Figure 53: TPD CO₂ concentration curve for thermal desorption treated SJV/BM1 soil. 2 samples of varying masses are shown.

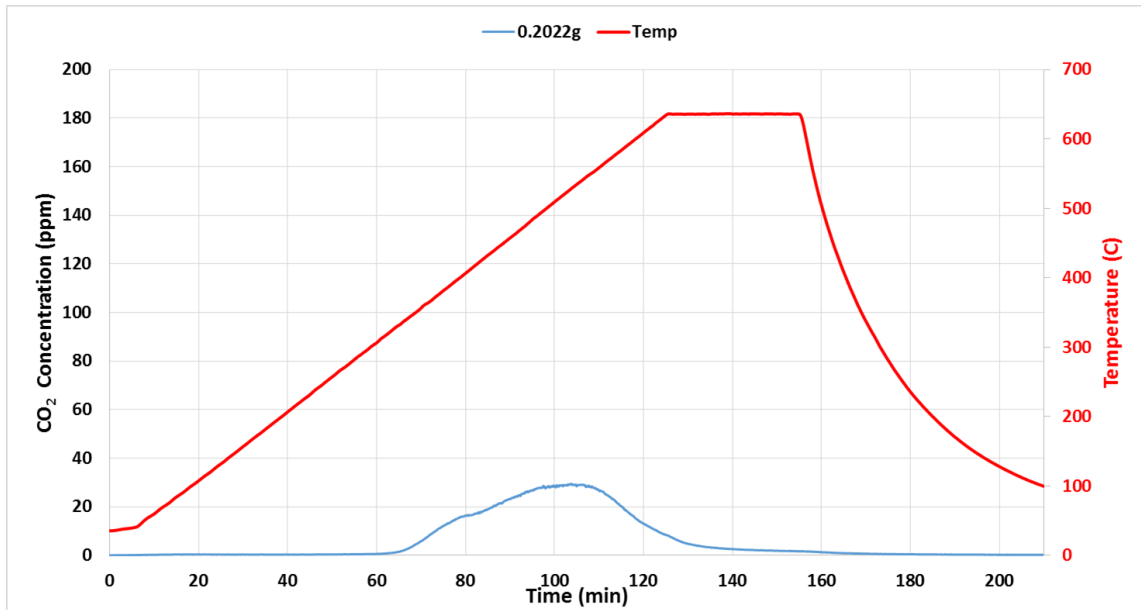


Figure 54: TPO Devol. CO₂ concentration curve for thermal desorption treated SJV/BM1 soil. 1 sample is shown.

APPENDIX D

PYROLYSIS (SJV/BM1) REPLICATE TPX

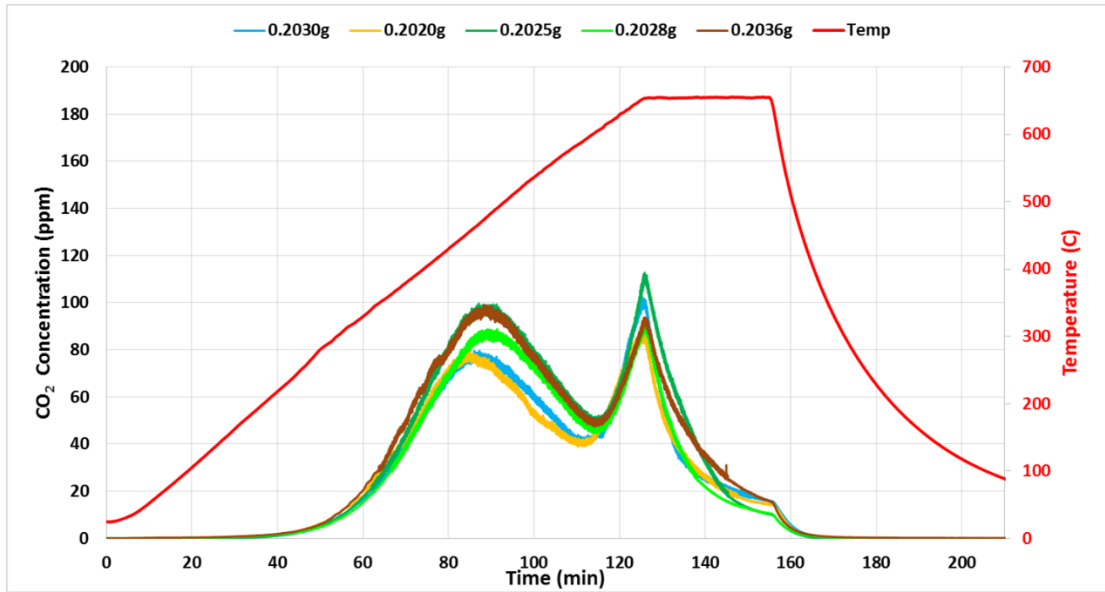


Figure 55: TPO CO₂ concentration curve for pyrolysis treated SJV/BM1 soil. 5 samples of varying masses are shown.

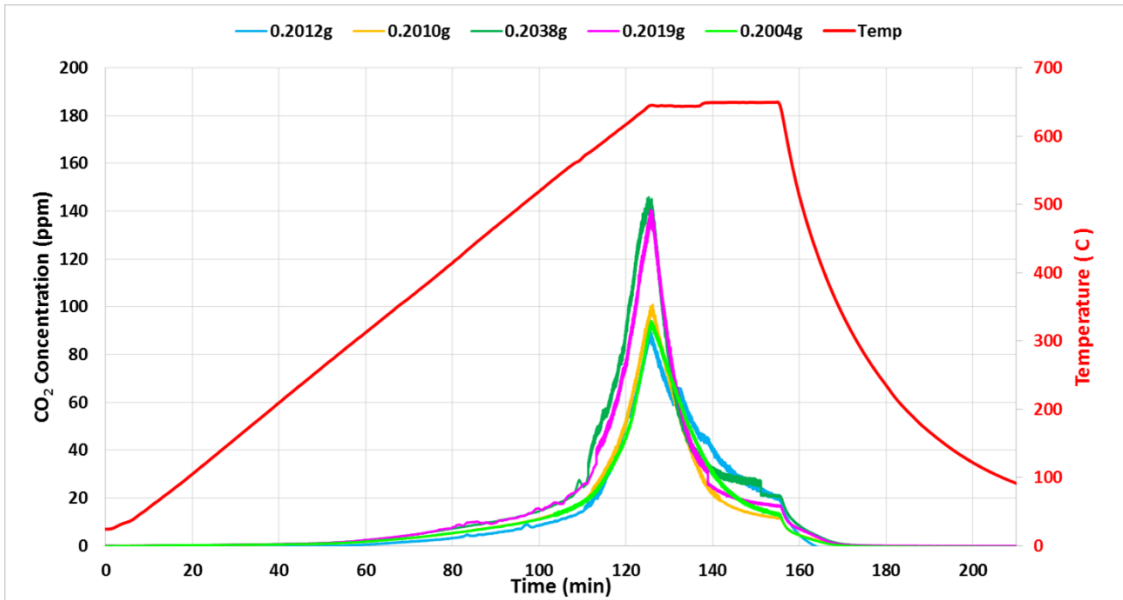


Figure 56: TPD CO₂ concentration curve for pyrolysis treated SJV/BM1 soil. 5 samples of varying masses are shown.

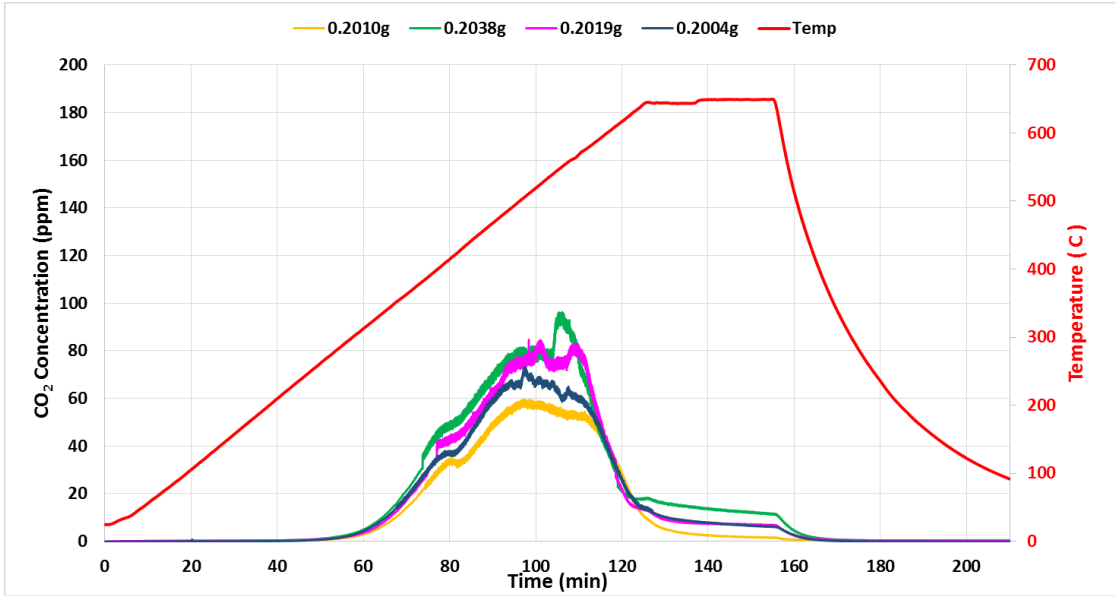


Figure 57: TPO Devol. CO₂ concentration curve for pyrolysis treated SJV/BM1 soil. 4 samples of varying masses are shown.

APPENDIX E

456 KGY (SJV/BM1) REPLICATE TPX

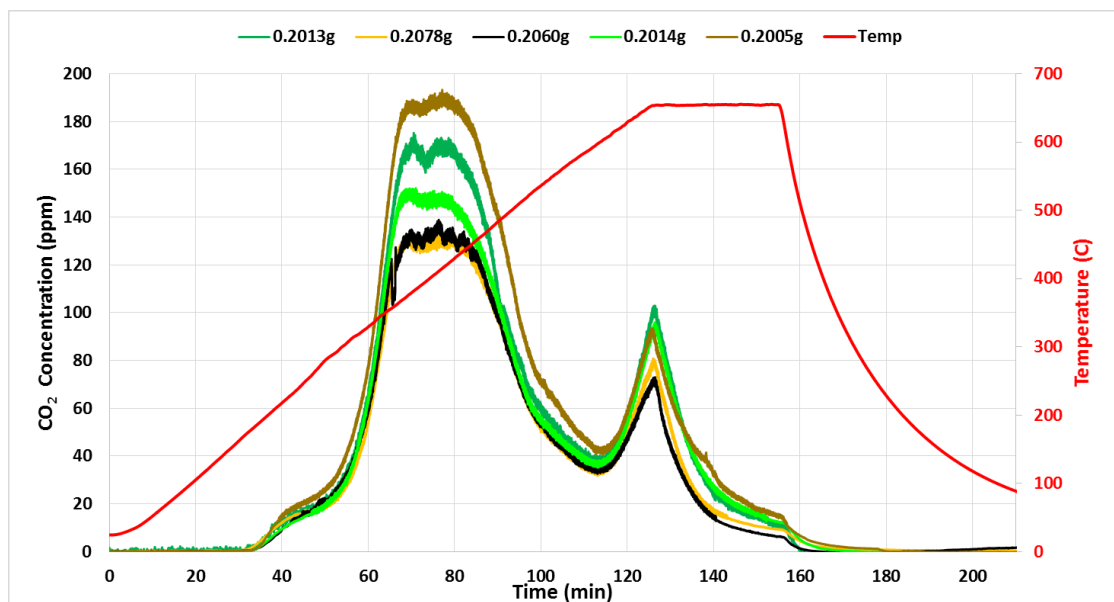


Figure 58: TPO CO₂ concentration curve for 456 kGy electron beam treated SJV/BM1 soil. 5 samples of varying masses are shown.

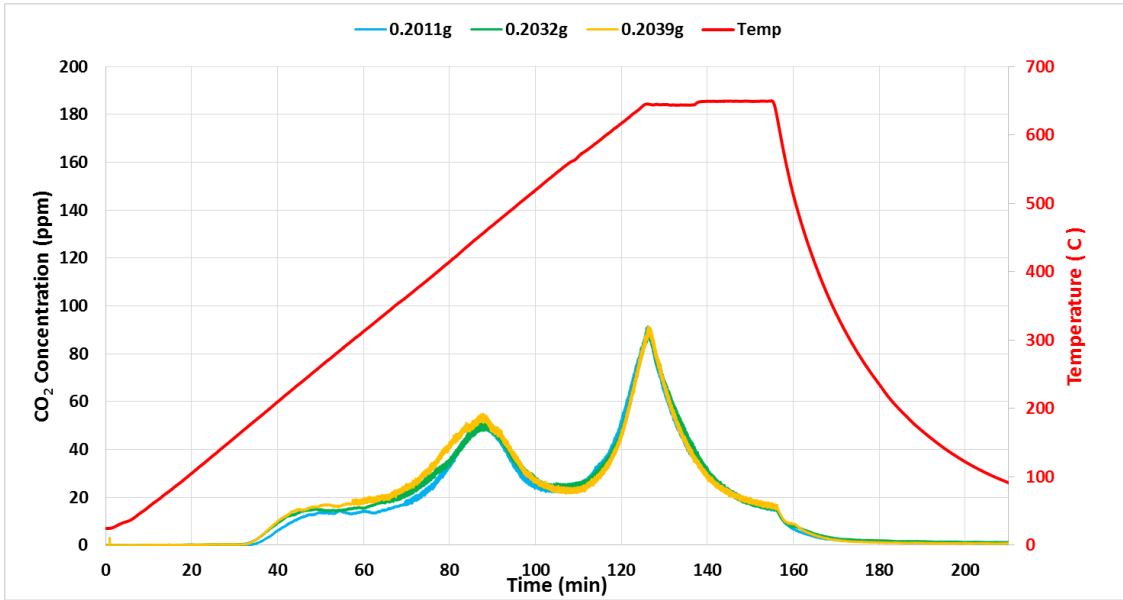


Figure 59: TPD CO₂ concentration curve for 456 kGy electron beam treated SJV/BM1 soil. 3 samples of varying masses are shown.

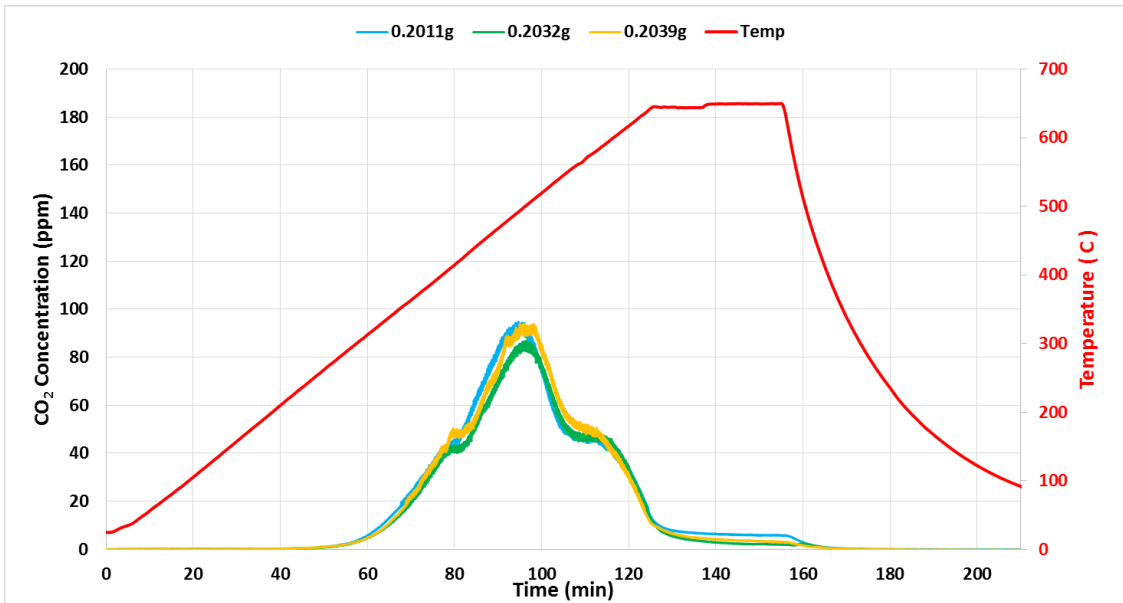


Figure 60: TPO Devol. CO₂ concentration curve for 456 kGy electron beam treated SJV/BM1 soil. 3 samples of varying masses are shown.

APPENDIX F

700 KGY (SJV/BM1) REPLICATE TPX

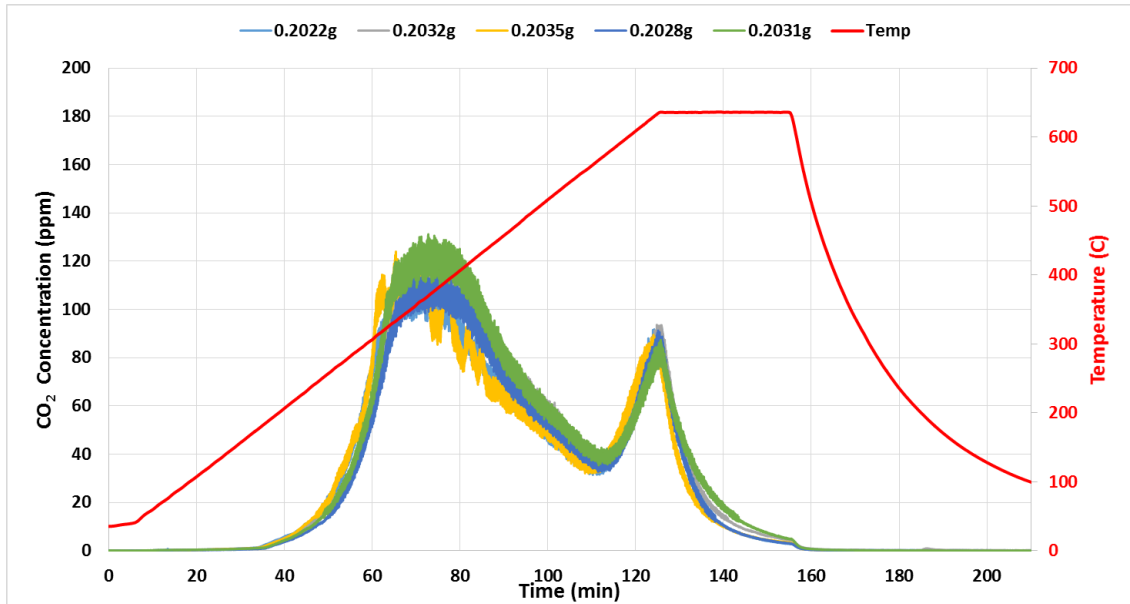


Figure 61: TPO CO₂ concentration curve for 700 kGy electron beam treated SJV/BM1 soil. 5 samples of varying masses are shown.

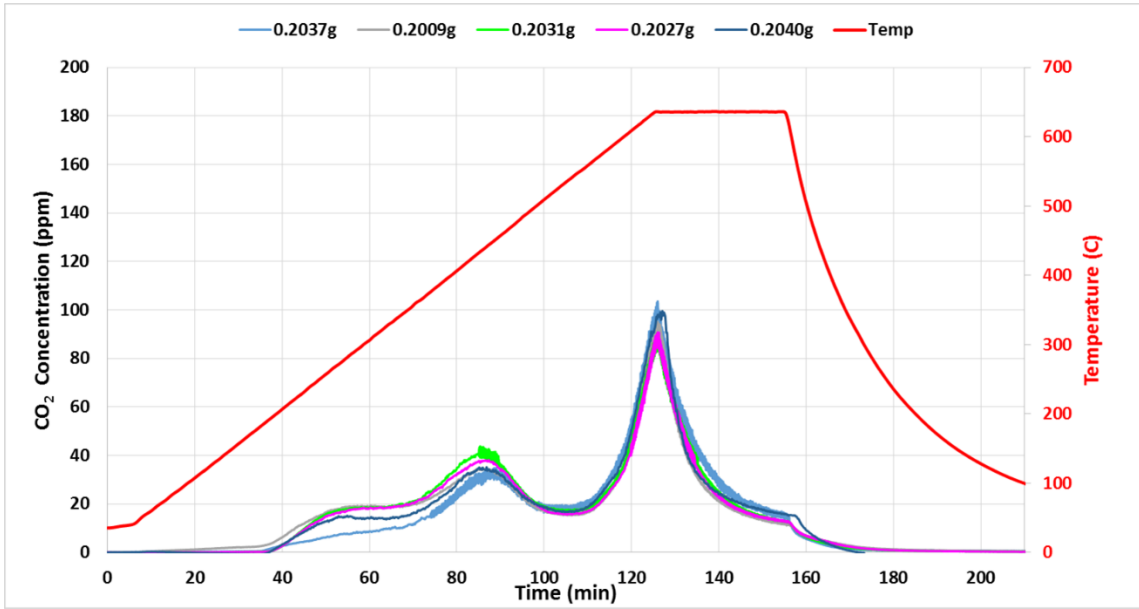


Figure 62: TPD CO₂ concentration curve for 700 kGy electron beam treated SJV/BM1 soil. 5 samples of varying masses are shown.

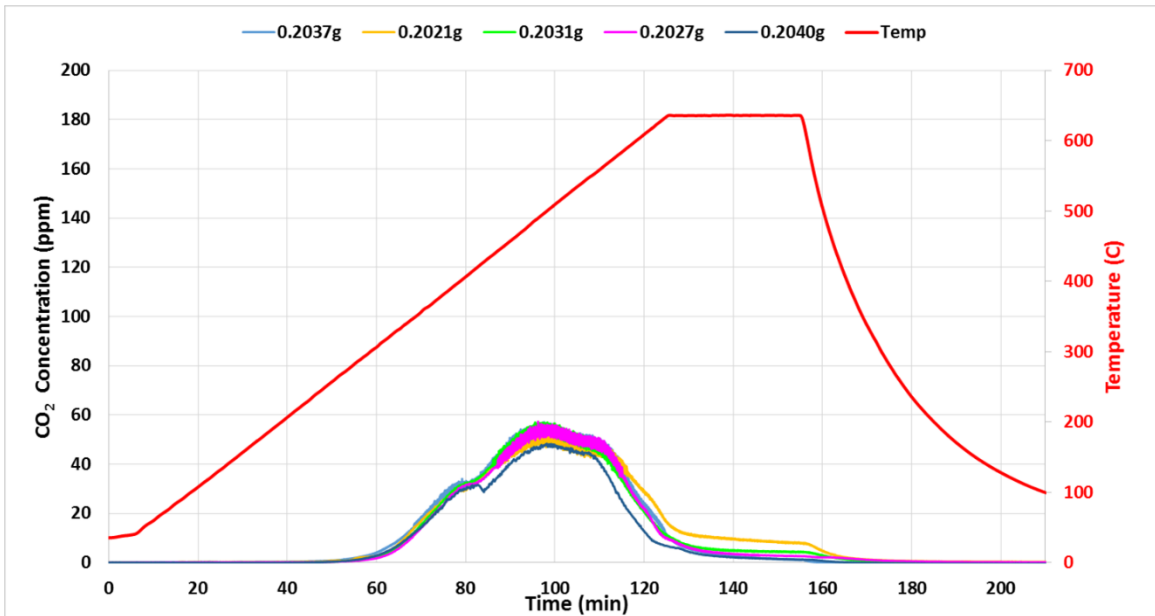


Figure 63: TPO Devol. CO₂ concentration curve for 700 kGy electron beam treated SJV/BM1 soil. 5 samples of varying masses are shown.

APPENDIX G

1200 KGY (SJV/BM1) REPLICATE TPX

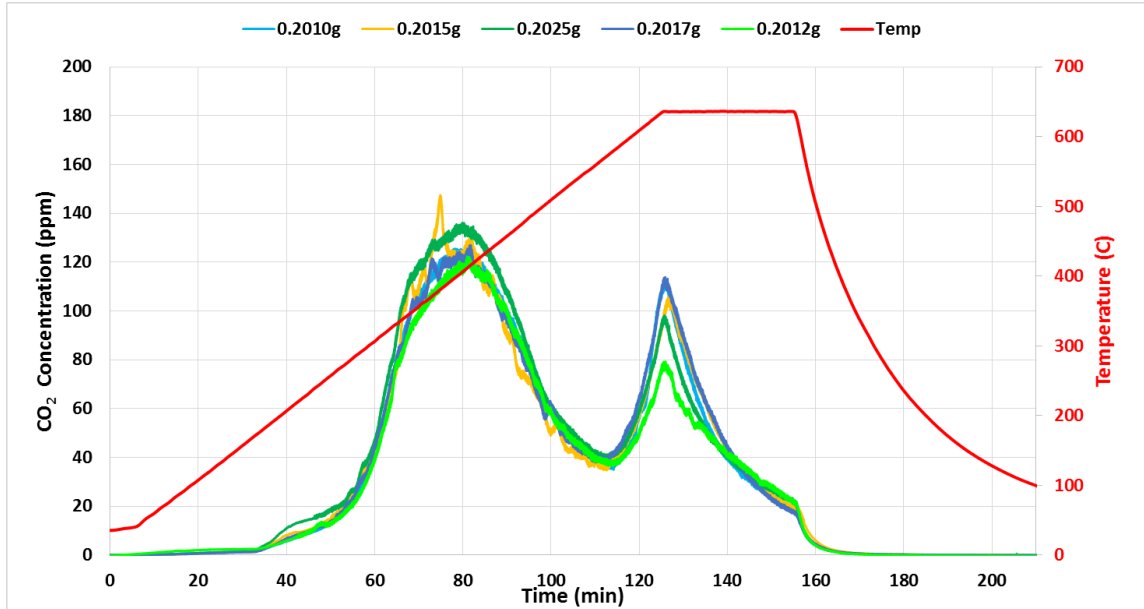


Figure 64: TPO CO₂ concentration curve for 1200 kGy electron beam treated SJV/BM1 soil. 5 samples of varying masses are shown.

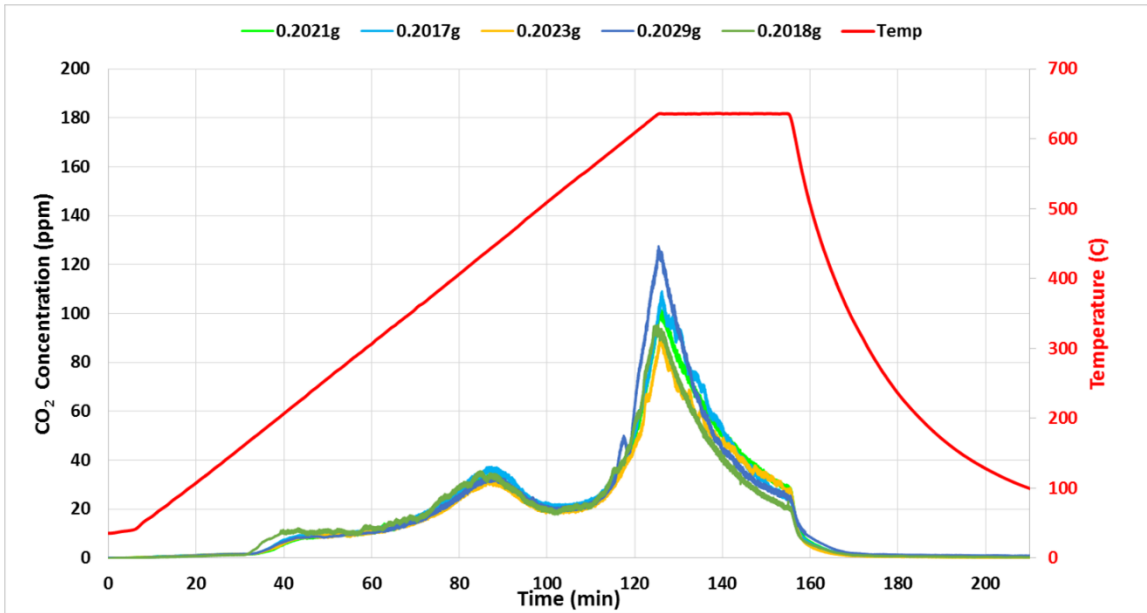


Figure 65: TPD CO₂ concentration curve for 1200 kGy electron beam treated SJV/BM1 soil. 5 samples of varying masses are shown.

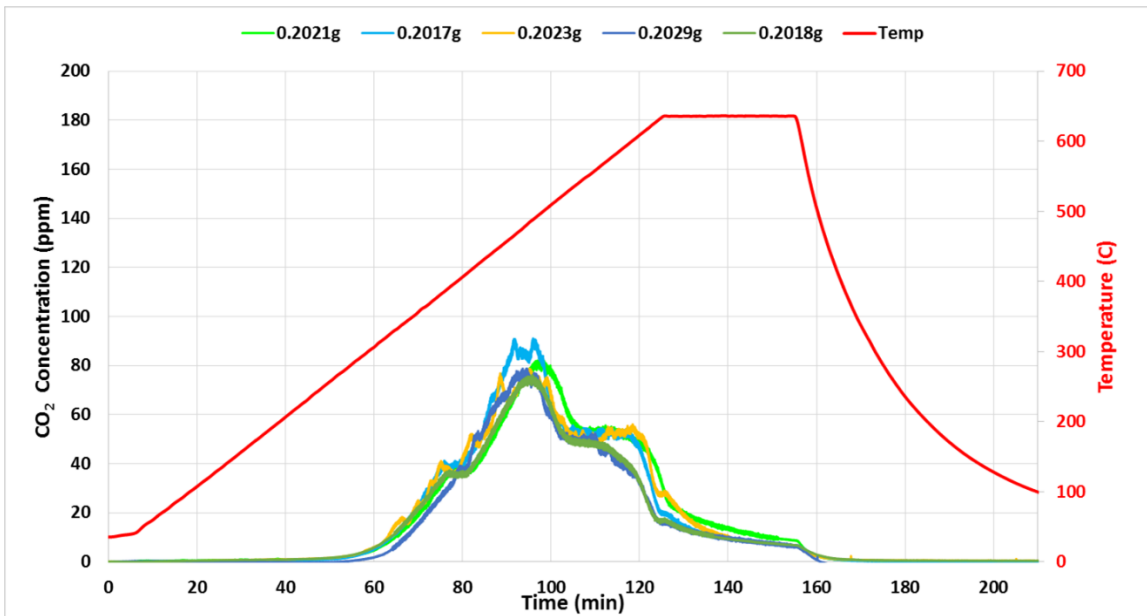


Figure 66: TPO Devol. CO₂ concentration curve for 1200 kGy electron beam treated SJV/BM1 soil. 5 samples of varying masses are shown.

APPENDIX H

2200 KGY (SJV/BM1) REPLICATE TPX

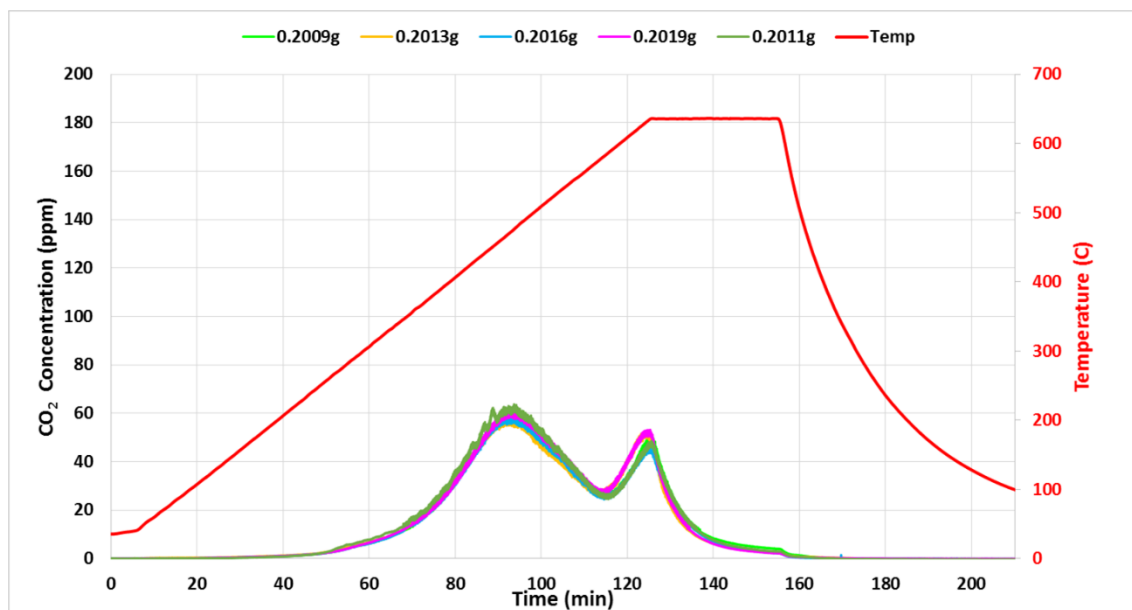


Figure 67: TPO CO₂ concentration curve for 2200 kGy electron beam treated SJV/BM1 soil. 5 samples of varying masses are shown.

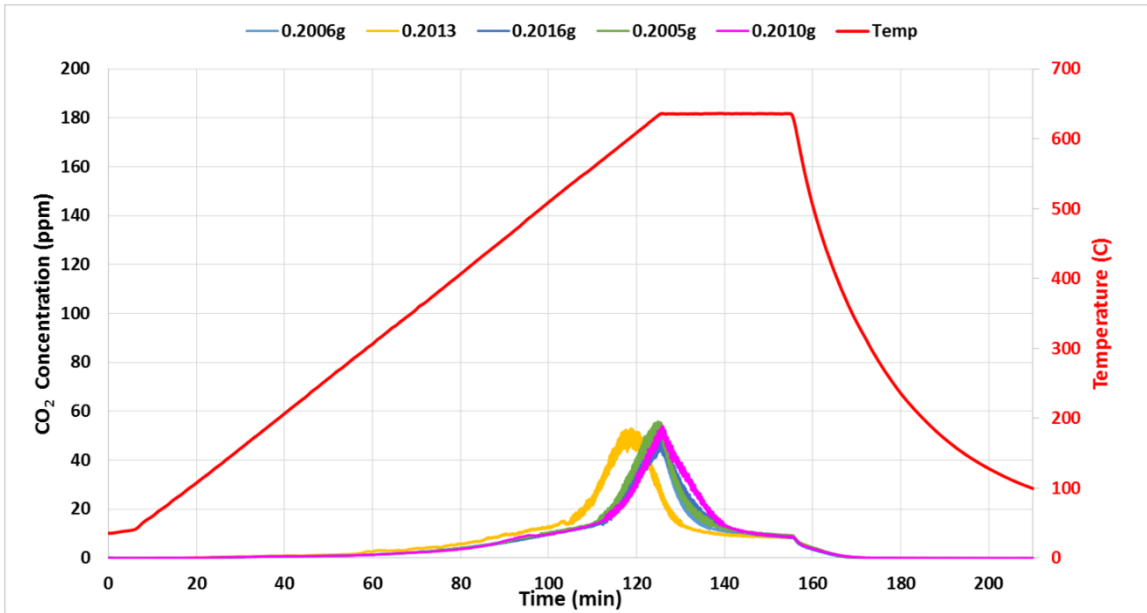


Figure 68: TPD CO₂ concentration curve for 2200 kGy electron beam treated SJV/BM1 soil. 5 samples of varying masses are shown.

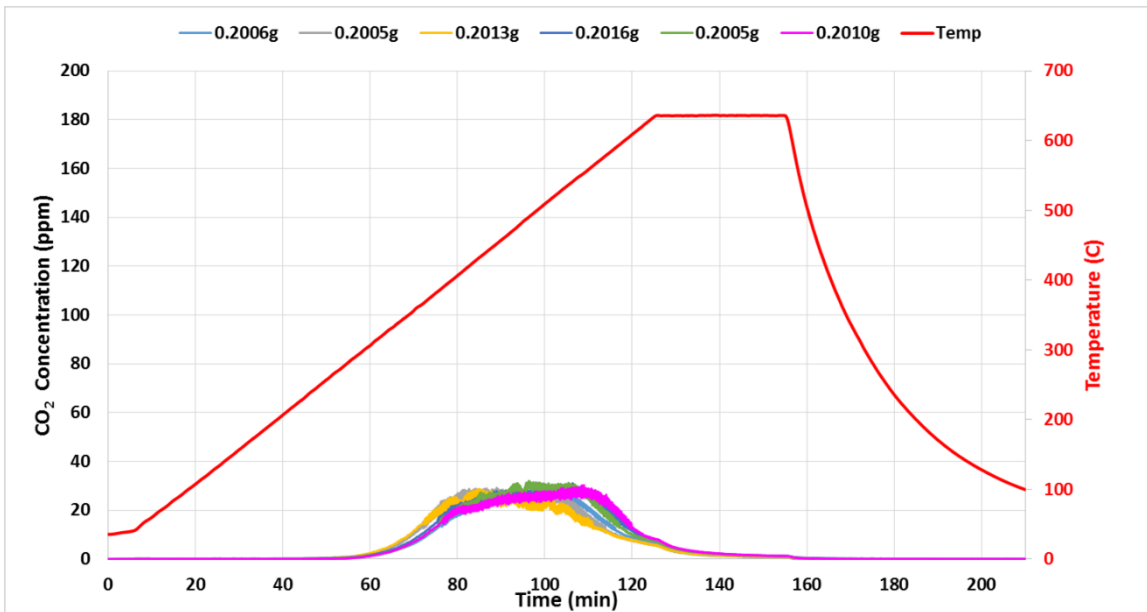


Figure 69: TPO Devol. CO₂ concentration curve for 2200 kGy electron beam treated SJV/BM1 soil. 6 samples of varying masses are shown.